8-2010

CHEMICAL MODIFICATION AND BIOLOGICAL ACTIVITY EXPLORATION OF THE NATURAL PRODUCT-GOSSYPOL

Juanjuan Yin

Clemson University, ci-anbi-an@hotmail.com

Follow this and additional works at: https://tigerprints.clemson.edu/all_dissertations

Part of the Chemistry Commons

Recommended Citation

CHEMICAL MODIFICATION AND BIOLOGICAL ACTIVITY EXPLORATION
OF THE NATURAL PRODUCT-GOSSYPOL

A Dissertation
Presented to
the Graduate School of
Clemson University

In Partial Fulfillment
of the Requirements for the Degree
Doctor of Philosophy
Food Technology

by
JUANJUAN YIN
August 2010

Accepted by:
Dr. Feng Chen, Committee Chair
Dr. Xi Wang
Dr. Jeff Adelberg
Dr. Alex Kitaygorodskiy

ABSTRACT

Gossypol is a naturally occurring, highly colored yellow pigment indigenous to the small intercellular pigment glands of the cotton plant genus Gossypium, which is proposed to be part of plant's defense system. Gossypol is characterized by wide contraceptive, antiviral, anticancer and antifungal properties. However, the relatively high toxicity of gossypol precludes its application in medical therapy. For this reason the syntheses and tests of gossypol derivatives, have been tried to enable their application as drugs. In our study, gossypol based methylation, glycosylation and nanoconjugate reactions were explored. The gossypol derivatives were all fully characterized by NMR, MS, FT-IR, UV spectrometry, HPLC and X-ray crystallography. Firstly, hexamethyl ethers of gossypol were synthesized, particularly, existence of four tautomers of gossypol tetramethyl ethers were chromatographically separated and confirmed. Gossypol exhibited the strongest antioxidant activity, while its ethers only remained partial antioxidant activity due to their conjugated naphthalene structure preserved in the derivatives. The result of alpha-amylase inhibitory activities of gossypol and its methylated ethers showed that the gossypol's methylated ethers were the alpha-amylase inhibitors, while gossypol was the alpha-amylase activator. Furthermore, it was found that anticancer activity of the gossypol and its methylated ethers depended on the degree of methylation level of gossypol. Secondly, novel glycosidic gossypol analogues were obtained by the ultrasound-assisted reaction of potassium salt of gossypol with 3, 4,

6-tetra-O-acetyl-α-D-glucopyranosyl bromide under phase transfer catalytic condition. The evaluation of anticancer, antitrypanosomal activities as well as cytotoxicity of those novel glycosidic gossypol derivatives implied that 6, 7'-gossypol diglycosidic tetraacetate (compound **8**) could be developed into a potential pharmaceutical candidate in the treatment of cancer since it exhibited powerful cancer cells inhibition with significantly low cytotoxicity. In addition, 7, 7'-gossypol diglycosidic tetraacetate (compound **7**) and 6, 7'- gossypol diglycosidic tetraacetate (compound **8**) possess antitrypanosomal activity with LD_{50} value of 2.12 and 2.44 µM, respectively. Finally, gossypol reacted with fullerene [60] in the presence of sarcosine through the Prato reaction, resulting in some unexpected N-methylfulleropyrrolidines, and different products in variable yields were obtained when choosing toluene or chlorobenzene as reaction medium. During the reaction, gossypol decomposed into benzaldehyde which was successfully detected as a new intermediate. In an *in vitro* assay of NO radical induced apoptosis in 3T3L1 cells for the N-methyl-2, 2-dimethylfulleropyrrolidine (compound **14**) showed dose dependent and stronger radical scavenging activities than the parent fullerene.

DEDICATION

This dissertation is dedicated to my beloved parents, Ying Wang and Xinsan Yin, my husband, Limei Jin, my lovely daughter, Ivy and the other members in my family and friends who have provided unconditional support and love throughout.

ACKNOWLEDGEMENTS

Table of Contents

Table of Contents (Continued)   Page

LIST OF TABLES

LIST OF FIGURES

Figure (Continued)   Page

CHAPTER 1

LITERATURE REVIEW

1.1 Introduction

Gossypol is a yellowish pigment and natural toxin found in the seeds of cotton plants (various Gossypium species). Its dimeric, bis-naphthalene structures are derived from sesquiterpenes of the cadinane family. The cadinanes are formed in the biogenetic cascade from the bisabolane intermediate by a series of putative 1, 2-shifts and cyclization. Gossypol exists as two atropisomers due to restricted rotation about the biaryl bond (Jung and Fahey, 1983; Cane, 1999).
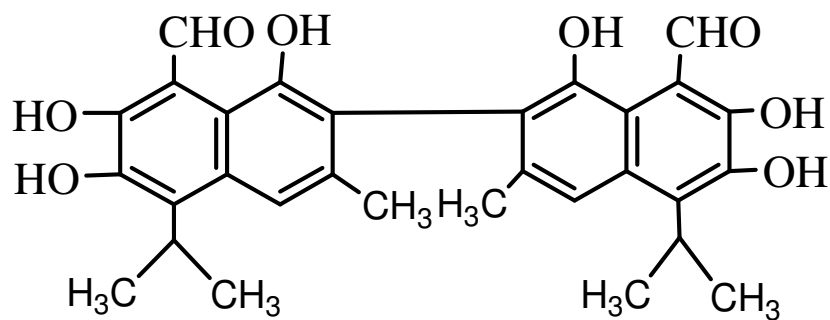
Figure 1.1 Chemical structure of gossypol

1.2 Discovery

Gossypol was first isolated by Longmore in 1886 from soapstock obtained on refining cold pressed cottonseed oil. Later, Marchlewski purified the chemical in 1899

by precipitating it from an ether solution using acetic acid to produce gossypol acetic acid. After further isolation, the chemical was named gossypol because of its originality from the vegetative family species gossypium and its polyphenolic chemical nature. Although cottonseed is the most familiar and abundant source of gossypol, the chemical has also been found in the bark and flowers of the tropic tree, Thespesia popolinea, common to Africa, Asia and the Pacific Islands, and in certain the members of the family Malvaceae (Varol et al., 2009). Okra, one of the staples of New Orleans creole cooking, also is a member of the same family and was reported to contain gossypol in its seeds (Hron et al., 2007). However, further careful evaluation of the chemical by chromatographic methods revealed it was not gossypol, but a degradation product of a reaction of hydroxylated unsaturated fatty acid triglycerides with aniline used in the gossypol analysis (Hron et al., 2007). The chemical structure of gossypol was first derived in 1938 by Adams and his students, who did extensive studies on its properties and reactions, and published a series of articles about the determination of the structure (Adams and Geissman, 1938). Twenty years later, Edwards (1970) confirmed Adams' structural formula by being the first to succeed in total synthesis of gossypol. Because of gossypol's uniqueness and challenging chemistry, it has been studied by many researchers since its discovery.

1.3 Initial research interest

Gossypol in cotton plants can slow down the reproduction of the insects that eat cotton bolls and seeds. This compound can also affect reproduction of mammals

(Saluja, 1988). Pressed cake of cotton seeds, a byproduct of the cotton industry, is sometimes fed to livestocks with unintentional contraceptive effects. Nevertheless, the most interest in gossypol derives from its activity as a contraceptive in human males. For example, the effect of gossypol on human male fertility has been known in China for many years. In 1929, a study of couples who used crude cottonseed oil for cooking showed that they were smaller than average families. Later, researchers were convinced that the oil affected male fertility. Eventually researchers isolated the contraceptive compound gossypol from the cotton seed oil. This discovery led to large scale testing of gossypol as a male contraceptive in China during the 1970s, which involved over 8,000 men, and continued for over a decade. The researchers found that men taking a daily gossypol pill had reliable contraception, but without significant change in libido (Taylor et al., 1991). Meanwhile, the chemical gossypol was confirmed to be able to affect the maturation and motility of sperm through inactivation of the enzymes required for the sperm to fertilize the ova (Ueno et al., 1988). The contraceptive effect appears to be associated with the (-)-isomer, while toxic effects (cardiac toxicity in cattle) appear to be associated with the (+)-isomer (Heywood et al., 1988). However, the studies revealed two serious flaws: disruption of potassium uptake and incomplete reversibility. The large-scale trials of gossypol in Chinese men showed an abnormally high rate of hypokalemia among subjects, varying from 1-10% (Bi et al., 1981). Hypokalemia is characterized by low levels of potassium in the blood. Since potassium is one of the key elements used by the muscles and nerves to transmit signals, low blood potassium can cause fatigue, muscle weakness and at its most extreme, paralysis. Hypokalemia is usually the result of kidney malfunction, and can be caused by excessive consumption of diuretics. Also,

there is evidence that the incidence of hypokalemia depends on intake dosage of potassium (Lohiya, 1990; Kumar, 1997). Therefore, Coutinho of Brazil (2002) claimed that previous reports of hypokalemia were the result of "the Chinese diet, which is poor in potassium, and not to the effect of gossypol on the kidneys." However, researchers are still full of questions of the observations on the effect of gossypol on kidney. Several studies of gossypol as a contraceptive in male monkeys tried to remedy potassium loss by giving the monkeys a daily potassium supplement, but the treatment did not stop the monkeys from losing potassium, which made the researchers believe that hypokalemia was an inevitable side effect, even though the dose the monkeys received were higher than the equivalent dose given to men.

Regardless of gossypol's possible causal relationship with hypokalemia, researchers at the World Health Organization (WHO) have other concerns about side effects due to natural toxicity. Therefore, some argue that this alone should disqualify it from further study (Waites, 1998).

1.4 Toxicity

The toxicity of gossypol has been shown on the reproductive system, heart, liver, and membranes. Besides, the compound exhibits both pro- and anti-oxidant behavior. Electron transfer (ET) functionalities, present in gossypol and its metabolites, comprise conjugated dicarbonyl, a quinone derivative, Schiff bases, and metal complexes. The parent possesses a reduction potential favorable for *in vivo* ET. Considerable evidence points out oxidative stress, formation of reactive oxygen species, DNA scission, and redox cycling by ET in biosystems, have similar

mechanism of action as gossypol. In a study on the apoptotic effect of gossypol on human lymphocytes, gossypol in a concentration of 20-50 mM could induce apoptosis in human lymphocytes without causing necrosis through cytotoxic effects. The combined use of steroid hormones (methyltestosterone and ethinyl estradiol) and gossypol (low dose) in an antifertility study in rats showed that the steroid hormone made the procedure of spermatogenesis slower, while low dose gossypol caused all sperm to lose their activity in the epididymis. Both affect the process of spermatogenesis from different endpoints and successfully induce infertility in the short term. A low dose of gossypol not only executes antifertility function in the epididymis, but also affects the quality of spermatozoal production in testis by impacting the procedures of both acrosomal formation and spermatozoal elongation. This assists in maintaining long term infertility (Kovacic, 2003).

1.5 Bioactivities

1.5.1 Antioxidant property

Gossypol is a polyphenolic compound from the viewpoint of its chemical structure. Like many other phenolic chemicals, such as butylated hydroxytoluene (BHT), coumaric acid, gallic acid, quercetin, myricetin, catechin, gallocatechin, etc., gossypol is an effective and potent natural antioxidant. For example, gossypol was found to be able to protect carotene *in vitro* against preformed fat peroxides many decades ago (Hove, 1944a,b). Hove confirmed that cottonseed products containing

gossypol could inhibit carotene destruction and rancidity development *in vitro*, and gossypol could act as a carotene-protecting antioxidant *in vivo*. Gossypol has shown potential in inhibiting rat liver microsomal peroxidation, which is caused by an incubation with ferric/ascorbate ($IC_{50} < 0.1\mu M$) (Laughton et al., 1989). Gossypol also exhibited a significant positive effect on oil and biodiesel stability. With a concentration of 0.1% gossypol, the oxidative stability indices (OSI) of cottonseed oil biodiesel could increase to 17.2 hours from 4.15 hours at 110 ^{o}C (Fan et al., 2008).

In some cases, modification of the functional groups on gossypol may not affect its original chemical and biological activities. For instance, the modification of aldehydic groups on gossypol to form dianilinogossypol, of which the free carbonyl groups were tied up by the anilido complex, did not decrease the antioxidant activity of the free compound (Bickford et al., 1954; Hove, 1944) Bickford and coworkers (1954) also found the other Schiff base-formed gossypol derivatives, gossypol-urea, gossypol-aminobenzene-thiol, and gossypol-glycineindicates, have roughly equivalent antioxidative ability to gossypol on a molar basis. Gossypol bis(piperinoethylimine) and bis(morpholinoethylimine) also showed potent antioxidant action in human blood serum and rat brain synaptosomes. At equal concentrations, these substances suppressed the peroxidation of lipids in enzymatic and nonenzymatic systems regarding the oxidation of rat liver microsomes (Dalimov et al., 1989).

On the contrary, in many other cases, the modification of phenolic hydroxyl groups on gossypol could significantly decrease the "chemical" antioxidative abilities regarding free radical scavenging activity, reducing power, and DNA damage prevention activity (Wang et al., 2008), demonstrating that the hydroxyl groups are critical for the antioxidative activities. For example, 6-methoxy gossypol exhibited a similar free radical scavenging activity as 6, 6'-dimethoxy gossypol, but both methylated derivatives of the gossypol possessed a weaker radical scavenging activity than gossypol. The concentrations of 6-methoxy gossypol and 6, 6'-dimethoxy gossypol needed to scavenge 50% of the free radicals in the test system were two-fold higher than that of gossypol (about 16ppm vs. 8ppm). Although gossypol, 6-methoxy gossypol, and 6,6'-dimethoxy gossypol all reduced ferric ions to ferrous ions in a dose-dependent manner, gossypol again showed greater reducing power and higher efficiency than 6-methoxy gossypol or 6,6'-dimethoxy gossypol. However, all three test compounds showed much stronger reducing power than commercial antioxidant butylated hydroxytoluene (BHT). For instance, 6,6'-dimethoxy gossypol at a concentration of 10 ppm exhibited the same reducing power as BHT at a 100 ppm concentration. The relative capability of gossypol and its methylated derivatives to prevent DNA damage caused by ultraviolet light and hydrogen peroxide was consistent with the compounds' antioxidant effects. This suggests that gossypol's protection of DNA may occur partially by quenching free radicals, therefore alleviating oxidative stress. A previous study (Li et al., 2000) also found that gossypol

demonstrated the ability, in a dose-dependent manner, to protect supercoiled plasmid DNA from damage caused by exposure to Fe^{3+}/ascorbate.

1.5.2 Anti-cancer activity

Gossypol is capable of inhibiting the growth of a variety of cancer cell lines including breast, colon, prostate, and leukemia cells (Balci et al., 1999; Benz et al., 1990; Huang et al., 2006; Zhang et al., 2003). These disruptions include inhibition of cytoplasmic and mitochondrial enzymes involved in energy production (Ueno et al., 1988) and uncoupling of oxidative phosphorylation (Flack et al., 1993; Abou-Donia et al, 1974). In addition, depletion of cellular adenosine triphosphate (ATP) has been demonstrated in cultured tumor cells (Keniry et al., 1989). Gossypol also inhibits key nuclear enzymes responsible for DNA replication and repair, including DNA polymerase α (Rosenberg et al., 1986) and topoisomerase II, and blocks DNA synthesis in HeLa cells (Wang, 1984). Hou et al. (2004) found that gossypol at 50 µM for 6 hours could induce apoptosis in human promyelocytic leukemia cells (HL-60) (DNA fragmentation, poly(ADP) ribose polymerase cleavage), and also induce the truncation of Bid protein, the loss of mitochondrial membrane potential, cytochrome c release from mitochondria into cytosol, and activation of caspases-3, -8, and -9. At a low dose of 5 µM, gossypol also could cause a significant elevation of caspases-3, -8 and -9, which resulted in cell apoptosis of human colon cancer cell line HCT 116 (Zhang et al., 2007). Recent studies on human leukemia U937 cells showed gossypol

at >10 µM resulted in significant cell cytotoxicity and DNA fragmentation, induced caspase-3 activation and poly (ADP) ribose polymerase cleavage. These properties make gossypol a potential antineoplastic agent.

It is reported that inhibition of DNA synthesis can be achieved with 10 µM gossypol by blocking the G1/S checkpoint in MCF-7 cells at 24 hours of incubation (Ligueros et al., 1997). Gossypol might regulate cell cycles by modulating the expression of cell cycle regulatory proteins Rb and cyclin D1 and the phosphorylation of Rb protein. Jiang et al. (2004) obtained a similar conclusion that inhibitory effect of gossypol on the proliferation of human prostate cancer PC3 cells was associated with induction of TGF-β1, which in turn influenced the expression of the cell cycle-regulatory protein, cyclin D1. In human alveolar lung cancer cells, gossypol induced Fas/Fas ligand mediated apoptosis (Moon et al., 2008a). Also, gossypol induced transcriptional downregulation and posttranslational modification of hTERT in human leukemia cells, causing inactivation of c-Myc and Akt, respectively. Both c-Myc and Akt are able to regulate various Bcl-2 proteins, the pro-apoptosis protein family members.

Gossypol also downregulates the expression of NF-kappaB-regulated gene products, including inhibitors of apoptosis such as protein (IAP)-1, IAP-2, and X-linked IAP. These results suggest that gossypol-induced apoptosis partially involves suppression of NF-kappaB activity (Moon et al., 2008b). Treatment of

Ramos cells with gossypol not only induced cell arrest on the G_0/G_1 phase, but also increased apoptosis and growth inhibition induced by etoposide, doxorubicin hydrochloride, vincristine, and paclitaxel (Li et al., 2008). Liu et al., (2002) found that (-)-gossypol was more active in inhibiting breast cancerous epithelial cells and cancerous stromal cells. Meanwhile, the inhibitory activity of (-)-gossypol was related to the reduction of the cell cycle regulator, cyclin D1, and the induction of the cell proliferation inhibitor, TGF-β. In the study of human prostate cancer cells, it was found that (-)-gossypol-induced apoptosis was mediated by the regulation of Bcl-2 and caspase families (Huang et al., 2006). Another *in vitro* study (Mohammad et al., 2005) demonstrated (-)-gossypol had significant inhibitive effects against the growth of lymphoma cell line WSU-DLCL2 and fresh cells obtained from a lymphoma patient with no effect on normal peripheral blood lymphocytes. (-)-Gossypol also induced complete cytochrome c release from mitochondria, increased caspases-3 and -9 activity, and caused apoptotic death without affecting protein levels of Bcl-2, Bcl-X (L), Bax, and Bak. Recent research has revealed that (-)-gossypol acts as a BH3 mimetic, binding to the BH3-binding domain in various pro-apoptotic proteins of the Bcl-2 family, displacing pro-death partners to induce apoptosis (Balakrishnan et al., 2008; Meng et al., 2008).

Sikora et al. (2008) found that the combination of gossypol with the antioxidant N-acetyl-cysteine to block reactive oxygen species (ROS) would increase the (-) gossypol-induced cytotoxicity in tumor cells, but not normal cells, indicating that

concurrent treatment with antioxidants to block ROS prevents oxidative inactivation of (-)-gossypol and limits off-target toxicity allowing more potent (-)-gossypol-induced anti-tumor activity. An *in vivo* study also showed that (-)-gossypol significantly enhanced the antitumor activity of X-ray irradiation, leading to tumor regression in the combination therapy by inhibiting both antiapoptotic proteins Bcl-2 and/or Bcl-xL (Xu, 2005). A combination of docetaxel and (-)-gossypol synergistically enhanced the antitumor activity of docetaxel both *in vitro* and *in vivo* in the human prostate cancer PC-3 xenograft model in nude mice. (-)-Gossypol exerts its antitumor activity through inhibition of the anti-apoptotic protein Bcl-xL accompanied by an increase of pro-apoptotic Noxa and Meng et al., 2008). One study on gossypol derivatives (Arnold et al., 2008)) showed that apogossypolone could inhibit the growth of the lymphoma cell line WSU-FSCCL with an IC_{50} of 109 nM, and the activation of caspases-9, -3, and -8 was observed. Hu et al. (2008) found that apogossypol selectively inhibited proliferation of three NPC cell lines (C666-1, CNE-1 and CNE-2) that highly expressed the anti-apoptotic Bcl-2 proteins with release of cytochrome c, activation of caspases-9 and -3, and apoptosis of sensitive NPC cells. The toxicity and efficacy study on mice (Kitada et al., 2008) showed that mice tolerate doses of apogossypol 2- to 4-times higher than gossypol. Apogossypol displayed superior activity to gossypol in terms of reducing splenomegaly and reducing B-cell counts in the spleens of Bcl-2-transgenic mice, indicating the potential of gossypol derivatives for cancer therapy. Gossypolone was

less potent than gossypol in inhibiting human breast cancer cells (Gilbert et al., 1995).

The reduced effectiveness of gossypolone compared to gossypol in breast cancer cells agrees with the antifertility effects (Kim et al., 1984), but is in contrast to the antisteroidogenic and antireproductive effects of gossypolone, which have shown similar potency as gossypol (Gu, 1991). Methylated gossypol, 6-methoxy gossypol, and 6, 6'-dimethoxy gossypol, compared with the parent compound, showed superior anti-cancer activity against cervical, breast, and colon cancer cells (Wang et al., 2008).

In summary, gossypol is believed to arrest cell growth at the G_0/G_1 phase and induce cell apoptosis, in cancer cells, by regulating the cell cycle, enzymes, anti-apoptosis, and pro-apoptosis proteins.

1.5.3 Anti-virus activity

Lin et al. (1989 and 1993) reported that gossypol inhibited the replication of human immunodeficiency virus-type 1 (HIV-1) and found (-)-gossypol to be more inhibitory (IC_{50}=5.2 µM) compared to the (+)-gossypol (IC_{50}=50.7µM). Besides HIV-1, gossypol also showed anti-viral activity in multiple enveloped viruses including herpes simplex virus type 2 (HSV-II), influenza virus, and parainfluenza virus (Vander Jagt et al., 2000).

Gossypol and a series of peri-acylated gossylic nitriles were compared for their anti-viral activities against HSV-II and for their toxicities to the host Vero cells. All of the peri-acylated gossylic nitriles exhibited lower cytotoxicities to the host cell than did the parent compound gossypol. Both gossypol and the series of derivatives exhibited anti-viral activities against HSV-II when the virus was treated with concentrations as low as $5x10^{-7}$ M. Two of the derivatives, gossylic nitrile-1, 1'-diacetate and gossylic nitrile-1, 1'-divalerate, were capable of inhibiting viral multiplication in Vero cells that were infected with virus before administration of the drug. The authors (Radloff et al., 1986) concluded that modification of gossypol's aldehydic groups lowered its toxicity to the host Vero cells but did not abolish the compound's anti-viral (HSV-II) activity. Derivatives of gossypol may be useful as anti-viral agents.

Later, Royer et al. (1991) found that gossypol and its derivatives, gossylic nitrile-1, 1'-diacetate, gossylic iminolactone, and gossylic lactone inhibited the replication of human immunodeficiency virus type 1 *in vitro*. Gossylic iminolactone displayed the greatest inhibition, followed by gossypol, gossylic nitrile-1, 1'-diacetate, and gossylic lactone, indicating that derivatives of gossypol can retain anti-viral activities. Then, Royer and coworkers (1995) tested several other gossypol derivatives for inhibition of HIV: 1, 1'-Dideoxygossypol, 1, 1'-dideoxygossylic acid (DDGA), 8-deoxyhemi -gossypol (DHG), and 8-deoxyhemigossylic acid (DHGA). The result showed that DDGA was the most effective in inhibiting the replication of

HIV in vitro with $EC_{50} < 1$ µM. Meanwhile, DDG was less effective than DDGA. DHG showed some anti-HIV activity, and DHGA was ineffective against HIV. Since all four gossypol derivatives were found to have much lower affinities for albumin than the parent compound gossypol, this would possibly enhance the anti-virus activity of the gossypol derivatives *in vivo* with less interference from *in vivo* proteins.

1.5.4 Anti-parasiticprotozoan activities

Malaria is a vector-borne infectious disease caused by protozoan parasites. Human malaria is usually caused by the infection of *Plasmodium falciparum*, *Plasmodium malariae*, *Plasmodium ovale*, and *Plasmodium vivax* (Mendis, 2001). It is widespread in tropical and subtropical regions, including Asia, Africa and parts of the Americas. Each year there are about 350-500 million cases of malaria, and more than one million people die (CDC, 2009). A series of gossypol derivatives with modified aldehydic groups and hydroxyl groups have been shown to inhibit the growth of *Plasmodium falciparum* (Razakantoanina et al., 2000; Royer et al., 1986). The derivatives with ethyl, propyl, or isopropyl side chains as well as gossylic nitrile 1,1'-divalerate with IC_{50} values close to gossypol (IC_{50}=16 µM) showed stronger inhibition than other gossypol derivatives against the growth of *Plasmodium falciparum*.

Royer et al. (1986) proposed that the antimalarial activity of gossypol and gossypol derivatives was through the inhibition of lactate dehydrogenase, which is the

most active and essential enzyme for anaerobic life cycle of *Plasmodium falciparum.* Any compound showing inhibition of this enzyme also kills the parasites (Razakantoanina et al., 2000; Royer et al., 1986). Similarly, the inhibition of LDH activity in *T. gondii* can also inhibit growth of the parasite in cultures (Dando et al., 2001). In the study on *Entamoeba histolytica* (Gonzalez-Garza et al., 1993a and 1993b)*,* gossypol also showed the inhibition to alcohol dehydrogenase and malic enzymes, and (-)-gossypol was found more active than racemic gossypol and (+)-gossypol. The (-)-gossypol was 3.6 and 13.0 times more potent than (+/-)-gossypol and (+)-gossypol, respectively, in inhibiting the malic enzyme, and 1.9 times and 2.9 times more potent than (+/-)-gossypol and (+)-gossypol, respectively, against the alcohol dehydrogenase.

Trypanosomes, protozoan parasites belonging to the subphylum Mastigophora, can cause a chronic infection called sleeping sickness. It has seriously affected the health of people in western and central African countries, and exerted significant mortality in man and livestock. Over 60 million people living in 36 sub-Saharan countries are threatened by sleeping sickness (WHO, 2001) and 48000 deaths were reported in 2002 (WHO, 2004). In addition, 46 million cattle are exposed to the risk of the sleeping disease. The disease costs an estimated 1,340 million USD per year (Kristjanson, 1999). However, few drugs are available for the treatment of trypanosomal infections that cause significant mortality in man and livestock in Africa. Gossypol was reported to be able to inhibit trypanosomes (Blanco et al., 1983;

Kaminsky and Zweygarth, 1989; Montamat et al., 1982). Montamat and coworkers (1982) reported that a 5-min exposure to 100 μM gossypol (~50 ppm) immobilizes cultures of *Trypanosoma cruzi*.   Blanco et al. (1983) reported that a 30-min exposure to 25 μM gossypol (~12 ppm) immobilizes and alters the cell morphology of *T. cruzi.* Later, Kaminsky and Zweygarth (1989) reported that, for three separate *Trypanosoma brucei* strains (including one drug resistant strain), the IC_{50} value for a 24h gossypol exposure was >10 ppm.   Our study showed a similar level of gossypol's anti-trypanosomal activity with IC_{50} value of 7.8 ppm after 24-h exposure. Moreover, methylated gossypol, both 6-methoxy gossypol (IC_{50} value, 3.98 ppm) and 6, 6'-dimethoxy gossypol (IC_{50} value, 3.21 ppm) showed more effective inhibition of growth than gossypol.   In the study of *T. cruzi,* gossypol was also reported to inhibit some oxidoreductases (Gerez de Burgos et al., *1984;* Montamat et al., 1982), such as, alpha-hydroxyacid and malate dehydrogenases, NAD-linked enzymes, and glutamate dehydrogenase, glucose-6-phosphate dehydrogenase, and NADP-dependent enzymes. Gossypol also inhibits the MDH enzyme of *T. cruzi* (Gerez de Burgos et al., 1984).

Accordingly, the possible mechanism of the antiparasitic effect of gossypol and gossypol derivatives could be the selective inhibition of vital enzymes in the parasites.

1.5.5 Anti-microbial activity

The anti-microbial properties of gossypol have been reported by several research groups. Gossypol has general antifungal activities with LD_{50} values from 20 to 100

ppm of pure gossypol (Bell, 1967), and has an inhibitory effect on microorganisms including aerobic sporeformers and lactobacilli and some yeasts (Margalith, 1967). Gossypol showed strong antibiotic activity against aerobic sporeformers and lactobacilli, and displayed antagonistic property to some of the more oxidative yeasts.

Later, Vadehra et al. (1985) investigated the effects of gossypol on the growth of a variety of bacteria and on spore formation and germination in *Bacillus cereus*. It was found that gossypol had more potent antibacterial properties against gram positive organisms (i.e. *Streptococcus* spp., *Bacillus* spp., *Staphylococcus aureus*) than gram negative bacteria such as *Pseudomonas aeruginosa*, *Salmonella spp.*, *Klebsiella pneumoniae*, *Shigella spp.*, *Proteus spp.*, and *Escherichia coli*. All of the gram positive organisms tested were completely inhibited at a concentration of 100 ppm. None of the tested gram negative strains was inhibited at 100 ppm of gossypol, and only 1/3 of the tested strains were inhibited at 200 ppm of gossypol. The authors proposed that the anti-bacterial activity of gossypol was related to the gram character of the organisms. Besides, the chemical and quantitative differences of the cell wall and cell membrane of the gram positive and negative groups may influence the transport of gossypol to its target site (i.e., Gram-positive organisms have high amount of peptidoglycan in the cell wall, and lack the outer membrane found in Gram-negative bacteria). The same research group also found that yeasts, such as *Saccharomyces cereviseae, S. uvarum, S. diasticu*) were sensitive to gossypol, and the growth were completely inhibited at 50 ppm of gossypol. Subsequent research

(Poprawski and Jones, 2001) found that fungi *Paecilomyces fumosoroseus* (associated with cutaneous and disseminated infections in dogs and cats) were highly tolerant to gossypol even at 500 ppm, but could be strongly inhibited at 1000 ppm of gossypol.

1.5.6 Lowering plasma cholesterol levels

Cholesterol is a fat-soluble compound found in the body. Having high "bad" cholesterol means you have too much low density lipoprotein (LDL) in your blood, which is linked to serious problems, such as atherosclerosis and coronary heart attack or stroke. A study on adult male cynomolgus monkeys (Shandilya and Clarkson, 1982) found that gossypol administered orally at 10 mg/kg/day for 6 months could cause a significant decrease in total plasma cholesterol (TPC) and LDL without any significant decrease in plasma high density lipoprotein cholesterol (HDL) levels. It was proposed that this cholesterol lowering activity might be attributed to: (a) gossypol might possibly reduce the intestinal absorption of dietary cholesterol; and (b) gossypol might reduce the hepatic synthesis of low density lipoproteins. Studies with rabbits also showed that dietary cottonseed protein effectively lowered the concentration of plasma cholesterol when compared to the animal protein casein, which was attributed to the presence of gossypol in the cottonseed protein. Thrice weekly subcutaneous injection doses of 20 mg/kg body weight to rats for 4 weeks also resulted in lower serum cholesterol. Another study on rats demonstrated that gossypol consumption not only had a significant effect on alcohol dehydrogenase, but also a

profound influence on the regulation of cholesterol level in the liver. A subsequent study on rats showed that the administration of gossypol at 20 mg/kg body weight/rat/day for 8 weeks could significantly decrease the serum level of cholesterol in both low and normal protein-fed male Wistar rats. The combined administration of gossypol and chloroquine (chloroquine, a 4-aminoquinoline, used for treatment of malaria) to the protein-malnourished rats had more profound effects in decreasing the levels of serum cholesterol and triglycerides compared to normal-protein fed rats, indicating the implication of the treatment and dietary effect on the level of serum cholesterol. However the mechanism by which gossypol lowers the serum cholesterol still needs further investigation.

1.6 References

Abou-Donia, M.B., and Dieckert, J.W. (1974). Gossypol: Uncoupling of respiratory chain and oxidative phosphorylation. *Life Sci.* **14**, 1955-1963.

Adams, R., and Geissman, T. A. (1938). Structure of gossypol. VII. gossypol dimethyl ether. *J. Am. Chem. Soc.* **60**, 2163-2166.

Arnold, A. A., Aboukameel, A., Chen, J., Yang, D., Wang, S., Al-Katib, A., and Mohammad, R. M. (2008). Preclinical studies of apogossypolone: a new nonpeptidic pan small-molecule inhibitor of Bcl-2, Bcl-XL and Mcl-1 proteins in Follicular Small Cleaved Cell Lymphoma model. *Mol. Cancer.* **7**, 20-29.

Balakrishnan, K., Wierda, W. G., Keating, M. J., and Gandhi, V. (2008). Gossypol, a BH3 mimetic, induces apoptosis in chronic lymphocytic leukemia cells. *Blood.* **112**, 1971-1980.

Balci, A., Sahin, F. I., and Ekmekci, A. (1999). Gossypol induced apoptosis in the human promyelocytic leukemia cell line HL 60. *Tohoku. J. Exp. Med.* **189**, 51-57.

Bell, A. A. (1967). Formation of gossypol in infected or chemically irritated tissues of gossypium species. *Phytopathol.* **57**, 759-764.

Benz, C. C., Keniry, M. A., Ford, J. M., Townsend, A. J., Cox, F. W., Palayoor, S., Matlin, S. A., Hait, W. N., and Cowan, K. H. (1990). Biochemical correlates of the antitumor and antimitochondrial properties of gossypol enantiomers. *Mol. Pharmacol.* **37**, 840-847.

Bi, X. F., Ye, Y. X., Yang, H. F., Zhang, Z. R. (1981). Preliminary study on gossypol induced hypokalemia. *Zhongguo Yixue Kexueyuan Xuebao*. **3**, 175-178.

Bickford, W. G., Pack, F. C., Castillon, L. E., and Mack, C. H. (1954). The antioxidant and antipolymerization properties of gossypol, dianilinogossypol, and related materials. *J. Am. Oil Chem. Soc.* **31**, 91-93.

Blanco, A., Aoki, A., Montamat, E. E., and Rovai, L. E. (1983). Effect of gossypol upon motility and ultrastructure of Trypanosoma cruzi. *J. Protozool.* **30**, 648-651.

Cane, D. E. (1999). Sesquiterpene biosynthesis: cyclization mechanisms. *Comprehensive Natural Products Chemistry*. Pergamon Press, Oxford, **2**, 155–200.

CDC. (2009). Department of Health and Human Sevice, Centers for Disease Control and Prevention. *http://www.cdc.gov/Malaria/.*

Coutinho, E. (2002). Gossypol: a contraceptive for men. *Contraception.* **59**, 259-263.

Dalimov, D. N., Mukhamedzhanova, E. N., Shneivais, V. B., Biktimirov, L., Isamilov, A. I., and Kamaev, F. G. (1989). Synthesis, structure, and action of some gossypol derivatives on the perozidation of the lipids of biosubstrates. *Khimiya. Prirodnykh. Soedinenii.* **5***, 707-712.

Dando, C., Schroeder, E. R., Hunsaker, L. A., Deck, L. M., Royer, R. E., Zhou, X., Parmley, S. F., and Vander Jagt, D. L. (2001). The kinetic properties and sensitivities to inhibitors of lactate dehydrogenases (LDH1 and LDH2) from Toxoplasma gondii: comparisons with pLDH from Plasmodium falciparum. *Mol. Biochem. Parasitol.* **118**, 23-32.

Edwards, J. D. (1970). Synthesis of gossypol and gossypol derivatives. *J. Am. Oil Chem. Soc.* **47**, 441-442.

Fan, X. H., Wang, X., Chen, F., Galler, D. P., and Wan, P. J. (**2008**). Engine performance test of cottonseed oil biodiesel. *The Open Energy and Fuels Journal .* **1***, 40-45.

Flack, M. R., Pyle, R. G., Mullen, N. M., Lorenzo, B., Wu, Y. W., Knazek, R. A., Nisula, B. C., and Reidenberg, M. M. (1993). Oral gossypol in the treatment of metastatic adrenal cancer. *J. Clin. Endocrinol. Metab.* **76**, 1019-1024.

Gerez de Burgos, N. M., Burgos, C., Montamat, E. E., Rovai, L. E., and Blanco, A. (1984). Inhibition by gossypol of oxidoreductases from *Trypanosoma cruzi. Biochem. Pharmacol.* **33**, 955-959.

Gilbert, N. E., O'Reilly, J. E., Chang, C. J. G., Lin, Y. C., and Brueggemeier, R. W. (1995). Antiproliferative activity of gossypol and gossypolone on human breast cancer cells. *Life Sci.* **57**, 61-67.

Gonzalez-Garza, M. T., Matlin, S. A., Mata-Cardenas, B. D., and Said-Fernandez, S. (1993a). Differential effects of the (+)- *and* (-)-gossypol enantiomers upon Entamoeba histolytica axenic cultures. *J. Pharm. Pharmacol.* **45**, 144-145.

Gonzalez-Garza, M. T., Matlin, S. A., Mata-Cardenas, B. D., and Said-Fernandez, S. (1993b). Entamoeba histolytica: inhibition of malic enzyme and alcohol dehydrogenase by (+/-)-, (+)-, and (-)- gossypol. *Arch. Med. Res.* **24**, 183-187.

Gu, Y., and Lin, Y. C. (1991). Suppression of adrenocorticotropic hormone (ACTH)-induced corticosterone secretion in cultured rat adrenocortical cells

by gossypol and gossypolone. *Res. Commun. Chem. Pathol. Pharmacol.* **72**, 27-38.

Heywood, R. (1988). The toxicology of gossypol acetic acid and (-) - gossypol. *Contraception*. **37**, 185-190

Hou, D. X., Uto, T., Tong, X., Takeshita, T., Tanigawa, S., Imamura, I., Ose, T., and Fujii, M. (2004). Involvement of reactive oxygen species-independent mitochondrial pathway in gossypol-induced apoptosis. *Arch. Biochem. Biophys.* **428**, 179-187.

Hove, E. L. (1944a). Gossypol as a carotene-protecting antioxidant, *in vivo* and *in vitro*. *J. Biol. Chem.* **156**, 633-642.

Hove, E. L., and Hove, Z. (1944b). A method for estimating total fat-soluble antioxidants based on the relation between fat peroxides and carotene destrction. *J. Biol. Chem.* **156**, 611-622.

Hron, R. J., Koltun, S. P., Pominski, J., and Abraham, G. (2007). The potential commercial aspects of gossypol. *J. Am. Oil Chem. Soc.* **64**, 1315-1319.

Hu, Z. Y., Zhu, X. F., Zhong, Z. D., Sun, J., Wang, J., Yang, D., and Zeng, Y. X. (2008). ApoG2, a novel inhibitor of antiapoptotic Bcl-2 family proteins, induces apoptosis and suppresses tumor growth in nasopharyngeal carcinoma xenografts. *Int. J. Cancer*. **123**, 2418–2429.

Huang, Y. W., Wang, L. S., Chang, H. L., Ye, W., Dowd, M. K., Wan, P. J., and Lin, Y. C. (2006). Molecular mechanisms of (-)-gossypol-induced apoptosis in human prostate cancer cells. *Anticancer Res.* **26**(3A), 1925-1933.

Jiang, J., Sugimoto, Y., Liu, S., Chang, H. L., Park, K. Y., Kulp, S. K., and Lin, Y. C. (2004). The inhibitory effects of gossypol on human prostate cancer cells-PC3 are associated with transforming growth factor beta1 (TGFbeta1) signal transduction pathway. *Anticancer Res.* **24**, 91-100.

Jung, H. G., and Fahey, G. C. (1983). Nutritional Implications of Phenolic Monomers and Lignin: a Review. *J. Anim. Sci.* **57**, 206-219.

Kaminsky, R., and Zweygarth, E. (1989). Feeder layer-free in vitro assay for screening antitrypanosomal compounds against *Trypanosoma brucei brucei* and *T. b. evansi*. *Antimicrob. Agents Chemother.* **33**, 881-885.

Keniry, M. A., Hollander, C., and Benz, C. C. (1989). The effect of gossypol and 6-aminonicotinamide on tumor cell metabolism: a ^{31}P-magnetic resonance spectroscopic study. *Biochem. Biophys. Res. Commun.* **164**, 947-953.

Kim, I. C., Waller, D. P., Marcelle, G. B., Cordell, G. A., Fong, H. H., Pirkle, W. H., Pilla, L., and Matlin, S. A. (1984). Comparative in vitro spermicidal effects of (+/-)-gossypol, (+)-gossypol, (-)-gossypol and gossypolone. *Contraception.* **30**, 253-259.

Kitada, S., Kress, C. L., Krajewska, M., Jia, L., Pellecchia, M., and Reed, J. C. (2008). Bcl-2 ;antagonist apogossypol (NSC736630) displays single-agent activity in Bcl-2-transgenic mice and has superior efficacy with less toxicity compared with gossypol (NSC19048). *Blood.* **111**, 3211-3219.

Kovacic, P. (2003). Mechanism of drug and toxic actions of gossypol: focus on reactive oxygen species and electron transfer. *Curr. Med. Chem.* **10**, 2711-2718.

Kristjanson, P. M., Swallow, B. M., Rowlands, G. J., Kruska, R. L., and de Leeuw, P. N. (1999). Measuring the costs of African animal trypanosomiasis, the potential benefits of control and returns to research. *Agr. Sys.* **59**, 79-98.

Kumar, M, S., Sharma, S., and Lohiya, N. K. (1997). Gossypol-induced hypokalemia and role of exogenous potassium salt supplementation when used as an antispermatogenic agent in male langur monkey. *Contraception.* **56**, 251-256.

Laughton, M. J., Halliwell, B., Evans, P. J., and Hoult, J. R. (1989). Antioxidant and pro-oxidant actions of the plant phenolics quercetin, gossypol and myricetin. Effects on lipid peroxidation, hydroxyl radical generation and bleomycin-dependent damage to DNA. *Biochem. Pharmacol.* **38**, 2859-2865.

Li, A., Bandy, B., Tsang, S. S., and Davison, A. J. (2000). DNA-breaking versus DNA-protecting activity of four phenolic compounds in vitro. *Free Rad. Res.* **33**, 551-566.

Li, Z. M., Jiang, W. Q., Zhu, Z. Y., Zhu, X. F., Zhou, J. M., Liu, Z. C., Yang, D. J., and Guang, Z. Z. (2008). Synergistic cytotoxicity of Bcl-xL inhibitor, gossypol and chemotherapeutic agents in non-Hodgkin's lymphoma cells. *Cancer Biol. Ther.* **7**, 51-60.

Ligueros, M., Jeoung, D., Tang, B., Hochhauser, D., Reidenberg, M. M., and Sonenberg, M. (1997). Gossypol inhibition of mitosis, cyclin D1 and Rb protein in human mammary cancer cells and cyclin-D1 transfected human fibrosarcoma cells. *Br. J. Cancer.* **76**, 21-28.

Lin, T. S., Schinazi, R. F., Zhu, J., Birks, E., Carbone, R., Si, Y., Wu, K., Huang, L., and Prusoff, W. H. (1993). Anti-HIV-1 activity and cellular pharmacology of various analogs of gossypol. *Biochem. Pharmacol.* **46**, 251-255.

Lin, T. S., Schinazi, R., Griffith, B. P., August, E. M., Eriksson, B. F. H., Zheng, D. K., Huang, L., and Prusoff, W. H. (1989). Selective inhibition of human immunodeficiency virus type 1 replication by the (-) but not the (+) enantiomer of gossypol. *Antimicrob. Agents Chemother.* **33**, 2149-2151.

Liu, S., Kulp, S. K., Sugimoto, Y., Jiang, J., Chang, H. L., Dowd, M. K., Wan, P., and Lin, Y. C. (2002). The (-)-enantiomer of gossypol possesses higher anticancer potency than racemic gossypol in human breast cancer. *Anticancer. Res.* **22**, 33-38.

Lohiya, N. K., Sharma, K., Humar, M., and Sharma, S. (1990). Limitations on developing gossypol acetic acid as a male contraceptive. *Contraception.* **41**, 519-532.

Longmore, J. (1886). Cottonseed oil: its colouring matter and mucilage, and description of a new method of recovering the loss occurring in the refining process. *J. Soc. Chem. Ind.* 200–206.

Marchlewski, L. (1899). Gossypol, ein bestandtheil der baumwollsamen. *J. Prakt. Chem.* **60**, 84–90.

Margalith, P. (1967). Inhibitory effect of gossypol on microorganisms. *Appl. Microbiol.* **15**, 952-953.

Mendis, K., Sina, B. J., Marchesini, P., and Carter, R. (2001). The neglected burden of plasmodium vivax malaria. *Am. J. Trop. Med. Hyg.* **64**, 97-106.

Meng, Y., Tang, W., Dai, Y., Wu, X., Liu, M., Ji, Q., Ji, M., Pienta, K., Lawrence, T., and Xu, L. (2008). Natural BH3 mimetic (-)-gossypol chemosensitizes human prostate cancer via Bcl-xL inhibition accompanied by increase of Puma and Noxa. *Mol. Cancer Ther.* **7**, 2192-2202.

Mohammad, R. M., Wang, S., Aboukameel, A., Chen, B., Wu, X., Chen, J., and Al-Katib, A. (2005). Preclinical studies of a nonpeptidic small-molecule inhibitor of Bcl-2 and Bcl-X(L) [(-)-gossypol] against diffuse large cell lymphoma. *Mol. Cancer Ther.* **4**, 13-21.

Montamat, E. E., Burgos, C., Gerez De Burgos, N. M., Rovai, L. E., and Blanco, A. (1982). Inhibitory action of gossypol on enzymes and growth of *trypanosoma cruzi*. *Science.* **218**, 288-289.

Moon, D. O., Kim, M. O., Choi, Y. H., Lee, H. G., Kim, N. D., and Kim, G. Y. (2008a). Gossypol suppresses telomerase activity in human leukemia cells via regulating hTERT. *FEBS Lett.* **582**, 3367-3373.

Moon, D. O., Kim, M. O., Lee, J. D., and Kim, G. Y. (2008b). Gossypol suppresses NF-kappaB activity and NF-kappaB-related gene expression in human leukemia U937 cells. *Cancer Lett*. **264**, 192-200.

Poprawski, T. J., and Jones, W. J. (2001). Host plant effects on activity of the mitosporic fungi *Beauveria bassiana* and *Paecilomyces fumosoroseus* against two populations of Bemisia whiteflies (Homoptera: Aleyrodidae). *Mycopathologia*. **151**, 11-20.

Radloff, R. J., Deck, L. M., Royer, R. E., and Vander Jagt, D. L. (1986) Antiviral activities of gossypol and its derivatives against herpes simplex virus type II. *Pharmacol. Res. Commun.* **18**, 1063-1073.

Razakantoanina, V., Nguyen Kim, P. P., and Jaureguiberry, G. (2000). Antimalarial activity of new gossypol derivatives. *Parasitol. Res*. **86**, 665-668.

Rosenberg, L. J., Adlakha, R. C., Desai, D. M., and Rao, P. N. (1986). Inhibition of DNA polymerase alpha by gossypol. *Biochim. Biophys. Acta.* **866**, 258-267.

Royer, R. E., Deck, L. M., Campos, N. M., Hunsaker, L. A., and Vander Jagt, D. L. (1986). Biologically active derivatives of gossypol: synthesis and antimalarial activities of peri-acylated gossylic nitriles. *J. Med. Chem*. **29**, 1799-1801.

Royer, R. E., Deck, L. M., Vander Jagt, T. J., Martinez, F. J., Mills, R. G., Young, S. A., and Vander Jagt, D. L. (1995). Synthesis and anti-HIV activity of 1, 1'-dideoxygossypol and related compounds. *J. Med. Chem.* **38**, 2427-2432.

Royer, R. E., Mills, R. G., Deck, L. M., Mertz, G. J., and Vander Jagt, D. L. (1991). Inhibition of human immunodeficiency virus type I replication by derivatives of gossypol. *Pharmacol. Res*. **24**, 407-412.

Saluja, A. K. (1988). Gossypol: a male contraceptive. *Eastern Pharmacist*. **31**, 55-56.

Shandilya, L. N., Clarkson, T. B., Adams, M. R., and Lewis, J. C. (1982). Effects of gossypol on reproductive and endocrine functions of male cynomolgus monkeys (Macaca fascicularis). *Biol. Reprod*. **27**, 241-252.

Sikora, M. J., Bauer, J. A., Verhaegen, M., Belbin, T. J., Prystowsky, M. B., Taylor, J. C., Brenner, J. C., Wang, S., Soengas, M. S., Bradford, C. R., and Carey, T. E. (2008). Anti-oxidant treatment enhances anti-tumor cytotoxicity of (-)-gossypol. *Cancer. Biol. Ther*. **7**, 767-776.

Taylor, G. T., Griffin, M. G., and Bardgett, M. (1991). Search for a male contraceptive: the effect of gossypol on sexual motivation and epididymal sperm. *J. Med.* **22**, 29-44.

Ueno, H., Sahni, M. K., Segal, S. J., and Koide, S. S. (1988). Interaction of gossypol with sperm macromolecules and enzymes. *Contraception*. **37**, 333-341.

Vadehra, D. V., Kalla, N. R., Saxena, M., Hashia, R., Kaur, P., and Gupta, L. K. (1985). Antimicrobial activity of gossypol acetic acid. *IRCS Med. Sci.* **13**, 10-11.

Vander Jagt, D. L., Deck, L. M., and Royer, R. E. (2000). Gossypol: prototype of inhibitors targeted to dinucleotide folds. *Curr. Med. Chem*. **7**, 479-498.

Varol, U., Karaca, B., Tunali, D., Degirmenci, M., Cirak, Y., Purcu, D. U., Uzunoglu, S., Sezgin, C., Karabulut, B., Sanli, U. A. and Uslu, R. (2009). The effect of racemic gossypol and at-101 on angiogenic profile of ovcar-3 cells: a preliminary molecular framework for gossypol enantiomers. *Exp. Oncol.* **31**, 220–225.

Waites, G. H., Wang, C., and Griffin, P. D. (1998). Gossypol: reasons for its failure to be accepted as a safe, reversible male antifertility drug. *Int. J. Andro*. **21**, 8-12.

Wang, X., Beckham, T., Morris, J., Chen, F., and Gangemi, D. (2008) Bioactivities of gossypol, 6-methoxy gossypol and 6, 6'-dimethoxy gossypol. *J. Agric. Food Chem.* **56**, 4393-4398.

Wang, Y. C., and Rao, P. N. (1984). Effect of gossypol on DNA synthesis and cell cycle progression of mammalian cells *in vitro*. *Cancer. Res.* **44**, 35-38.

WHO. (2001). World Health Organization. African trypanosomiasis or sleeping sickness. *259 World Health Organ Fact Sheet.* (http://www.who.int/mediacentre/factsheets/fs259/en/).

WHO. (2004). World Health Organization. The world health report 2004: changing history Geneva.

Xu, L. Y., Wang, S., Tang, W., Liu, M., Davis, M., Chen, J., Rae, J. M., Lawrence, T., and Lippman, M. E. (2005). (-)-Gossypol enhances response to radiation therapy and results in tumor regression of human prostate cancer. *Mol. Cancer Ther*. **4**, 197-205.

Zhang, M., Liu, H., Guo, R., Ling, Y., Wu, X., Li, B., Roller, P. P., Wang, S., and Yang, D. (2003). Molecular mechanism of gossypol-induced cell growth

inhibition and cell death of HT-29 human colon carcinoma cells. *Biochem. Pharmacol.* **66**, 93-103.

Zhang, M., Liu, H., Tian, Z., Huang, J., Remo, M., and Li, Q. Q. (2007). Differential growth inhibition and induction of apoptosis by gossypol between HCT116 and HCT116/Bax (-/-) colorectal cancer cells. *Clin. Exp. Pharmacol. Physiol.* **34**, 230-237.

Zhang, W. J., Xu, Z. R., Sun, J. Y., and Yang, X. (2006a). Effect of selected fungi on the reduction of gossypol levels and nutritional value during solid substrate fermentation of cottonseed meal. *J. Zhejiang. Univ. Sci. B*. **7**, 690-695.

Zhang, W. J., Xu, Z. R., Zhao, S. H., Jiang, J. F., Wang, Y. B., and Yan, X. H. (2006b). Optimization of process parameters for reduction of gossypol levels in cottonseed meal by Candida tropicalis ZD-3 during solid substrate fermentation. *Toxicon*. **48**, 221-226.

CHAPTER 2

CHEMICAL CHARACTERIZATION AND BIOACTIVITIES OF GOSSYPOL

AND ITS METHYLATED ETHERS

2.1 Abstract

Tetramethyl and hexamethyl ethers of gossypol were synthesized from gossypol that was extracted from cotton plant. The gossypol ethers were fully characterized by NMR, MS, and HPLC methods. Particularly, existence of four tautomers of gossypol tetramethyl ethers were chromatographically separated and confirmed by the combination of NMR and LC/MS. Antioxidant activity in terms of DPPH free radical scavenging capability of gossypol and its methyl ethers were compared. Gossypol exhibited the strongest antioxidant activity, while its ethers only remained partial antioxidant activity due to their conjugated naphthalene structure preserved in the derivatives. In addition, alpha-amylase inhibitory activities of gossypol and its methylated ethers were determined. The result showed that the gossypol's methylated ethers were the alpha-amylase inhibitors, while gossypol was the alpha-amylase activator. Furthermore, it was found that anticancer activity of the gossypol and its methylated ethers against MCF-7 cancer cells depended on the degree of methylation level of gossypol.

2.2 Introduction

Gossypol is a polyphenolic aldehyde isolated from the members of various *Gossypium* species, which is a natural toxin present in the cotton plant that protects it

from insect damage (Smith et al., 1972). Gossypol exists as two atropisomers due to the restricted rotation of its binaphthyl bond (**Figure 2.1**). As we mentioned in Chapter 1, the initial research interest on gossypol derived from the (-)-gossypol isomer that is active in male sterility discovered in in 1970s when it was found to be able to affect the maturation and motility of sperm, and inactivate the enzymes required for the sperm to fertilize the ova (Anonymous, 1978; Anonymous, 1980). In addition, a number of potential biological activities of gossypol, such as antiviral (Radloff et al., 1986; Lin et al., 1993), antiamoebic (Gonzalez-Garza et al., 1991), and antiprotozoan effects (Blanco, et al., 1983; Gerez de Burgos, et al., 1984; Montamat et al., 1982), were reported. While gossypol displays a certain degree of toxicity due to its aldehyde groups which can easily bind nucleophilic targets of biological importance (Clark et al., 1927; DePeyster et al., 1993; Gallup et al., 1931), various gossypol derivatives such as apogossypol (Clark et al., 1928; Meltzer et al., 1985; Zhu et al., 1992), gossypolone (Haas et al., 1965), gossypol ethers (Adams and Geissman, 1938; Adams et al., 1938; Datta et al., 1972; Haar et al., 1952; Morris et al., 1937; Seshadri et al., 1973; Seshadri et al., 1975) and gossypol Schiff base (Dao et al., 2000; Liang et al., 1995; Kim et al., 1987; Przybylski et al., 2003; Zheng et al., 1992), which have been prepared since 1930s, have not been studied thoroughly for their bioactivities. This prompted us to synthesize some of these gossypol derivatives, and explore their novel bioactivities.

In this study, we synthesized, separated and fully characterized gossypol tetramethyl ethers, hexamethyl ether and their tautomers. In addition, their DPPH free radical scavenging activities, alpha-amalyse inhibitory activities and anticancer activities were determined.
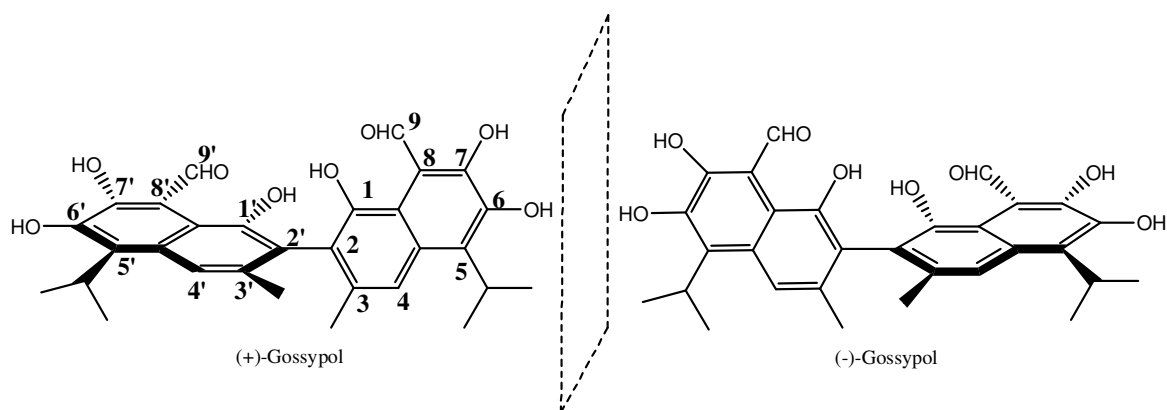
Figure 2.1 Two Atropisomers of gossypol

2.3 Experimental

2.3.1 Material

Structures of gossypol and all of its tested derivatives are shown in **Figure 2.2**.

2′-Bi [8-formyl-1, 6, 7-trihydroxy-5-isopropyl-3-methylnaphthalene]) acetic acid (**1**, gossypol acetic acid, MW=578.6, $C_{30}H_{30}O_8 \bullet C_2H_4O_2$, HPLC purity >95%, racemic form) was purchased from Zhejiang Yixin Pharmaceutical Co., Ltd. P. R. China. 6-Methoxygossypol (**5**) and 6, 6′-dimethoxygossytpol (**6**) (see **Figure 2.2**) were isolated as previously reported (Kim et al., 1987). Racemic gossypol and possible derivatives were biologically tested. 1, 1-diphenyl-2-picrylhydrazyl (DPPH free radicals), butylated hydroxytoluene (BHT), 3, 5-dinitrosalicylic acid (98%) (DNSA), alpha-amylase (type VI-B: from porcine pancreas), dimethyl sulfoxide (DMSO), potassium carbonate (K_2CO_3), and phosphoric acid (H_3PO_4) were purchased from Sigma Chemical Co., (St. Louis, MO). Starch from potatoes (($C_6H_{10}O_5)_n$, Mr=162.14_n) was purchased from Fluka, Germany. Potassium sodium tartrate ($KNaC_4H_4O_6 \bullet 4H_2O$,

Figure 2.2 Structures of gossypol and its ethers *4a=A: lactol form, B: lactol form, R$_1$=CH$_3$, R$_2$=H; 4b= A: aldehyde form, B:lactol form, R$_1$=CH$_3$,R$_2$=H; 4c= A: aldehyde form, B: aldehyde form, R$_1$=CH$_3$,R$_2$=H; 4d= A: lactol form, B:lactol form, R$_1$=H, R$_2$=CH$_3$;

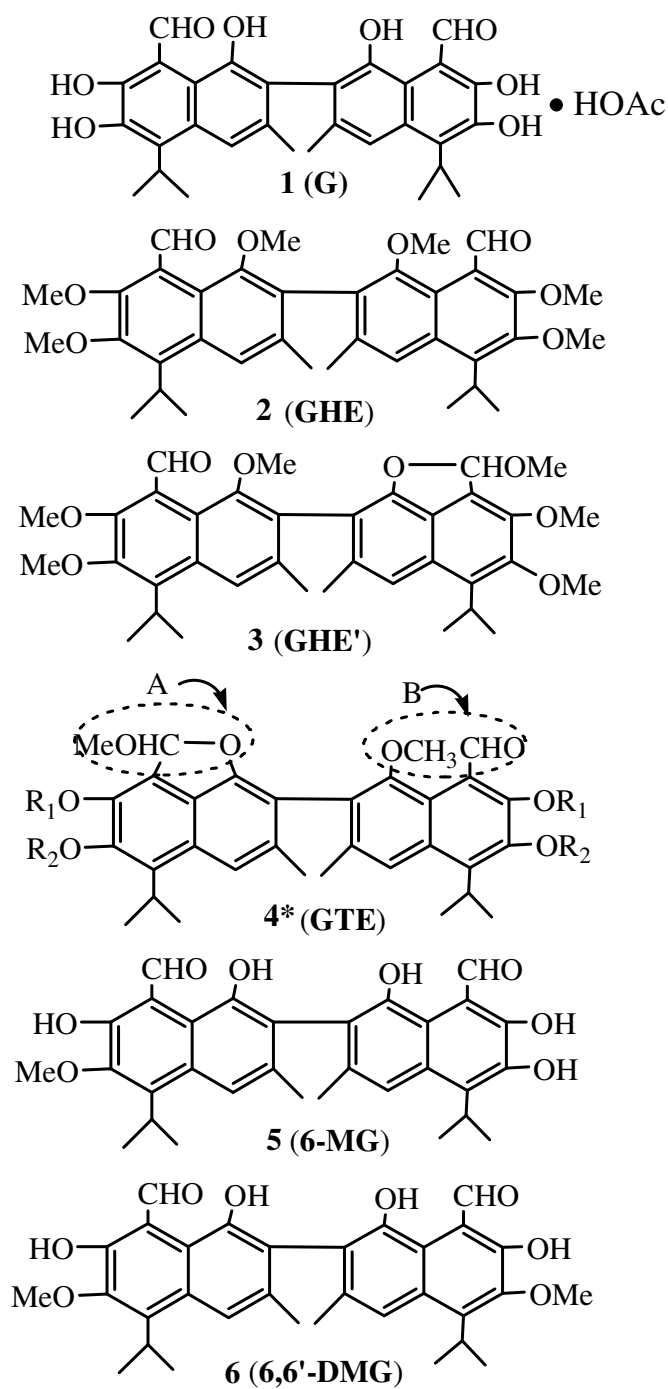FW=282.231), and sodium hydroxide were purchased from J. T. Baker Chemical Co. (Phillipsburg, N.J. USA). Sodium phosphate (Na_2HPO_4, FW=141.96) and sodium chloride were purchased from Fisher Scientific Company (Fair lawn, N.J. USA). Iodomethane (CH_3I 99.5% pure, 2.2789 g cm^{-3} at 20°C, molar mass 141.94 g mol^{-1}), and dimethyl sulfate (($CH_3O)_2SO_2$, d=1.33 g ml^{-1}, molar mass 126.13 g mol^{-1}) were from Alfa Aesar company (Ward Hill, MA, USA). All solvents for chromatographic isolation were of analytical grade. HPLC grade methanol, dichloromethane, acetone, acetonitrile, and chloroform were purchased from Fisher Scientific Company (Fair lawn, N.J. USA). Tissue culture plates were purchased from Costar Corp. (Cambridge, MA). Heat-inactivated fetal bovine serum, fetal bovine serum, and newborn calf serum were purchased from Hyclone Laboratories, Inc. (Logan, UT). MCF-7 (human breast cancer) cancer cell lines were purchased from the American Type Culture Collection (ATCC) (Rockville, MD).

2.3.2 Instruments for Chemical Analysis

 HPLC analysis was carried out on a Shimadzu HPLC system that included LC-20AT solvent delivery pumps, a CBM-20A communication bus module, a SPD-M20A photo-diode array detector, and the ClassVP operating software. The HPLC was equipped with a Kromasil RP C18 column (particle size of 5µm, column size of 150 mm×4.6 mm, Alltech Associates, Inc. Deerfield, IL), which was placed in a column oven (CTO-20A) under a constant temperature at 25°C. The mobile phase consisted of methanol: H_2O = 87:13 (v/v) containing 0.1% aqueous H_3PO_4. The column flow rate was set at 1 ml min^{-1}, while the HPLC pressure was controlled between 1020-1040 psi.

LC/MS analysis was performed on an Agilent 6100 series LC/MS in which a quadruple mass spectrometer was coupled to an Agilent 1200 HPLC that consisted of a G1329A high performance autosampler (hp-ALS-SL), a G1312A binary pump (BIN-SL), a G1379B vacuum degasser, a G1316A thermostatted column compartment (TCC-SL) and a G1314B variable wavelength detector (VWD-SL). The quadrupole mass spectrometer was operated with an atmospheric pressure electrospray ionization (API-ES) source in positive mode. The flow rate of HPLC was maintained at 1 mL min^{-1} through a Kromasil RP C18 column (particle size of 5 µm, column size of 150 mm×4.6 mm, Alltech Associates, Inc. Deerfield, IL). The mobile phase in an isocratic elution consisted of methanol and water (v/v=87:13) containing 0.1% formic acid. Mass spectra were recorded within the *m/z* range of 100-1000. The dry gas flow for MS was 13.0 L min^{-1}, the nebulizer pressure was 30 psig, dry gas temperature was 350℃, and the Vcap voltage was 3500 V. Data was acquired from and processed by the Agilent LC/MSD ChemStation software.

Some mass spectrum were obtained by a nanoflow capillary HPLC coupled with a quadrupole time-of-flight micro mass spectrometer (Q-TOF-MS) (Waters Corp., Milford, MS) with an electrospray ionization (ESI) in both ESI-MS and ESI-MS-MS modes operated by the Masslynx software (V4.0, Waters Corp., Milford, MS). Each separated and purified sample was directly injected from the sample vial into the ESI source in methanol at a flow rate of 1.5 µL min^{-1}. The ion source voltages were set at ±3000V for positive and negative ion mode acquisitions, respectively. In both modes, the source temperature was maintained at 100℃ and the mass spectrum was scanned from 100 to 800 *m/z* at 1 second with 0.1-second inter-scan delay in continuum mode. For MS/MS analysis, mass spectrum was scanned from 50-800 *m/z.*

Glu-fibrinopeptide (Sigma) as a mass standard in ESI-MS and ESI-MS-MS mode was infused through the nanoLockspray (Waters Corp., Milford, MS) for single point, real time, and accurate mass calibration. Raw spectra were processed using the MassLynx software (V4.0). Precursor ion scans on positive and negative ion modes using low energy collision induced dissociation (CID) resulted in more structural fragments, which helped structural identification of compounds of interest.

1D and 2D NMR (^{1}H NMR, ^{13}C NMR, DEPT, HMQC, HMBC) spectra were acquired from a Bruker AV-500 spectrometer or JEOL operated at 300 MHz for ^{1}H NMR and 75 MHz for ^{13}C NMR. Data were processed by the Bruker XWINNMR 3.50 programs.

In addition, thin layer chromatography (TLC) analysis was performed on F_{254} plates precoated with silica gel 60 and fluorescent reagent (Merck, Darmstadt, Germany). The TLC was visualized at 254 nm in a UV-viewing system purchased from Fisher Biotech. Silica gel (300 meshes), which was purchased from QingDao Haiyang Chemical Co., Ltd. P. R. China, was used for column chromatography.

The *in vitro* DPPH free radical scavenging assay and the alpha-amylase enzymatic assay were measured by the Thermo Scientific Genesys 20 visible spectrophotometer.

2.4 Chemical Syntheses and Structural Characterization

2.4.1 Chemical Syntheses

A sample of gossypol acetic acid (500 mg, 0.97 mmol), potassium carbonate (1 g, 7 mmol) and dimethyl sulfate (1.5 g, 12 mmol) in acetone (10 mL) was refluxed for 48 hours according to the Adams' method with minor modification (**Figure 2.3**)
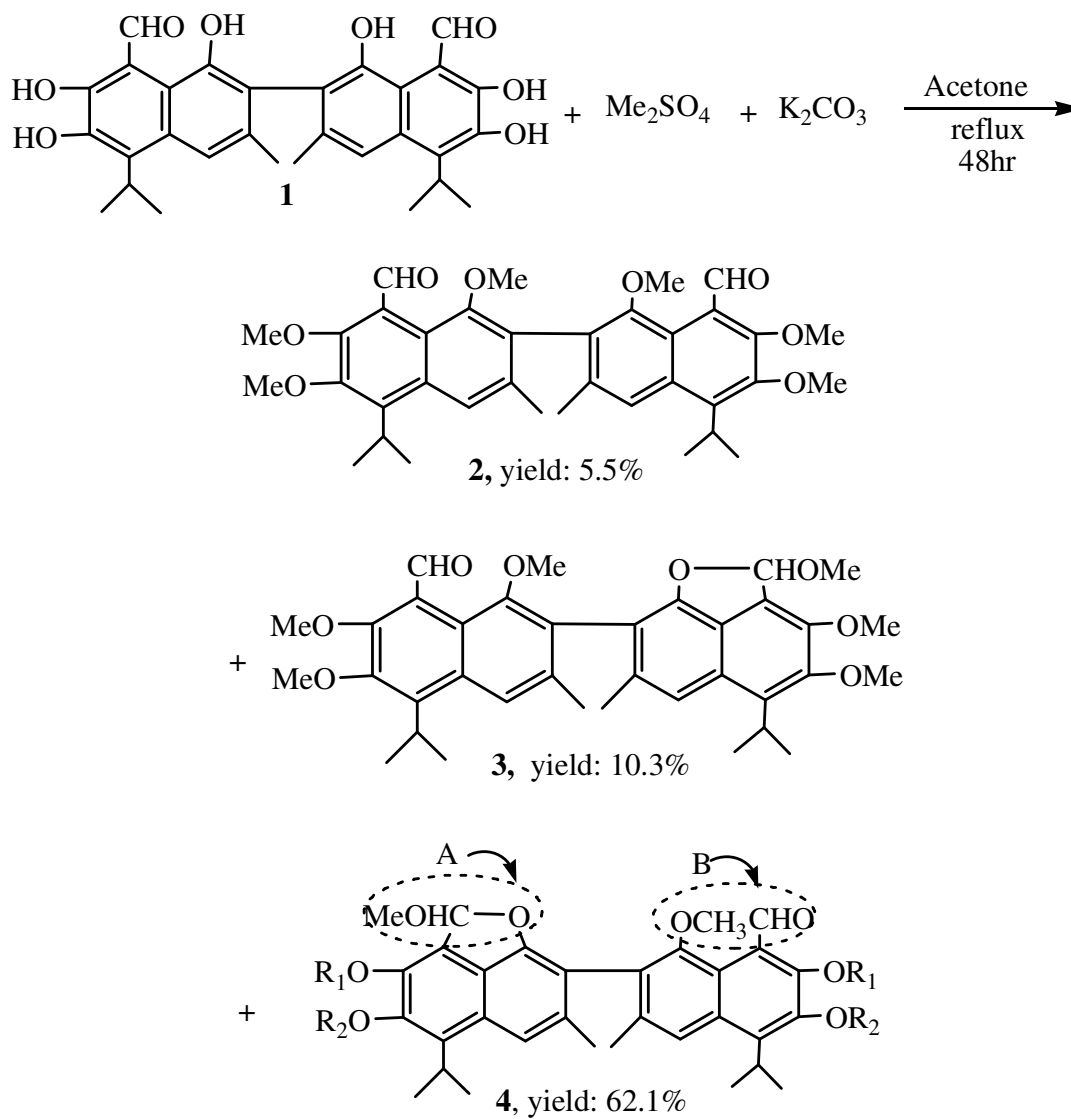
Figure 2.3 Methylation of gossypol with dimethyl sulfate

(Morris et al. 1937). Then acetone was removed under vacuum. The residue was

reconstituted into a solution by adding 15 mL of water before it was heated for 0.5 h

to thoroughly hydrolyze the excess dimethyl sulfate. After the mixture was cooled down to room temperature, ethyl ether (50 mL × 3) was added to extract the gossypol's methylated products that were separated and purified by preparative TLC eluted with chloroform and methanol (150:1, v/v) to afford compounds **2**, **3** and **4**, with 5.5%, 10.3%, 62.1% yield, respectively.

To obtain the compound **2** in a higher yield, the Haar's method (Haar et al., 1952) was applied with a minor modification. A solution of 500 mg of gossypol acetic acid (0.97 mmol), 10 ml of anhydrous acetone, 1 g of potassium carbonate (7 mmol, excess) and 1.4 g of methyl iodide (9.7 mmol) were mixed and refluxed gently for 48 hrs (**Figure 2.4**). Then the volatile solvent was removed by rotary evaporation. The residue was purified with flash chromatography (silica gel, 300 – 400 meshes, $CHCl_3$/MeOH = 150/1, vol) to give compounds **2, 3** and **4** with yield of 43%, 9.1%, 7.4%, respectively.

2.4.2 Spectral data of gossypol derivatives

(The carbon position numbering of gossypol refers to **Figure 2.2**)

Gossypol hexamethyl ether in dialdehyde form (GHE, compound **2**)

^{1}H-NMR (300 M Hz, in $CDCl_3$) δ *(ppm)*: 10.65 (2H, s, two protons of –CHO) 7.90 (2H, s, two sp[2] protons of naphthol ring), 3.98 (6H, s, protons of two methoxyl group at position 7 and 7′), 3.94 (6H, s, protons of two methoxyl group at position 6 and 6′), 3.96 (2H, m, protons attached to tertiary carbon in two isopropyl groups), 3.25 (6H, s,

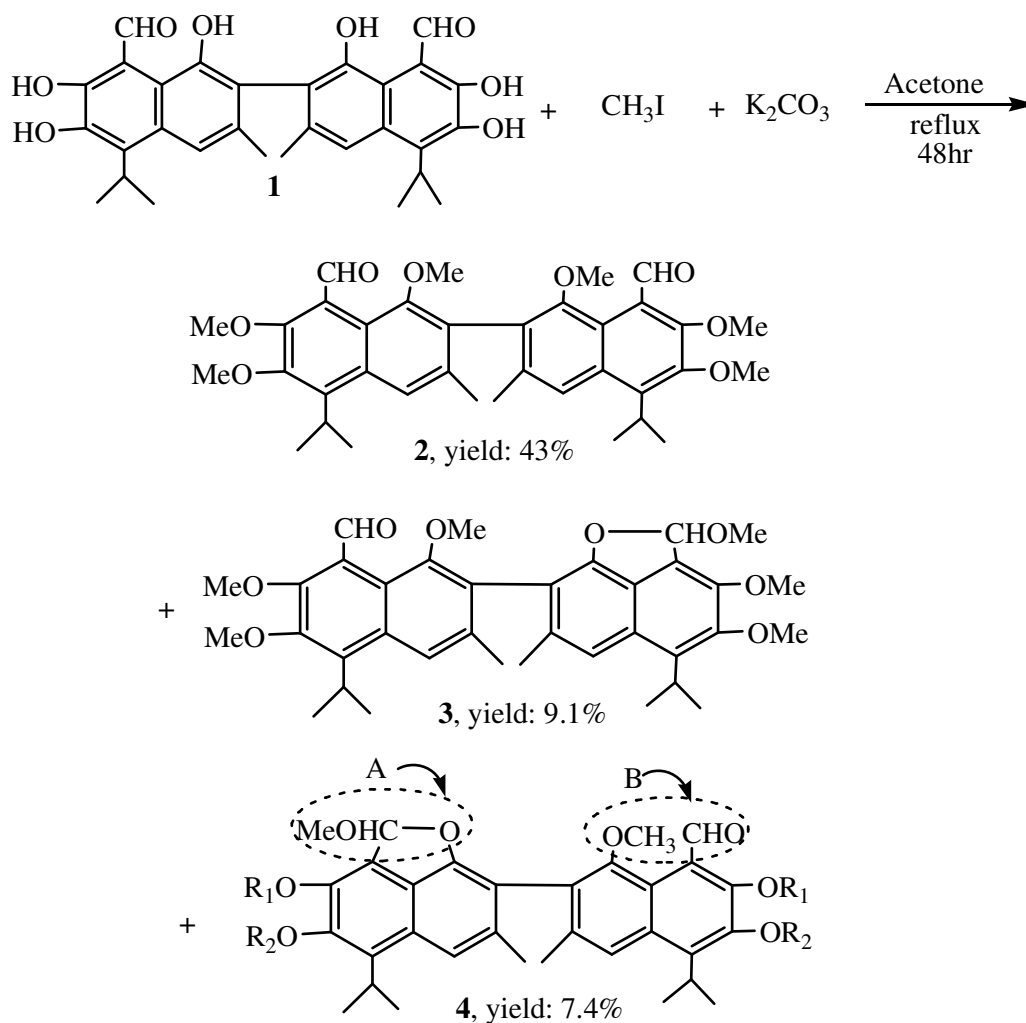**Figure 2.4** Methylation of gossypol with methyl iodine

protons of two methoxyl group at position 1 and 1′), 2.22 (6H, s, protons of methyl group at position 3 and 3′), 1.57 (12H, m, protons of four methyl groups in the isopropyl groups); ^{13}C NMR (125 MHz, in CDCl$_3$) δ *(ppm)*: 21.10, 22.18, 59.62, 61.10, 62.19, 122.81, 126.06, 127.85, 131.01, 135.29, 137.72, 149.60, 152.98, 193.19;

UV-Vis: $\lambda_{max/nm}$: 255, 294, 420; HRESI-MS *m/z*: 603.2816 [M+H]$^+$, (Calcd for C$_{36}$H$_{42}$O$_8$, 602.2880); HPLC: T$_R$=18.55 min;

Gossypol hexamethyl ether in monoaldehyde-monolactol form (GHE′, compound **3**)

^{1}H-NMR (300 M Hz, in CDCl$_3$) δ *(ppm)*: 10.60 (1H, s, the proton of –CHO) 7.91 (1H, s, the sp^2 proton of naphthol ring at position 4), 7.50 (1H, s, the sp^2 proton of naphthol ring at position 4′), 7.20 (1H, s, the proton at position 9′), 4.21(3H, s, protons of methoxyl group attached to 9′ carbon), 3.96 (6H, s, protons of two methoxyl group at 7 and 7′), 3.91(6H, s, protons of two methoxyl group at 6 and 6′), 3.05 (3H, d, protons of two methoxyl group at 1), 2.24 (6H, s, protons of methyl group in 3 and 3′), 1.56 (12H, m, protons of four methoxyl group in isopropyl groups); ^{13}C NMR (125 M Hz, in CDCl$_3$) δ:20.96, 21.00, 22.08, 27.17, 29.71, 58.39, 58.43, 60.43, 60.47, 62.18, 103.04, 112.11, 115.59, 117.98, 122.55, 127.48, 130.89, 136.00, 136.29, 137.38, 137.75, 147.73, 149.37, 150.09, 153.92, 192.91; HRESI-MS *m/z*: 603.2948 [M+H]$^+$, (Calcd for C$_{36}$H$_{42}$O$_8$, 602.2880);

Gossypol tetramethyl ethers (compound **4**)

^{1}H-NMR (300 M Hz, in CDCl$_3$) δ *(ppm)*: 10.60, 7.93, 7.92, 7.50, 7.09 , 6.98, 6.95, 4.16, 4.14, 3.98, 3.91, 3.54, 3.28, 2.35, 2.23, 1.58; Retention time for **4a-d** in LC-MS were 17.056, 18.825, 14.631, 13.635min (see Figure 2.5) with area percentage of 39.31%, 35.38%, 19.64% and 5.67%, respectively. HRESI-MS of **4a-d** showed *m/z*: 573.2595 [M+H]$^+$, (Calcd for C$_{34}$H$_{38}$O$_8$, 574.2880);

2.5 DPPH antioxidant assay

The DPPH free radical scavenging activity was determined by the modified method (Yamaguchi et al., 1998). Solution of each sample (i.e., G stands for gossypol acetic acid **1**, GHE for gossypol hexamethyl ether in dialdehyde form **2**, GHE′ for gossypol hexamethyl ether in monoaldehyde and monolactol form **3**, GTE for gossypol tetramethyl ether **4**, and BHT for butylated hydroxytoluene) dissolved in dichloromethane were prepared for 0 - 200 ppm. An aliquot of 0.5 mL of the solution was mixed with 0.4 mL of 0.25 mM solution of DPPH in dichloromethane. The solution was sealed and shaken vigorously and then incubated in the dark at room temperature for 15 min. Absorbance at 517 nm was measured. The DPPH antioxidant activity was calculated as scavenging activity (%) = (1-absorbanceof sample at 517 nm/ absorbance of control at 517 nm) ×100% (Dowd et al., 2006).

2.6 Alpha-amylase inhibition assay

The DNSA regent (Wang et al., 2008) was prepared as a mixture of 1 g of 3, 5-dinitrosalicylic acid, 20 mL of NaOH (2 M), 50 mL of H_2O and 30 g of potassium sodium tartrate. After ultra sonication, certain amount of water was added to make the mixture in total volume to 100 mL.

The alpha-amylase inhibitory activity was determined using the type VI-B porcine pancreatic alpha-amylase. An aliquot of DMSO (100 µL, containing sample with certain concentration) was added into starch solution (500 µL, 1%). The mixture were incubated at 45^oC for 10 min immediately after adding alpha-amylase solution (400 µL, 50 µg mL^{-1} in 0.02 mol L^{-1} sodium phosphate buffer, pH=6.9 with 6 mmol L^{-1} NaCl), incubation was timed accurately. After incubation, the reaction was terminated by adding 2 mL of DNSA regent. Then, the test tubes were incubated at 90^oC in water

bath for 10 min accurately. At the end of this period, the test tubes were cooled down in tap water and diluted by addition of 22 mL of distilled water. Absorbance was measured at 540 nm by the Genesys 20 visible spectrophotometer. Each absorbance subtracted the absorbance measured under the exact same condition without the amylase (same volume, same temperature, same time intervals, same ratio of starch solution, etc.). The control absorbance was measured for that of the mixture without sample at the same condition. In addition, the control should also subtract the absorbance without the amylase and sample.

Standard curve was prepared by maltose. In brief, 1 mg mL^{-1} of stock solution of maltose was diluted into final concentrations of 8-80 µg mL^{-1}. Each test tube was added by 2 mL of DNSA regent and 2 mL of maltose solution (final concentration is 8-80 µg mL^{-1}). After incubation at 90°C in water bath for 10 min, the mixtures were cooled down in tap water and diluted with 21 mL of distilled water. The absorbance was measured at 540 nm. The enzymatic regression equation was determined as Y= 0.0044X-0.0367 and R^2 = 0.9985, where Y stands for the absorbance at 540 nm, and X stands for maltose concentration (µg mL^{-1}). Alpha-amylase activity was reflected by resultant reducing sugar content during the reaction within certain time interval.

2.7 Anticancer assay

The MCF-7 cancer cells were cultured in RPMI with 10% fetal bovine serum respectively. The cell line was incubated at 5% CO_2 and 90-100% relative humidity at 37°C. Medium renewal was carried out 2-3 times per week, and cells were subcultured when they achieved 80-90% confluence. Prior to chemical treatment, 10^4 cells well^{-1} were seeded into a 96-well tissue culture plate and were allowed to attach

for 24 h. The cells were then treated with a defined concentration of the test compound dissolved in DMSO, which was limited to a 1% concentration in each well. As negative controls, cells were treated with DMSO only. After a 24-hour's incubation, cell proliferation was determined with the CellTiter 96 aqueous nonradioactivity cell proliferation assay (Promega, Madison, WI). Results were recorded on a universal EL800 Bio-Tek microplate reader at 490 nm.

2.8 Results and discussion

Gossypol methylated ethers were prepared by using iodomethane and dimethyl sulfate to produce selective gossypol ether tautomers in desired yields. In case of mono-lactol and mono–aldehyde forms such as compounds **2** and **4b**, the chemical shift of the proton in lactol ring moved from 10.6 ppm to 7.09 ppm, and the tertiary protons in benzene ring (position 4 and 4′) displayed two unequivalent signals around 7.5 and 7.9 ppm. In addition, the protons of methoxyl groups in position 1 and 1′ showed up around 3.4 ppm if they were in the aldehyde form, while the protons of methoxyl groups in position 9 and 9′ had a downfield movement to around 4.1 ppm in the lactol form. Moreover, the chemical shifts of the protons in the methyl groups at 6 and 6′, and 7 and 7′ pairs were found to have an upfield movement (or the nucleus
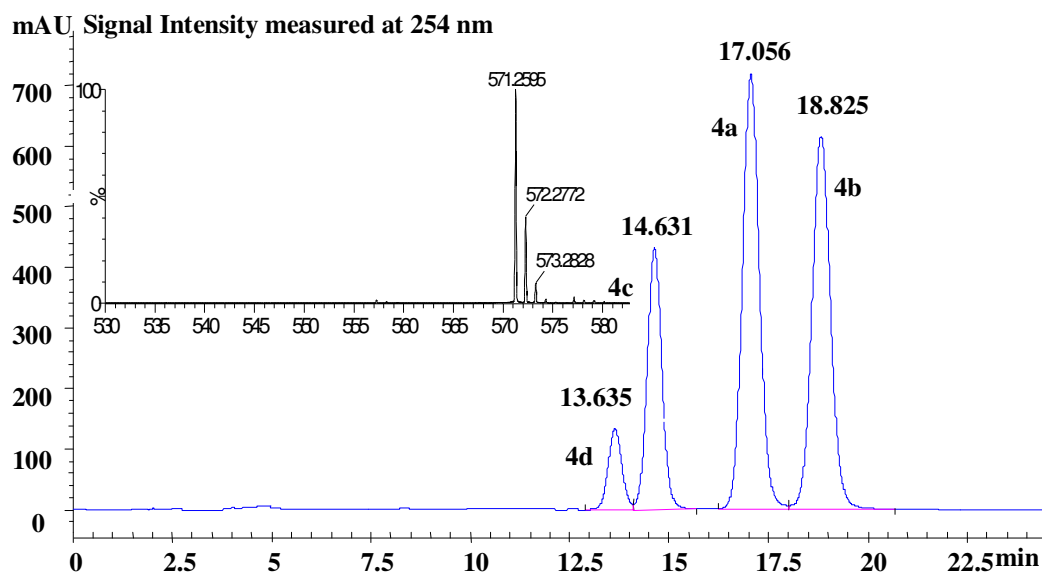
Figure 2.5 The LC/MS chromatogram of compounds **4a-d**

were more shielded) from 3.94 ppm and 3.98 ppm in the dialdehyde form (compound **2**) to 3.91ppm and 3.96 ppm in the monoaldehyde and monolactol form (compound **3**), respectively. The retention time of compounds **4a-d** (**Figure 2.5**) was 17.056, 18.825, 14.631, 13.635 min respectively in the LC/MS chromatogram. The concentration ratio of **4a**:**4b**:**4c**:**4d** is 39.31: 35.38: 19.64: 5.67, which are exactly consistent with the integration ratio of protons in the aldehyde groups and lactol groups from ^{1}H NMR spectra.

The DPPH free radical scavenging activity was used to evaluate the antioxidant activities of gossypol and its ethers in different degree of methylation. Antioxidant properties, especially radical scavenging activities, are very important due to the deleterious role of free radicals in biological systems. Our results provide interesting

42

insights into the antioxidants of gossypol and its derivatives, and shed more light onto
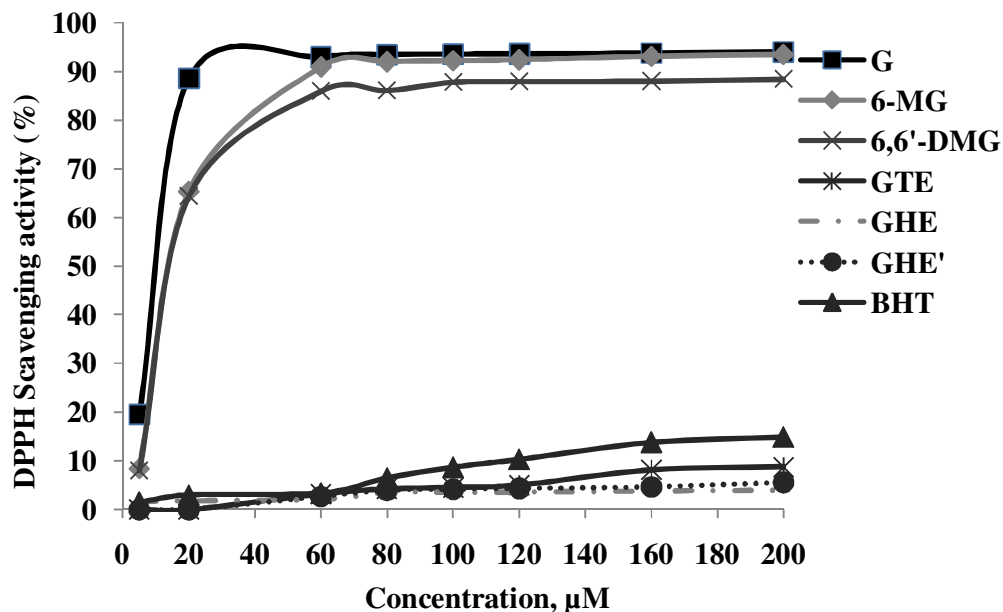

Figure 2.6 The DPPH free radical scavenging activities of G, 6-MG,
6, 6'-DMG, GTE, GHE, GHE′ and BHT. (The numbering refers to
Figure 2.2)

their mechanisms as free radical scavengers. As shown in **Figure 2.6**, gossypol possesses a significantly high antioxidant activity with its DPPH free radical scavenging capacity over 80% within the concentration range of 20-200 ppm, of which the IC_{50} value for gossypol was 9.2 ppm. Our previous research demonstrated that the IC_{50} values for the 6-methoxygossypol (compound **5**), and 6, 6′-dimethoxy-gossypol (compound **6**) to scavenge the DPPH free radicals in the same experimental system were 16.4 and 16.8 ppm, respectively, which were relatively higher than that of gossypol. In this study, it was further confirmed that more methylation of gossypol resulted in remarkably lower DPPH free radical scavenging activities below 20% within the concentration range of 0-200 ppm, although the

43

gossypol ethers still remained parts of antioxidant activity comparable to that of BHT. Based on our experiments and study on this structure-activity relationship, it seems the overall tendency of the functional modification of gossypol follows the rule of that more hydroxyl group in gossypol is replaced by methyl group, the lower free radical scavenging activity of the derivatives will have.

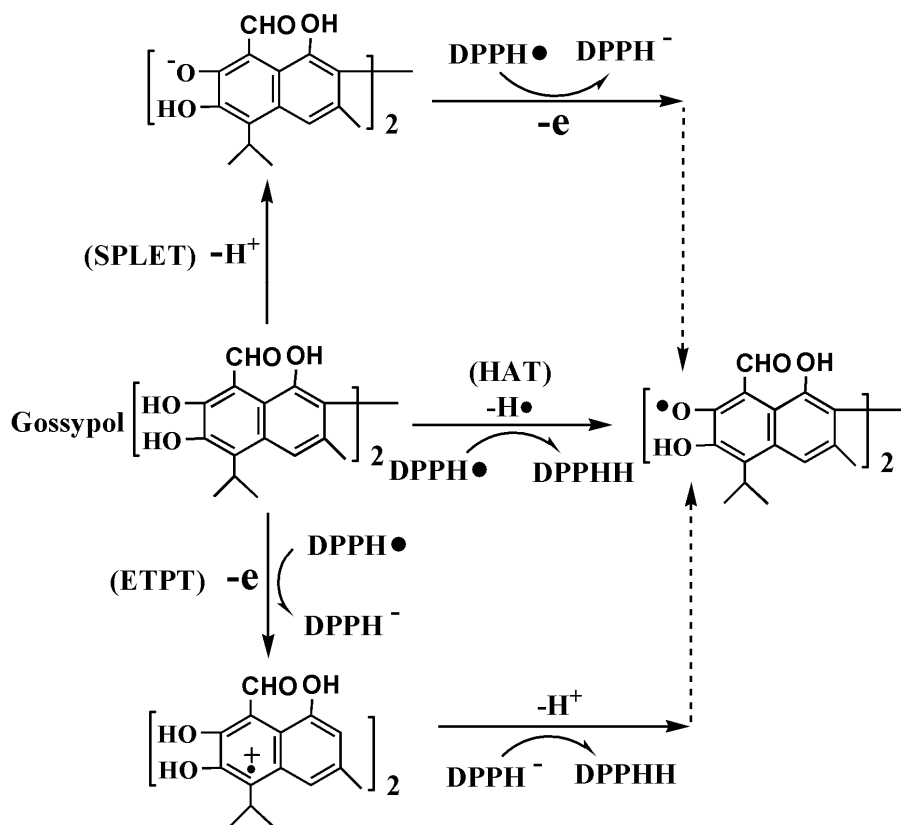Besides, three possible antioxidant mechanisms of gossypol are shown in the **Figure 2.7**.

Figure 2.7 Three possible antioxidant mechanisms of gossypol

Antioxidant polyphenols have been recognized that they are able to neutralize radicals by three pathways, e.g., donating hydrogen atom through one-step H-atom transfer (HAT), stepwise electron transfer proton transfer (ETPT) and sequential proton loss electron transfer (SPLET)) (Zhang et al., 2006). These antioxidant pathways also fit for the antioxidant gossypol and some of its derivatives. Yet, the antioxidant capacity of gossypol derivatives also depends on their modified molecular structures.

It is clear from this investigation that the numbers and positions of hydroxyl groups and other functional groups are important for the antioxidant and free radical scavenging activities of gossypol and its derivatives. After the hydroxyl groups in gossypol were partially and/or completely methylated, the H-atom donating capability significantly decreased although partial free radical scavenging activity of the methylated gossypol derivatives was preserved. This demonstrated that the conjugated binaphthalene ring of the backbone of gossypol could also stabilize some free radicals through the ETPT mechanism, although other aforementioned pathways might coordinate and play the critical role for the free radical scavenging activity.

The alpha-amylase inhibitory activities of gossypol as well as their di/tetra/hex methyl ethers were also examined (**Figure 2.8**). It was found that gossypol hexamethyl ether (GHE), gossypol tetramethyl ether (GTE), 6-methoxygossypol (6-MG), and 6, 6′-dimethoxygossypol (6, 6′-DMG) all displayed enzymatic inhibitory ability at lower levels compared to acarbose, which is a well-known inhibitor of α-glucosidases, α-amylases, cyclomaltodextrin glucanyltransferase (CGTase) and dextransucrase and used as an anti-diabetic drug (Morris et al., 1937). However, in

our surprise, it was found that gossypol activated rather than inhibited the enzyme. It is postulated that the alpha-amylase have several tertiary structural forms in solution that are in dynamic equilibrium with each other. The additives that give maximum
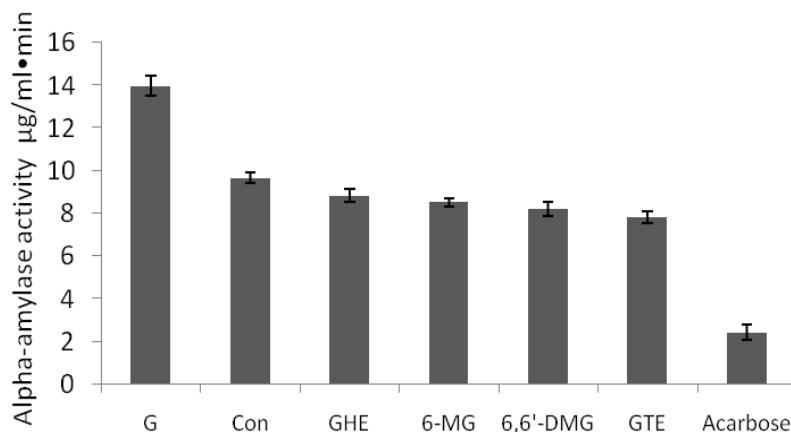

Figure 2.8 Alpha-amylase activity treating with G, GTE, GHE,
6-MG, 6, 6'-DMG and Acarbose at 8mM concentration

activation bind to the protein-enzymes to give a single, optimum structure that is fixed and gives the maximum activity with activation. Our study attempts to give a hint for further understanding of the fundamental issues behind the enzyme activation and inhibition.

Furthermore, gossypol exhibited dose-dependent growth inhibition against the breast cancer cell line MCF-7. Although the low-leveled methylated gossypol ethers such as 6- methoxygossypol and 6, 6′- dimethoxygossypol have been demonstrated to possess higher anticancer activity than gossypol to some extent (Wang et al., 2008), the highly methylated gossypol ethers like compounds **2-4** (e.g., GTE, GHE, and

GHE′) exhibited a remarkably weak or no anticancer activity against each cell line in our experiment (**Figure 2.9**). We postulated that partial methylation of gossypol could increase the lipophilic affinity of 6-MG and 6, 6′-DMG with cancer cells resulting in
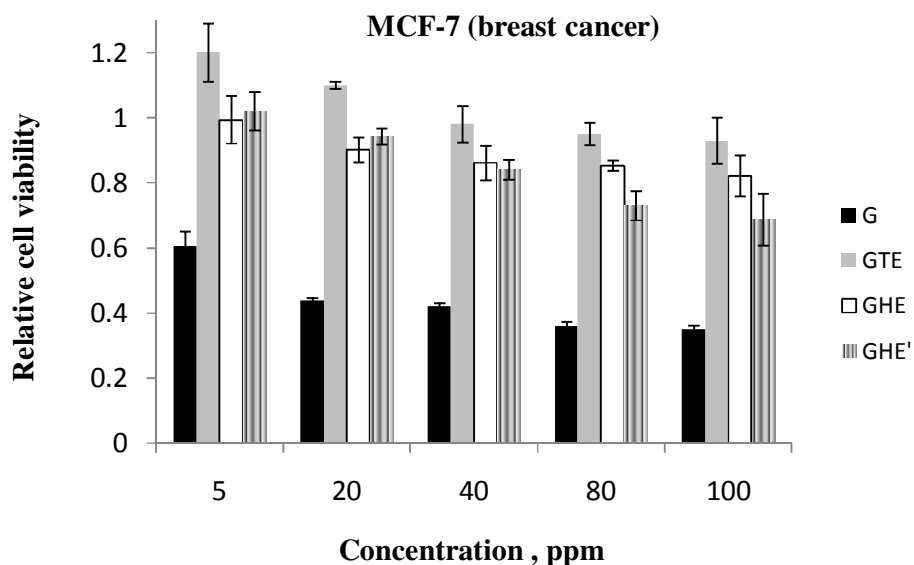

Figure 2.9 Growth inhibition of breast cancer MCF-7 incubated with G, GTE, GHE and GHE′. Error bars represent standard deviations of three experiments.

higher toxicity against those cells, but higher methylation of hydrpoxyl groups could, on the contrary, decrease and/or deprive the gossypol's original strong activity that relied on the hydroxyl and aldehydic groups. This unexpected finding needs further investigation regarding the functionalities of the aldehyde and hydroxyl groups on gossypol.

2.9 Conclusion

In this experiment, the tetra/hexmethyl ethers of gossypol were synthesized by two modified methods using iodomethane and dimethyl sulfate. The gossypol ether was successfully separated and fully characterized by NMR, MS, and HPLC. Four

gossypol tetramethyl ether tautomers were also determined by LC/MS. In addition, their free radical scavenging activity and inhibitory alpha-amylase activities were measured. Gossypol possesses a high antioxidant activity, and also is a good alpha-amylase activator, while gossypol hexamethyl ether (GHE), gossypol tetramethyl ether (GTE), methoxygossypol (6-MG), and 6, 6′-dimethoxygossypol (6, 6′-DMG) all exhibited their inhibitory tcapability against the alpha-amylase. In addition, gossypol ethers showed very weak or no anticancer activities, which were correlated with the methylation level. Nevertheless, our results demonstrated that gossypol and its derivatives possess many biological activities, and have potential to be developed as drugs for some chronic diseases.

2.10 References

Adams, R., and Geissman, T. A. (1938).   Structure of gossypol. VII. gossypol dimethyl ether. *J. Am. Soc. Chem.* **60**, 2163-2166.

Adams, R., Geissman, T. A., and Morris, R. C. (1938). Structure of gossypol.XVI. reduction of gossypolone tetramethyl ether and gossypolonic acid tetramethyl ether. *J. Am. Soc. Chem.* **60**, 2967-2970.

Anonymous. (1978). Gossypol, a new antifertility agent for males. *Chinese. Med. J.* **4**, 417-428.

Anonymous. (1980). Gossypol as an oral contraceptive for men. *J. Med. Soc. N. J.* **77**, 5.

Blanco, A., Aoki, A., Montamat, E. E., and Rovai, L. E. (1983). Effect of gossypol upon motility and ultrastructure of *Trypanosoma cruzi*. *J. Protozool.* **30**, 648–651.

Clark, E. P. (1927). Studies on gossypol. I. The preparation, purification and some of the properties of gossypol, the toxic principle of cottonseed. *J. Biol. Chem.* **75**, 725-739.

Clark, E. P. (1928). Studies on gossypol. IV. apogossypol. *J. Biol. Chem.* **78**, 159–166.

Dao, V. T., Gaspard, C., Mayer, M., Werner, G. H., Nguen, S. N., and Michelot, R. J. (2000). *Eur J. Med. Chem.* **35**, 805-813.

Datta, S. C., Murti, V. V. S., and Seshadri, T. R. (1972). Isolation & study of (+)-gossypol from the spesia populnea. *Indian. J. Chem.* **10**, 263-266.

DePeyster, A., and Wang, Y. Y. (1993). Genetic toxicity studies of gossypol. *Mutation Research, Reviews in Genetic Toxicology.* **297**, 293-312.

Dowd, M. K., and Pelitire, S. M. (2006). Isolation of 6-methoxy gossypol and 6, 6′-dimethoxy gossypol from *gossypium barbadense* seaisland cotton. *J. Agric. Food. Chem.* **54**, 3265–3270.

Gallup, W. D. (1931a). Studies on the toxicity of gossypol. I. The response of rats to gossypol administration during avitaminosis. *J. Biol. Chem.* **93**, 381-405.

Gallup, W. D., and Reder, R. (1931b). Studies on the toxicity of gossypol. II. The effect of gossypol upon the apparent digestibility of protein, fat and carbohydrate and upon the absorption of glucose from the gastrointestinal tract of the rat. *J. Biol. Chem.* **94**, 221-232.

Gerez de Burgos, N. M., Burgos, C., Montamat, E. E., Rovai, L. E., and Blanco, A.

(1984). Inhibition by gossypol of oxidoreductases from *Trypanosoma cruzi. Biochem. Pharmacol.* **33**, 955-959.

Gindler, M. E. (1976). Determination of amylase. *United States Patent 3953297*, Pierce Chemical Company (Rockford, IL).

Gonzalez-Garza, T., Matlin, S. A., Mata-Cardenas, B. D., and Said-Fernandez, S. (1991). *In vitro* evaluation of gossypol as potential antiamoebic drug. *Proc. West. Pharmacol. Soc.* **34**, 359-361.

Haar, P. V. D., and Pominski, C. H. (1952). Pigments of cottonseed. V. methylation of gossypururin. *J. Org. Chem.* **17**, 177–180.

Haas, R. H., and Shirley, D. A. (1965). The oxidation of gossypol. 11. formation of gossypolone with ferric chloride. *J. Org. Chem.* **30**, 4111-4113.

Kenar, J. A. (2006). Reaction chemistry of gossypol and its derivatives. *J. Am. Oil Chem. Soc.* **83**, 269-302.

Kim, I., Mercelle, G. B., Waller, D. D., Cordell, G. A., and Fong, H. H. S. (1987). *Contraception.* **35**, 289-310.

Liang, X. S., Rogers, A. J., Webber, C., Ormsby, T. J., Tiritan, M. E., Mathieu, S. A. and Benz, C. C. (1995). *Interest. New. Drugs.* **13**, 181-185.

Lin, T. S., Schinazi, R. F., Zhu, J., Birks, E., Carbone, R., Si, Y., Wu, K., Huang, L., and Prusoff, W. H. (1993). Anti-HIV-1 activity and cellular pharmacology of various analogs of gossypol. *Biochem. Pharmacol.* **46**, 251–255.

Meltzer, P. C., Bickford, P. H., and Lambert, G. A. (1985). Regioselective route to gossypol analogues: the synthesis of gossypol and 5, 5'-didesisopropyl-5, 5'-diethylgossypol. *J. Org. Chem.* **50**, 3121-3124.

Montamat, E. E., Burgos, C., Gerez de Burgos, N. M., Rovai, L. E., Blanco, A., and Segura, E. L. (1982). Inhibitory action of gossypol on enzymes and growth of *Trypanosoma cruzi. Science.* **218**, 288-289.

Morris, R. C., and Adams, R. (1937). The structure of gossypol. III. gossypol ethers. *J. Am. Soc. Chem.* **59**, 1731-1735.

Przybylski, P., Wojciechowski, G., Schilf, W., Brzezinski, B., and Bartl, F. (2003). *J. Mol. Struct.* **646**, 2003-2010.

Radloff, R. J., Deck, L. M., Royer, R. E., and Vander, D. L. (1986). Antiviral activities of gossypol and its derivatives against herpes simplex virus type II. *Pharmacol. Res. Commun.* **18**, 1063-1073.

Seshadri, T. R., and Sharma, N. N. (1973). Isolation of the hexamethyl ether of the monolactol-monoaldehyde form of (+) gossypol. *Curr. Sci.* **42**, 821-822.

Seshadri, T. R., and Sharma, N. N. (1975). Further study of the three forms of (+)-gossypol hexamethyl ether. *Indian. J. Chem.* **13**, 866-868.

Smith, F. H., (1972). Effect of gossypol bound to cottonseed protein on growth of weanling rats. *J. Agric. Food. Chem.* **20**, 803-804.

Wang, X., Beckham, T. H., Morris, J. C., Chen, F., and Gangemi, J. D. (2008). Bioactivities of gossypol, 6-methoxygossypol, and 6, 6′-dimethoxygossypol. *J. Agric. Food. Chem.* **56**, 4393–4398.

Yamaguchi, T., Takamura, H., Matoba, T., and Terao, J. (1998). HPLC method for evaluation of the free radical-scavenging activity of foods by using 1, 1-diphenyl-2-picrylhydrazyl. *Biosci. Biotechnol. Biochem.* **62**, 1201–1204.

Zhang, H. Y., and Ji, H. F. (2006). How vitamin E scavenging DPPH radicals in polar protic media. *New. J. Chem.* **30**, 503-504.

Zheng, B., Brett, S., Tite, J. P., Brodie, T. A., and Phodes, J. (1992). *Science.* **256**, 1560-1563.

Zhu, G. D., Chen, D. H., Huang, J. H., and Chi, C. S. (1992). Regioselective bromination and fluorination of apogossypol hexamethyl ether. *J. Org. Chem.* **57**, 2316-2320.
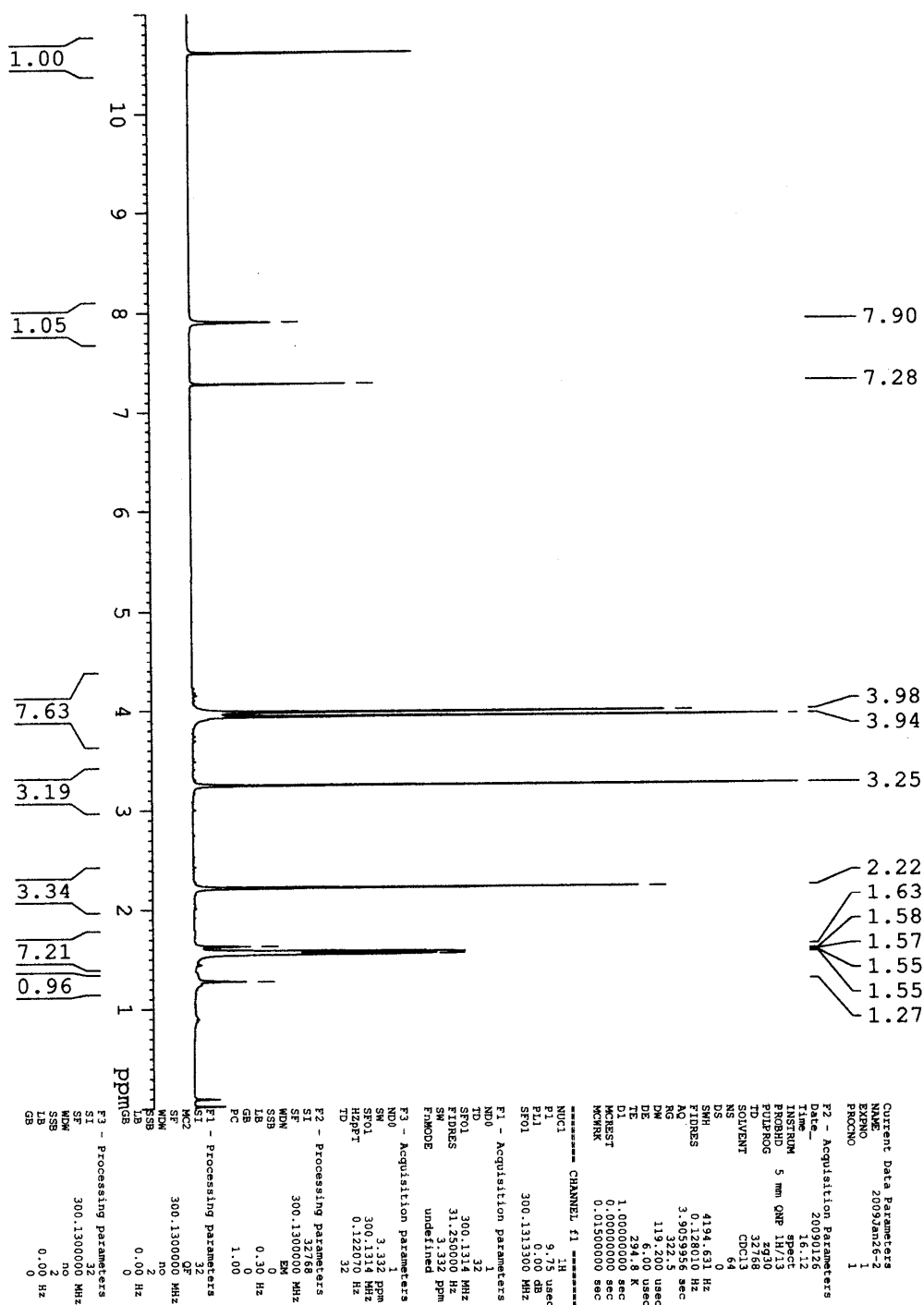
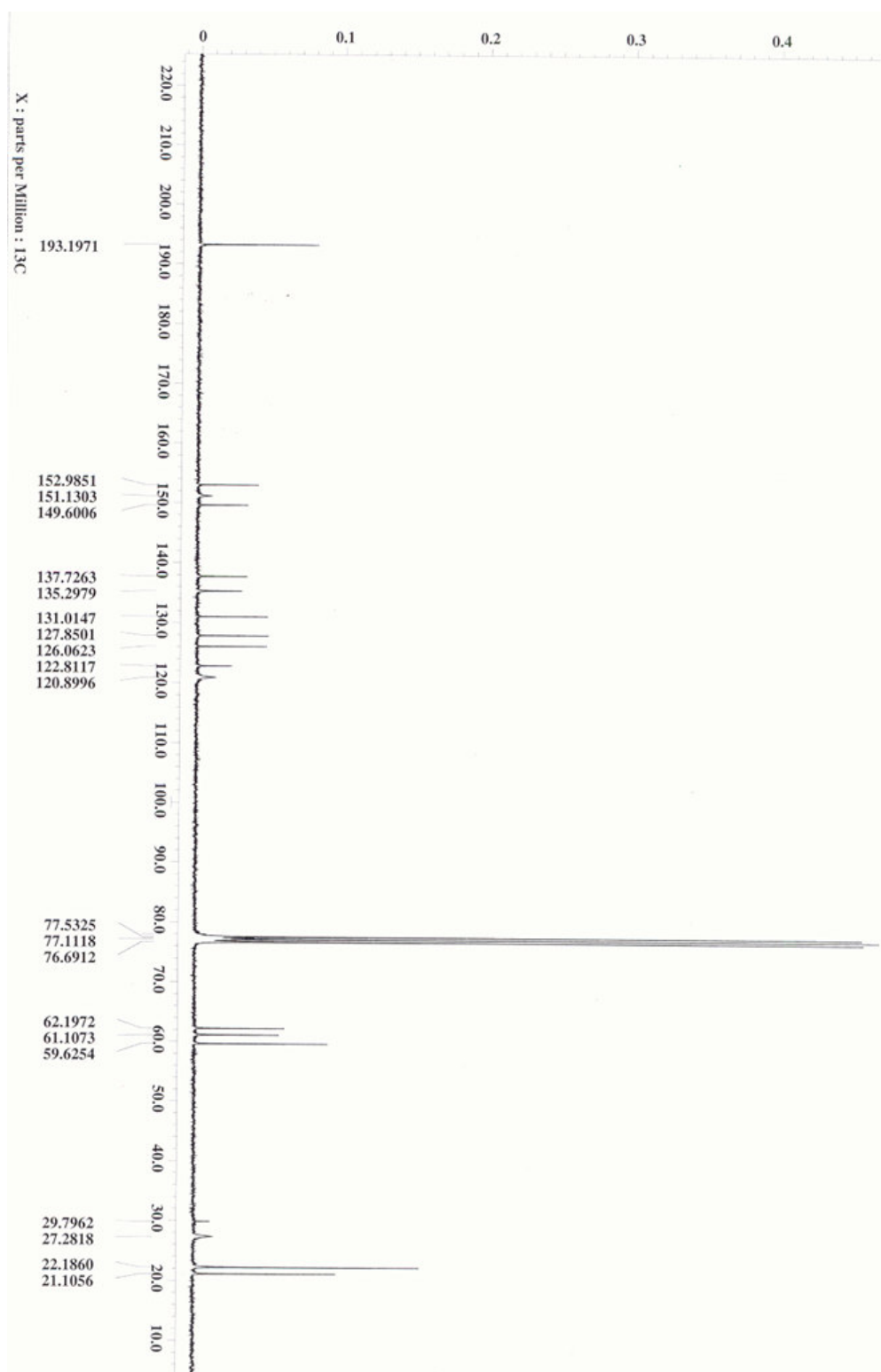**Figure A2.1** The ^{1}HNMR spectra of **2** (300MHz, CDCl$_3$)

Figure A2.2 The ^{13}CNMR spectra of **2** (300MHz, CDCl$_3$)

X : parts per Million : 13C

193.1971

152.9851
151.1303
149.6006

137.7263
135.2979

131.0147
127.8501
126.0623
122.8117
120.8996

77.5325
77.1118
76.6912

62.1972
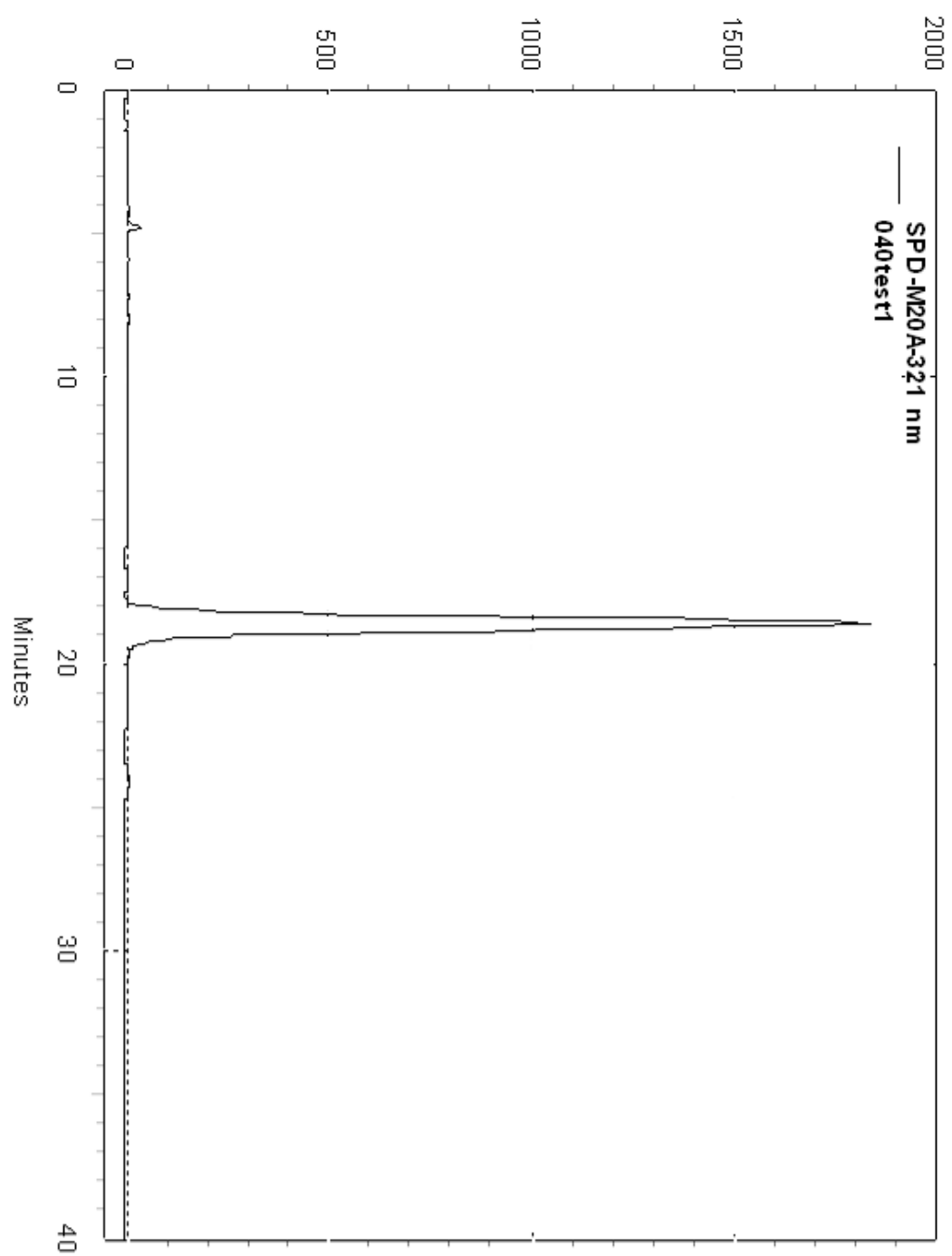61.1073
59.6254

29.7962
27.2818

22.1860
21.1056

53

Figure A2.3 The chromatogram HPLC of **2**

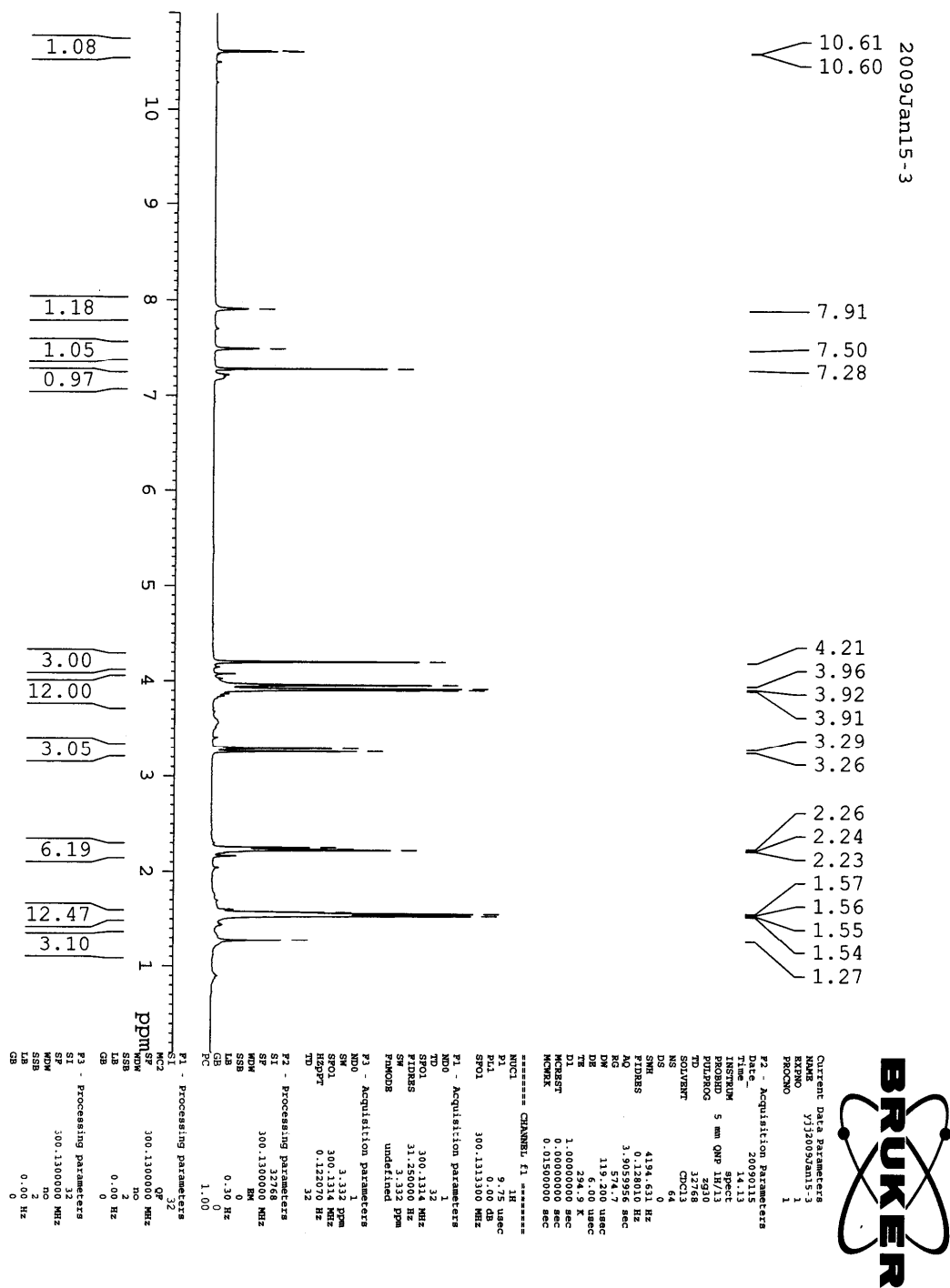**Figure A2.4** The ^{1}HNMR spectra of **3** (300MHz, CDCl$_3$)

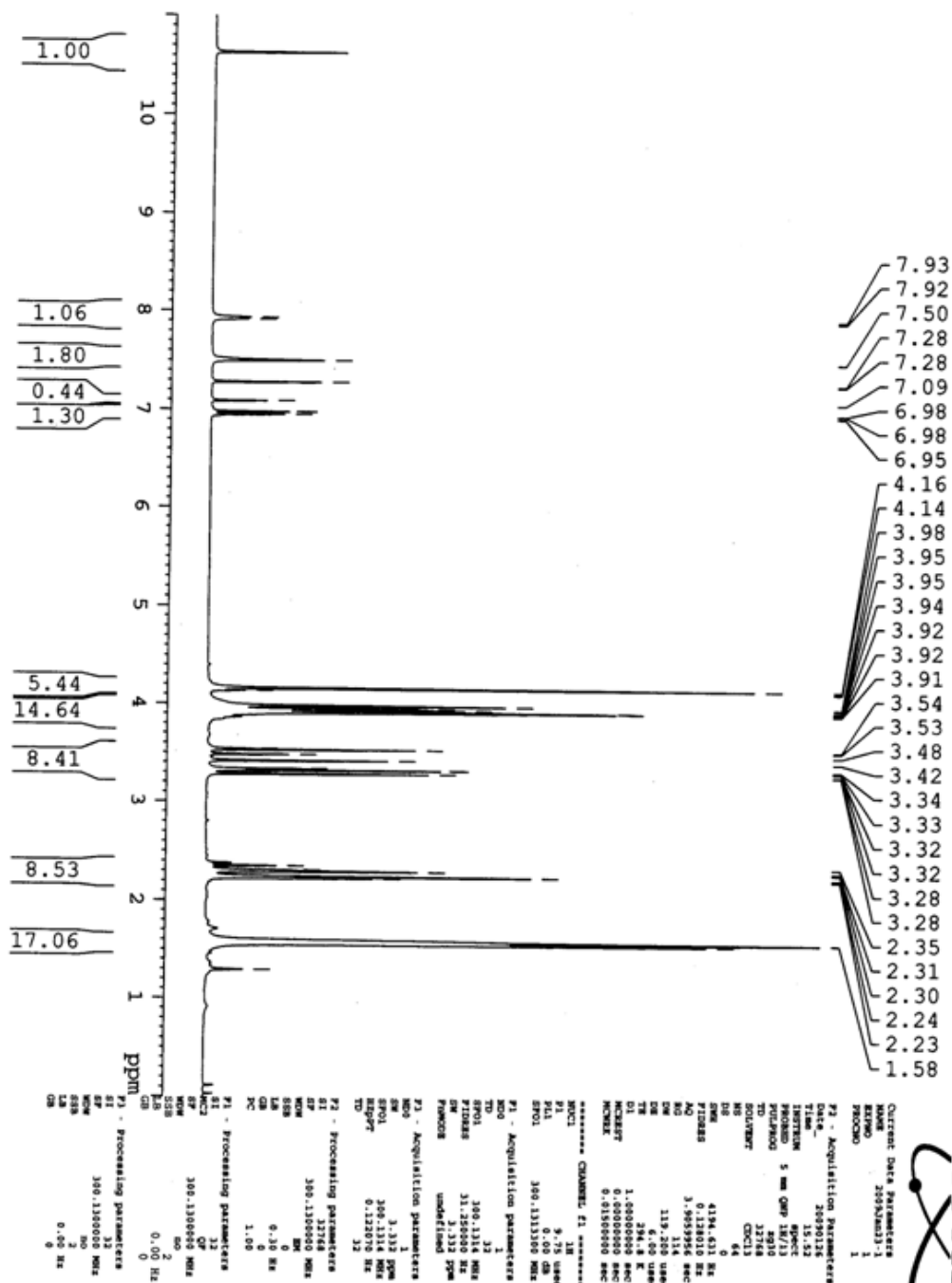**Figure A2.5** The ^{13}CNMR spectra of **3** (300MHz, CDCl$_3$)

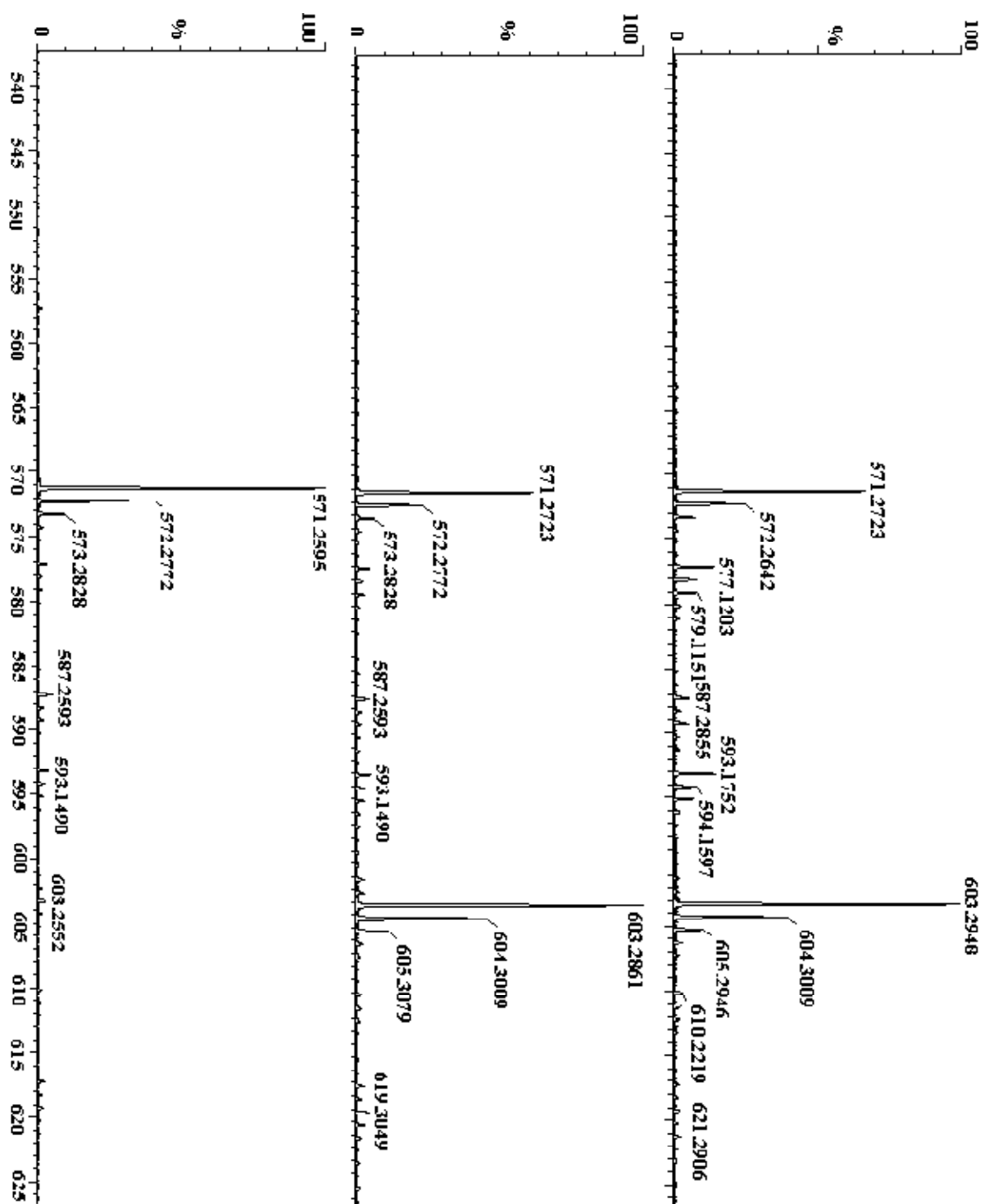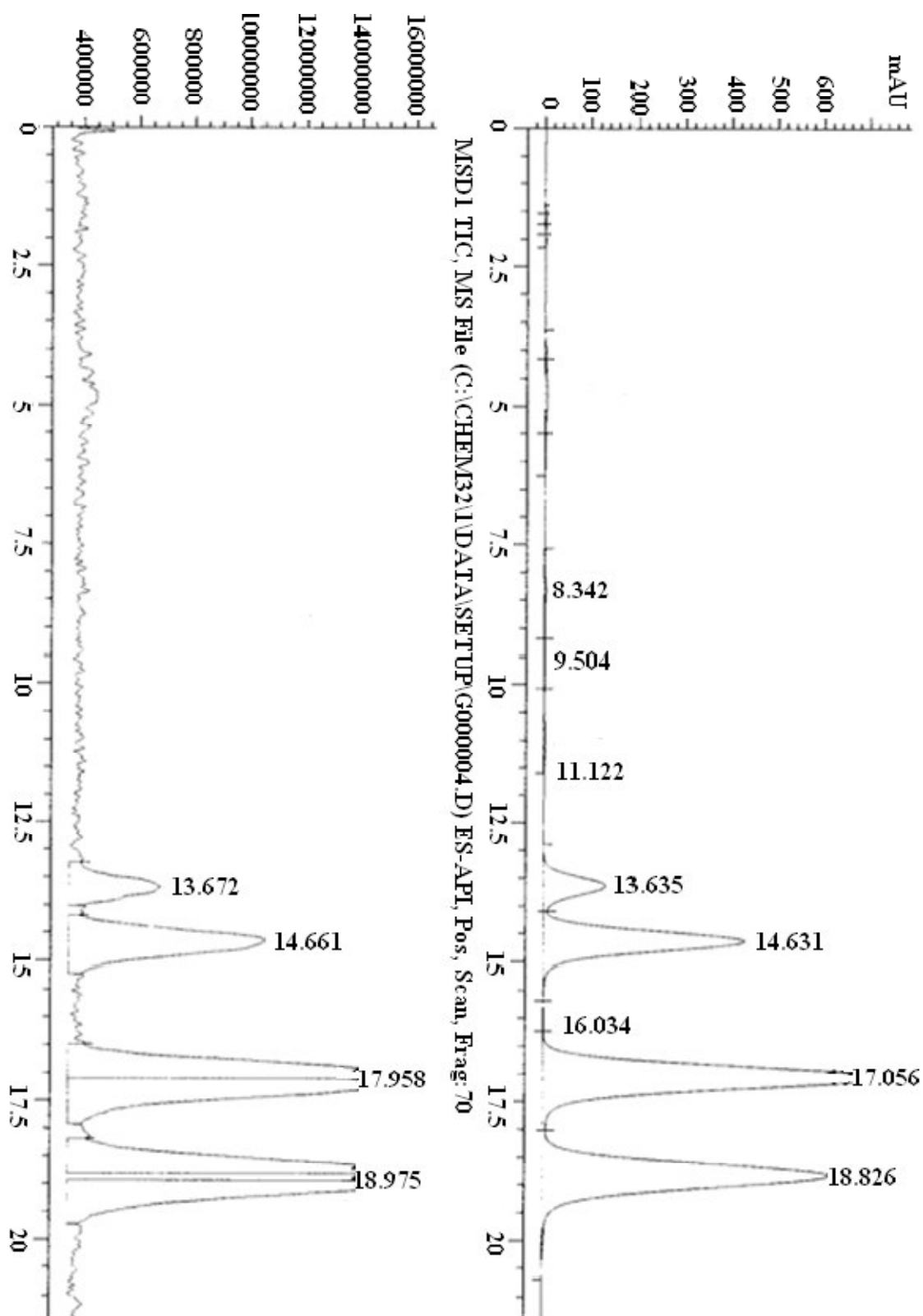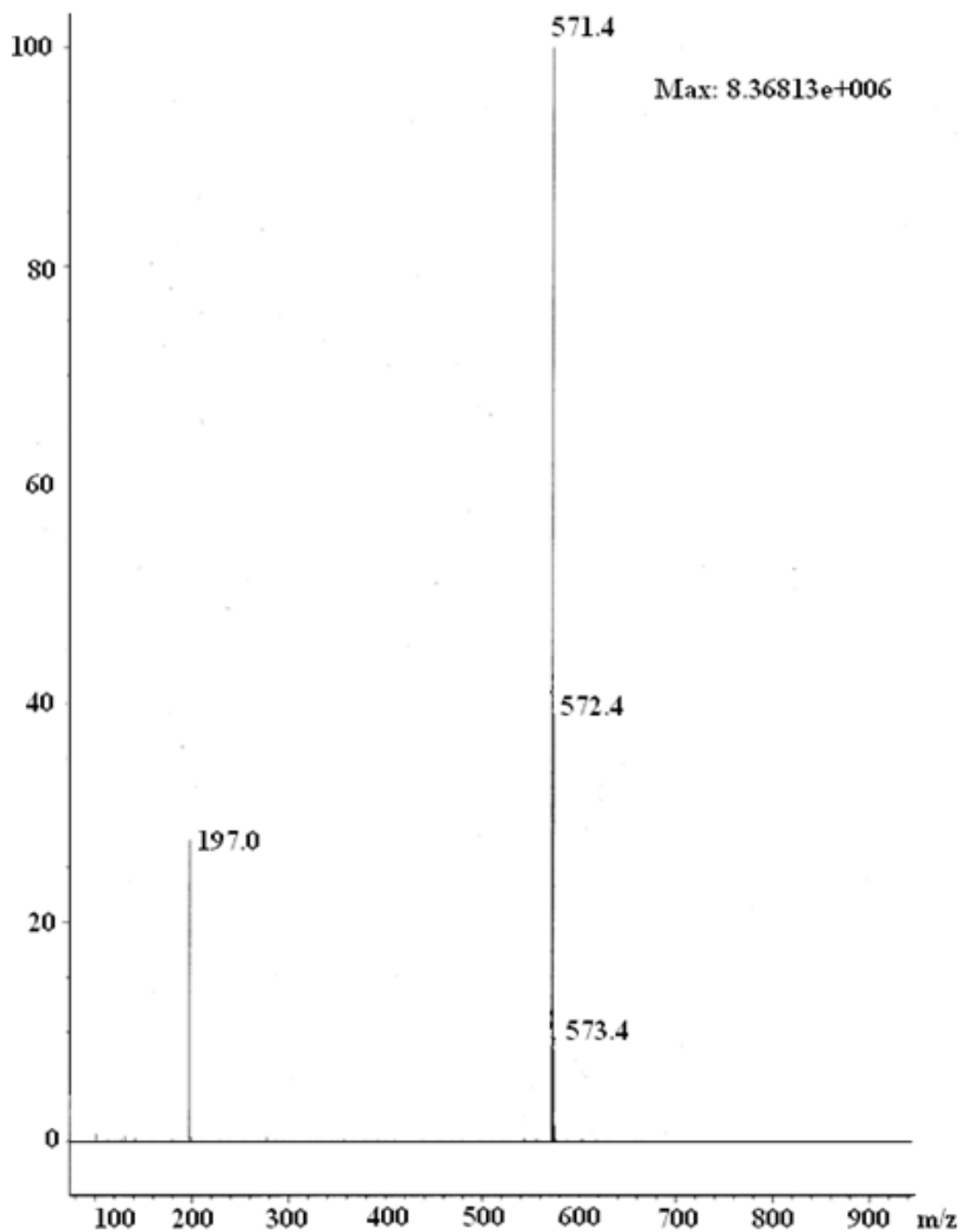**Figure A2.6** The ^{1}HNMR spectra of **4** (300MHz, CDCl$_3$)

Figure A2.7 The ESI-MS spectra of **3**, **2**, **4** (form the top to the end respectively)

(Figure A2.8-1)

*MSD1 SPC, time=19.022 of C:\CHEM32\1\DATA\SETUP\
MS Spectrum G000004.D ES-API, Pos, Scan, Frag 70

(Figure A2.8-2)

*MSD1 SPC, time=17.109 of C:\CHEM32\1\DATA\SETUP\ G000004.D ES-API, Pos, Scan, Frag 70

MS Spectrum

Max:8.3881e+006
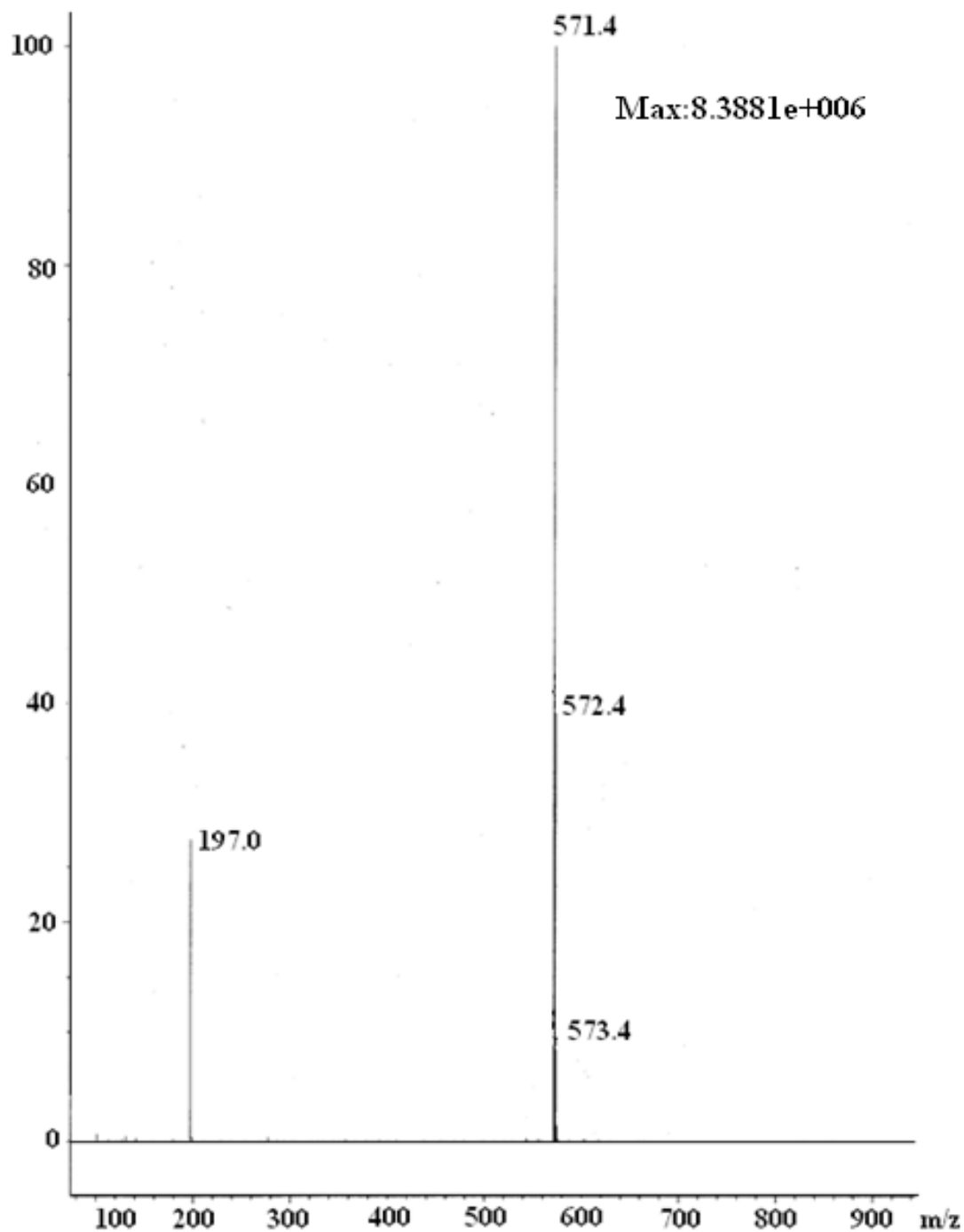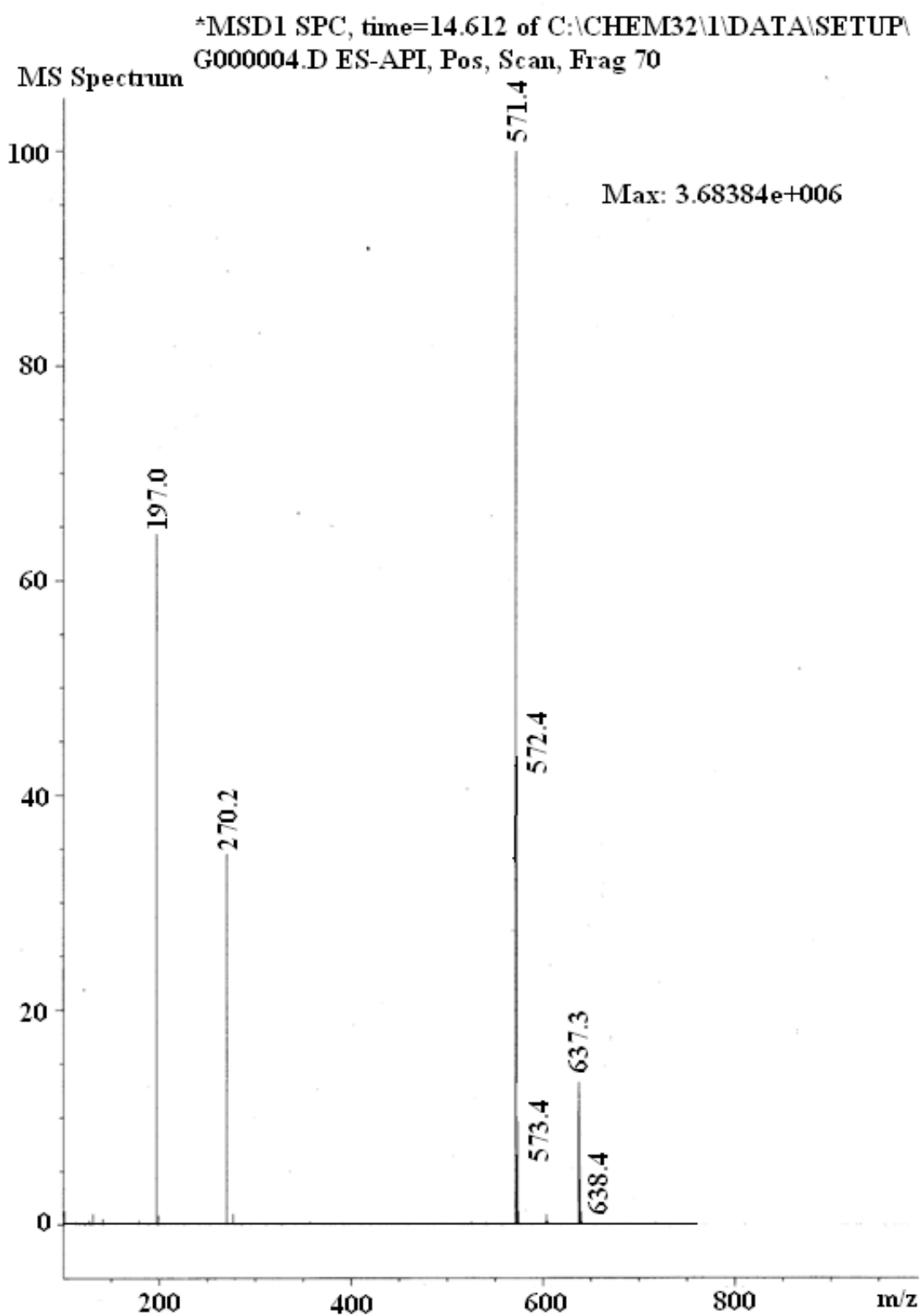
(Figure A2.8-3)

(Figure A2.8-4)
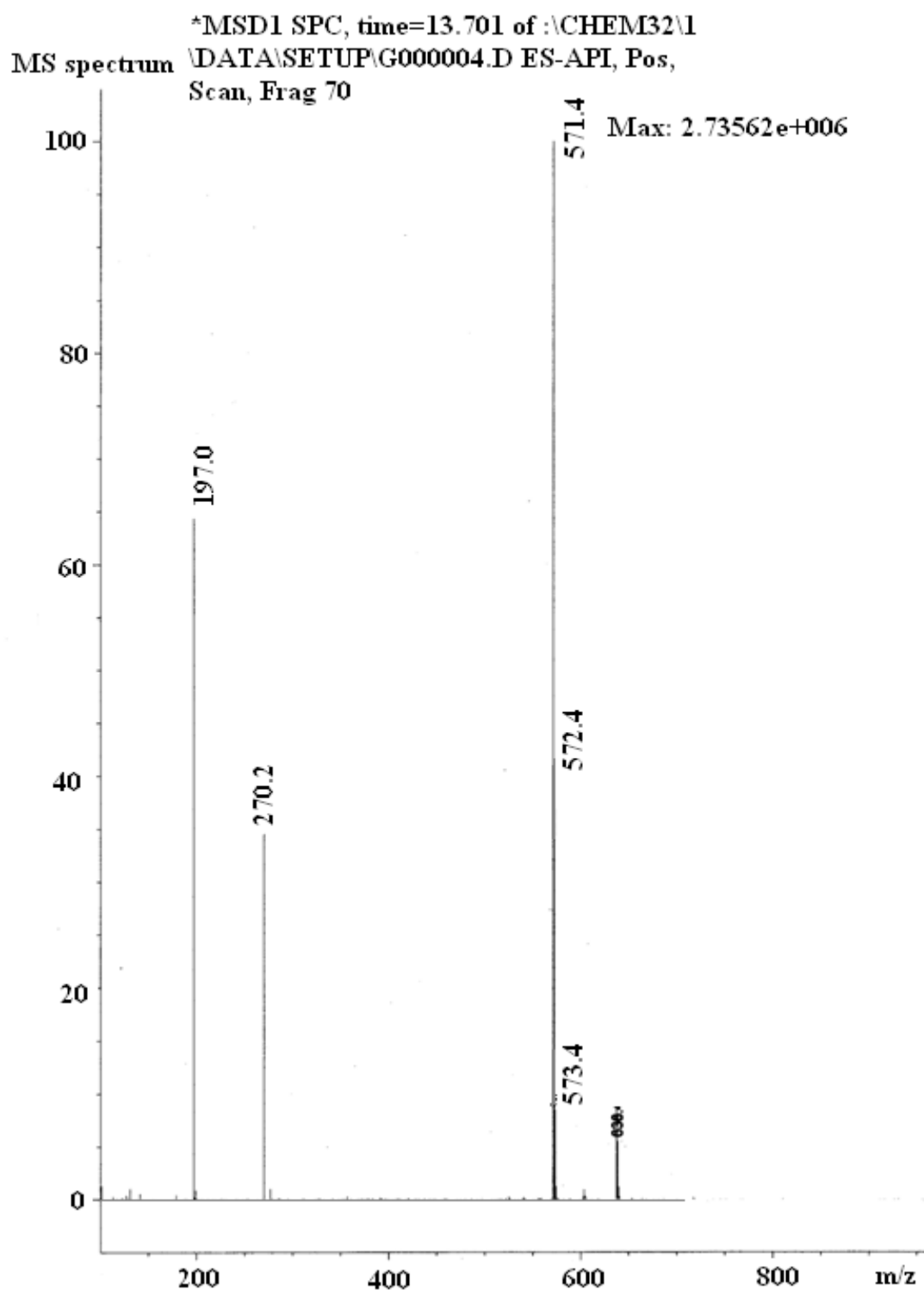
(Figure A2.8-5)

Figure A2.8 The LC-MS spectra of **4** (the MS spectra parts are for 19.0, 17.1, 14.5, 13.7min form the top the end respectively)

CHAPTER 3

NOVEL-*O*-GLYCOSIDIC GOSSYPOL ISOMERS AND THEIR BIOACTIVITIES

3.1 Abstract

Novel glycosidic gossypol analogues, gossypol diglycosidic tetraacetate **7**, gossypol diglycosidic tetraacetate **8**, gossypol mono-glycosidic tetraacetate **9** gossypol diglycoside **10** and gossypol diglycoside **11** were obtained by the ultrasound-assisted reaction of potassium salt of gossypol with 3, 4, 6-tetra-O-acetyl-α-D-glucopyranosyl bromide under phase transfer catalytic (PTC) condition. The new glycosidic gossypol derivatives were fully characterized by 1D NMR (^{1}H NMR, ^{13}C NMR, DEPT, 1D NOE), 2D NMR (HMBC, HMQC) spectroscopy, HRMS/MS spectrometry, UV spectrometry as well as HPLC-PDA technique. The biological activities of the novel glycosidic gossypol analogues were explored in detail. The anticancer, antitrypanosomal activities as well as cytotoxicity evaluation of those novel glycosidic gossypol derivatives exhibited that gossypol diglycosidic tetraacetate **8** could be developed into a potential pharmaceutical candidate in the treatment of cancer since it elicited powerful inhibition against cancer cells (MCF–7 Human breast and HT-29 Human colon carcinoma cells) with significantly low cytotoxicity compared with unfunctional gossypol. In addition,

gossypol diglycosidic tetraacetate **7** and **8** possess antitrypanosomal activity with LD$_{50}$ value of 2.12 and 2.44 µM, respectively.

3.2 Background

A glycoside is any molecule in which a sugar group is bonded through its anomeric carbon to another group via a glycosidic bond.
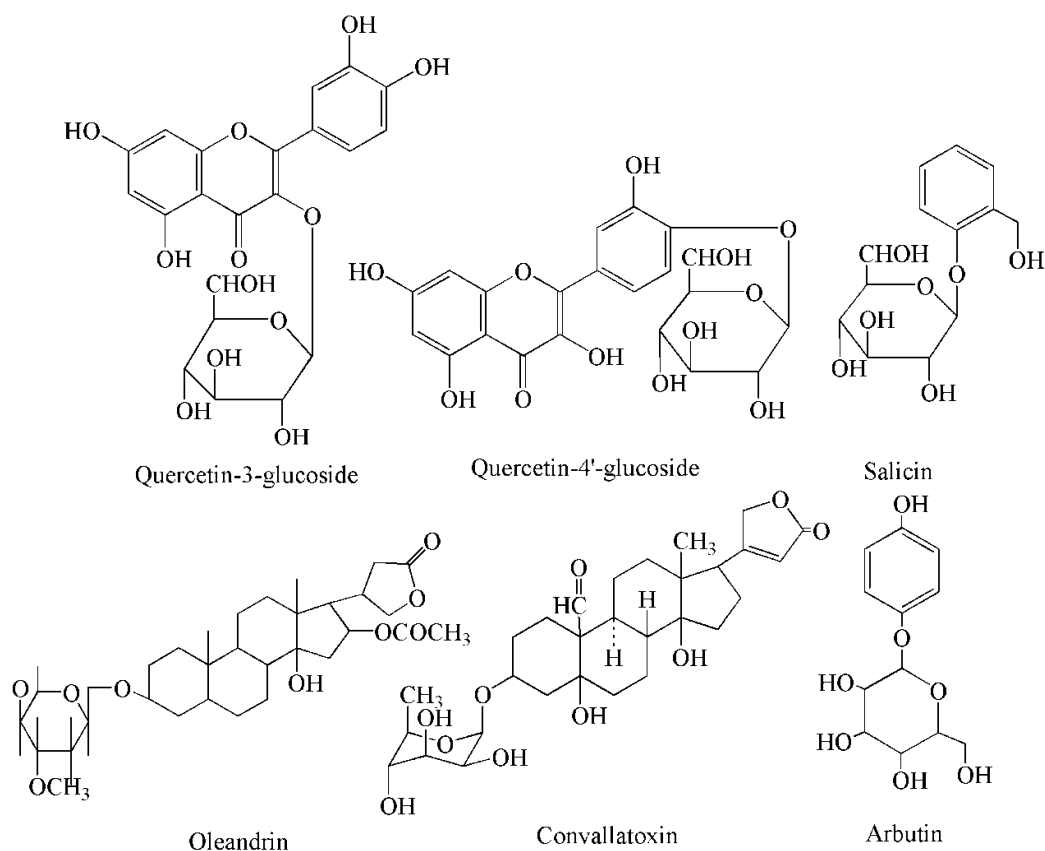
Figure 3.1 Structure of some phenolic glycosides existing in natural plants

Glycosides can be linked by an O-(an O-glycoside), C-(a C-glycoside), N-(a glycosylamine) or S-(a thioglycoside) glycosidic bond. The sugar group is then known as the glycone and the non-sugar group as the aglycone or genin part of the glycoside. In addition, the glycone can consist of a single sugar group (monosaccharide) or several sugar groups. Common types of glycosides include saponins, cardiac glycosides (cardenolides), cyanogenic glycosides, anthraquinone glycosides and glucosinolates, many of which possess various biological functions, e.g, as deterrents to herbivores (Majak, 1992; Duffey, S. S. 1980). Some examples of natural phenolic glycosides are given in **Figure 3.1**.

Carbohydrates carrying aromatic aglycones are important natural products with versatile bioactivities and thus key synthetic targets. The most common carbohydrate donors used for aromatic O-glycosylation are anomeric acetates, halides, trichloroacetimidates and thioglycosides as well as some other less common donors. Anomeric acetates or trichloroacetimidates, which are activated under acidic conditions, are preferred for electron rich aromatic aglycons; while glycosyl halides, which are activated using basic conditions, are preferred for electron deficient aromatic residues (Jacobsson et al., 2006).

Before the introduction of gossypol glycosylation, it is worth to mention an important reaction: the Koenigs–Knorr reaction (**Figure 3.2**) which was reported in 1901 and thus, it is one of the oldest, simplest but most useful reactions for preparation of a wide variety of O-glycosides. It is useful for coupling reactions with either alkyl or aromatic alcohols as well as for coupling between sugars. The

methodology requires silver salts as catalysts. Among them, the oxide, carbonate, nitrate, triflate silver salts are the most commonly employed. Also a drying agent such as calcium sulfate, calcium chloride or molecular sieves is recommended (Fischer et al., 1901; Koenigs et al., 1901).
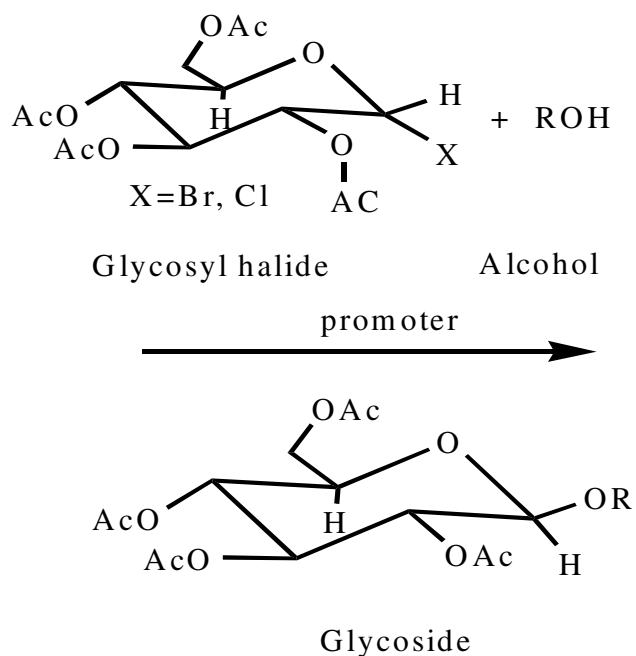
Promoters	Conditions
Ag_2CO_3	PhH, drierite (drying agent), I_2
Ag_2O	S-collidin (acid scavenger)
$AgNO_3$	HgO (acid scavenger)
$AgClO_4$	$AgClO_3$ (acid scavenger),THF or toluene, r.t.
AgOTf	CH_2Cl_2, r.t.

Figure 3.2 The Koenigs–Knorr reaction

3.3 Introduction

The naturally occurring sesquiterpene dimer gossypol and its derivatives have long been a subject of interest to medicinal chemists due to their great potentials in pharmaceutical and industrial applications. This polyphenolic pigment displays various promising biological properties including contraceptive (Porat, 1990), anticancer (Moon et al., 2008; Shelley et al., 2000), antiviral (Radloff et al., 1986), and antifungal properties (Przybylski et al., 2009b). However, the relatively high toxicity of gossypol (Clark, 1927; Gallup et al., 1931) precludes its application in medical therapy, for this reason the syntheses and tests of potentially less toxic gossypol analogues are desired to enable their application as drugs. Many gossypol derivatives including its Schiff bases (Przybylski et al., 2009a), gossypol ethers (Adams et al., 1938; Morris et al., 1937), apogossypol series derivatives (Meltzer et al., 1985), gossypolone (Haas, 1965), gossindane (Talipov et al., 1999), halogenated gosspol (Zhu et al., 1992), periacetylated gossylic nitriles, periacetylated gossylic imino-lactones, azo-derivatives, hydrazones, thioderivatives of gossypol have been obtained and tested for their antipsoriatic, antimalarial, antitumor, interferon-inducing as well as anti-HIV activities (Przybylski et al., 2009c; Dodou et al., 2005; Razakantoanina et al., 2000; Rezhepov et al., 2002; Liang et al., 1995; Royer et al., 1995).

However, among those gossypol derivatives, no studies about gossypol glycosides have been reported up to now. As mentioned above in Section **3.2**

background, glycosides are a main type of sources of natural medicines, cosmetics, and some functional food ingredients, which possess essential biological functions that make them the key synthetic targets. On one hand, gossypol glycosylation products may have increased solubility and thus make them more easily absorbed by the intestine; on the other hand, gossypol glycosides may undergo different metabolism pathways with reduced toxicity. However, regardless of these potential advantages, phenols such as gossypol are difficult to be glycosylated due to the electron-withdrawing properties of aromatic rings (Jacobsson et al., 2006).

In this paper, novel glycosidic gossypol isomers were synthesized through ultrasound assisted reaction of 2, 3, 4, 6-tetra-O-acetyl-α-D-glucopyranosyl bromide with potassium salt of gossypol under PTC conditions and were fully characterized by 1D NMR (^{1}H NMR, ^{13}C NMR, DEPT, 1D NOE), 2D NMR (HMBC, HMQC), HRMS, HPLC. Besides, we explored the antioxidant capacity, antitumor effects and the cytotoxicity of the glycosidic gossypol isomers and their hydrolyzed products.

3.4 Experimental

3.4.1 Material

2, 2′-Bi [8-formyl-1, 6, 7-trihydroxy-5-isopropyl-3-methylnaphthalene]) acetic acid (gossypol acetic acid, MW=578.6, $C_{30}H_{30}O_8 \bullet C_2H_4O_2$, HPLC purity >95%) was purchased from Zhejiang Yixin Pharmaceutical Co., Ltd. P. R. China. Tetrabutylammonium bromide, 99+% (MW=322.36 $C_{16}H_{36}BrN$), 2, 3, 4,

6-tetra-O-acetyl-alpha-D-galactopyranosyl bromide (MW=411.21, $C_{14}H_{19}BrO_9$), were products form Acros organics, New Jersey, USA. Dimethyl sulfoxide (DMSO), potassium carbonate (K_2CO_3), and phosphoric acid (H_3PO_4) were purchased from Sigma Chemical Co., (St. Louis, MO). Amerlite ion exchange resin (IR-120 H. C. P.) has medium porosity and moisture holding capacity of 44-48%, which is composed of strong acidic, sulfonated polystyrene type cation exchange resin (RSO_3-H^+). All solvents for chromatographic isolation were of analytical grade. HPLC grade methanol, dichloromethane, acetone, and chloroform were purchased from Fisher Scientific Company (Fair lawn, N.J. USA). Tissue culture plates were purchased from Costar Corp. (Cambridge, MA). Heat-inactivated fetal bovine serum, fetal bovine serum, and newborn calf serum were purchased from Hyclone Laboratories, Inc. (Logan, UT). MCF-7 (human breast cancer), HT-29 (colon cancer) cancer cell lines and 3T3L1 preadipocytic cell line were purchased from the American Type Culture Collection (ATCC) (Rockville, MD). MCF-7 cells were cultured in RPMI-1640 with 10% newborn calf serum and HT-29 cells were cultured in RPMI with 10% fetal bovine serum instead of the newborn calf serum. The base medium for 3T3L1 preadipocytic cells is ATCC-formulated Dulbecco's Modified Eagle's Medium, Catalog No. 30-2002. To make the complete growth medium, the following components were added to the base medium: bovine calf serum to a final concentration of 10%. All cell lines were incubated at 5% CO_2 and 90-100% relative humidity at 37°C. Medium renewal was carried out 2-3 times per week, and cells

were subcultured when they achieved 80-90% confluence. 1, 1-diphenyl-2-picrylhydrazy (DPPH), butylated hydroxytoluene (BHT), 3, 5-dinitrosalicylic acid (98%)(DNSA), alpha-amylase (Type VI-B, from porcine pancreas), starch from potatoes (($C_6H_{10}O_5$) $_n$, Mr=162.14$_n$) was purchased from Fluka, Germany. Potassium sodium tartrate ($KNaC_4H_4O_6 \cdot 4H_2O$, FW=282.231), sodium hydroxide were purchased from J. T. Baker Chemical Co., (Phillipsburg, N.J. USA). Sodium phosphate (Na_2HPO_4, FW=141.96), Sodium chloride were purchased from Fisher Scientific Company (Fair lawn, N.J. USA).

3.4.2 Instruments for chemical analysis

HPLC analysis was carried out on a Shimadzu HPLC system that included LC-20AT solvent delivery pumps, a CBM-20A communication bus module, a SPD-M20A photo-diode array detector, and the ClassVP operating software.

The HPLC was equipped with a Kromasil RP C18 column (particle size of 5μm, column size of 150 mm×4.6 mm, Alltech Associates, Inc. Deerfield, IL), which was placed in a column oven (CTO-20A) under a constant temperature at 25°C. The mobile phase consisted of methanol: H_2O = 87:13 (v/v) containing 0.1% aqueous H_3PO_4. The column flow rate was set at 1 ml min^{-1}, while the HPLC pressure was controlled between 1020-1040 psi.

Mass spectrum were obtained by a nanoflow capillary HPLC coupled with a quadrupole time-of-flight micro mass spectrometer (Q-TOF-MS) (Waters Corp., Milford, MS) with an electrospray ionization (ESI) in both ESI-MS and ESI-MS-MS modes operated by the Masslynx software (V4.0, Waters Corp., Milford, MS). Each

separated and purified sample was directly injected from the sample vial into the ESI source in methanol at a flow rate of 1.5 µL min^{-1}. The ion source voltages were set at ±3000V for positive and negative ion mode acquisitions, respectively. In both modes, the source temperature was maintained at 100°C and the mass spectrum was scanned from 100 to 800 *m/z* at 1 second with 0.1-second inter-scan delay in continuum mode. For MS/MS analysis, mass spectrum was scanned from 50-800 *m/z*. Glu-fibrinopeptide (Sigma) as a mass standard in ESI-MS and ESI-MS/MS mode was infused through the nanoLockspray (Waters Corp., Milford, MS) for single point, real time, and accurate mass calibration. Raw spectra were processed using the MassLynx software (V4.0). Precursor ion scans on positive and negative ion modes using low energy collision induced dissociation (CID) resulted in more structural fragments, which helped structural identification of compounds of interest.

LC/MS analysis was performed on an Agilent 6100 series LC/MS in which a quadrupole mass spectrometer was coupled to an Agilent 1200 HPLC that consisted of a G1329A high performance autosampler (hp-ALS-SL), a G1312A binary pump (BIN-SL), a G1379B vacuum degasser, a G1316A thermostatted column compartment (TCC-SL) and a G1314B variable wavelength detector (VWD-SL).

The quadrupole mass spectrometer was operated with an atmospheric pressure electrospray ionization (API-ES) source in positive mode. The flow rate of HPLC was maintained at 1 mL/min through a Kromasil RP C18 column (particle size of 5 µm, column size of 150 mm×4.6 mm, Alltech Associates, Inc. Deerfield, IL). The mobile phase in an isocratic elution consisted of methanol and water (v/v=87:13) containing 0.1% formic acid. Mass spectra were recorded within the *m/z* range of 100-1000. The

dry gas flow for MS was 13.0 L/min, the nebulizer pressure was 30 psig, dry gas temperature was 350 ^{0}C, and the Vcap voltage was 3500 V. Data was acquired from and processed by the Agilent LC/MSD ChemStation software.

The instrument used for infrared (IR) spectral analysis was a PerkinElmer 1725 series FTIR spectrometer (PerkinElmer Corporation, Norwalk, CT) equipped with a room temperature deuterated triglycine sulfate detector and controlled by a PerkinElmer 7300 PC.

The software used for collecting the FTIR data was the Spectrum version 5.3.1. The instrument was purged with dry nitrogen and maintained with two automatic dehumidifiers to minimize CO_2 and water vapor interference. Melted drops of each standard were placed in a transmission cell with sodium chloride (NaCl) windows. The transmission path of 25 μm was adjusted using a polytetrafluoroethylene spacer. The cell was then placed in the cell holder in the FTIR spectrometer before the sample was scanned. The transmission cell was rinsed three times with acetone and then dried with a soft tissue before the next sample was put in. Calibration spectra were collected by 81 scans of each of the 45 standards at a resolution of 4 cm^{-1}, gain of 1.0, and strong apodization throughout the mid-IR region of 4000–400 cm^{-1}.All the spectra were subtracted from the background KBr spectrum. All the samples were scanned in duplicate.

The UV-Vis absorbance spectra are recorded by the SPD-M20A photo-diode array spectrophotometer.

1D and 2D NMR (^{1}H NMR, ^{13}C NMR, DEPT, HMQC, HMBC) spectra were acquired from a Bruker AV-500 spectrometer or JEOL operated at 300 MHz for ^{1}H NMR and 75 MHz for ^{13}C NMR. Data were processed by the Bruker XWINNMR 3.50 programs.

In addition, thin layer chromatography (TLC) analytic plates were F$_{254}$ plates precoated with silica gel 60Å and fluorescent reagent (Merck, Darmstadt, Germany & Whatman, New Jersey, USA). The TLC preparative plates are Partisil PK6F, precoated with silica gel 60Å, 20×20cm, layer thickness is 250 or 1000 µm., purchased from Whatman Inc, New Jersey, USA. The TLC was visualized at 254 nm in a UV-viewing system purchased from Fisher Biotech. Silica gel (300 meshes), which was purchased from QingDao Haiyang Chemical Co., Ltd. P. R. China, was used for column chromatography.

3.4.3 Chemical syntheses and structural characterization

The synthetic procedure for the glycosidic gossypol isomers is depicted in **Figure 3.3**. To a mixture of gossypol acetate (500 mg, 0.864 mmol, 1eq) in dichloromethane/acetone (v/v=5:1, 25 ml) and 2, 3, 4, 6- tetra-O-acetyl-α -D-glucopyranosyl bromide (711mg, 1.728 mmol, 2eq) in dichloromethane (5 ml), aqueous KOH (0.3 g, 5mmol in 10 ml water) and tetrabutylammonium bromide (0.6 g, 1.86 mmol in 10 ml water) were added. The mixture was ultrasonicated until the completion of the reaction (at least 6 hrs at room temperature), which was indicated by phase separation and analyzed by TLC (dichloromethane/methanol
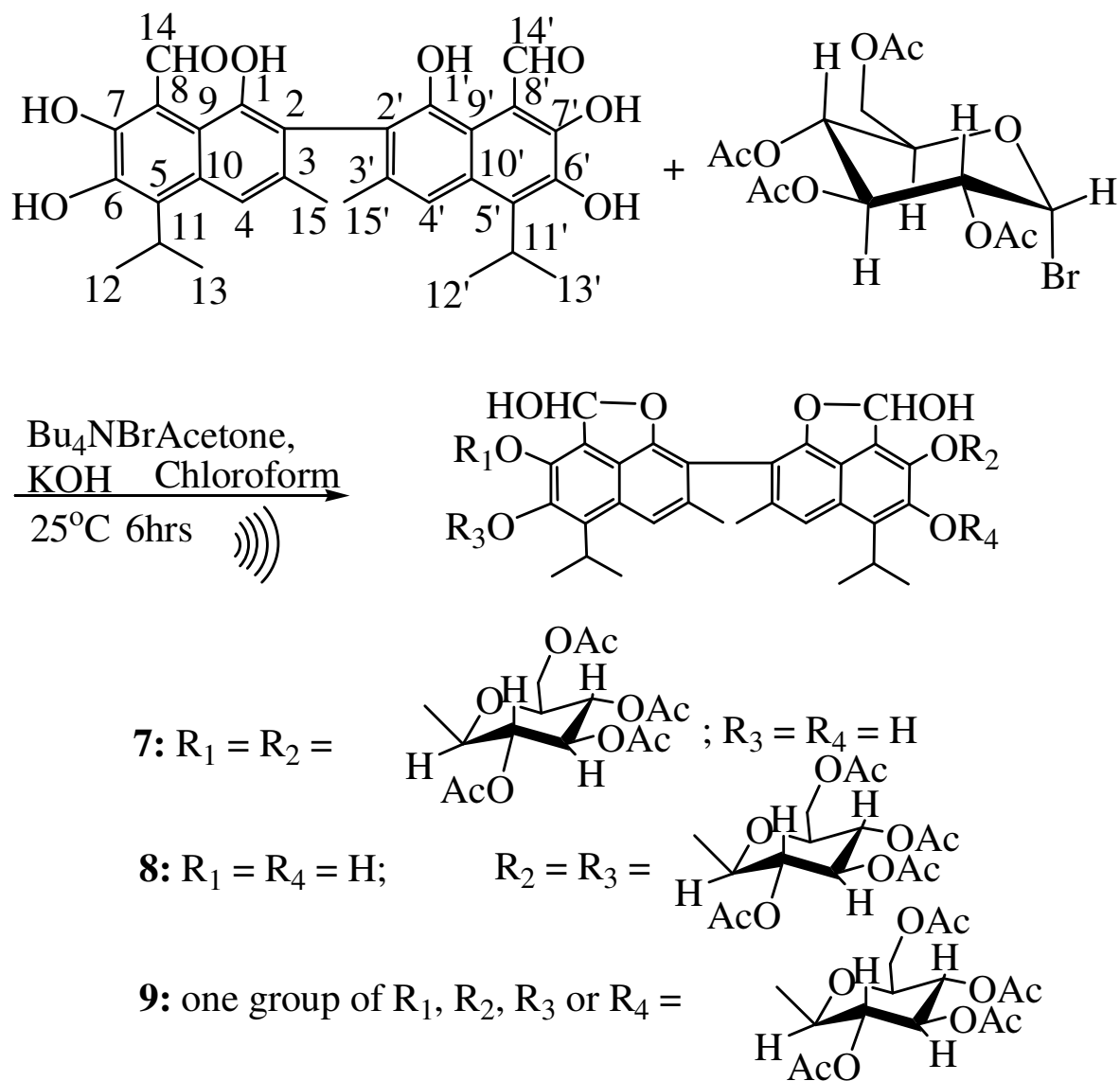
Figure 3.3 The glycosylation of gossypol
(**7** or **GS1**:7, 7'-gosspol di-glucosidic tetraacetate
8 or **GS2**:6, 7'-gosspol di-glucosidic tetraacetate)

=20:1). The organic layer was washed with water, dried over anhydrous sodium

sulfate and distilled under reduced pressure. The crude sample was loaded onto a

silica gel (300 mesh) column and eluted out with gradient from 100% petroleum ether

to the mixture of petroleum ether-acetone in 10/1 to the final concentration ratio 3/1

(V/V). The isomers were finally elaborately separated by preparative TLC

(dichloromethane/ methanol=20:1), pure fractions were pooled and evaporated to

afford 7, 7'-gosspol di-glucosidic tetraacetate **7** in 36% yield (0.36g) and 6, 7'-gosspol

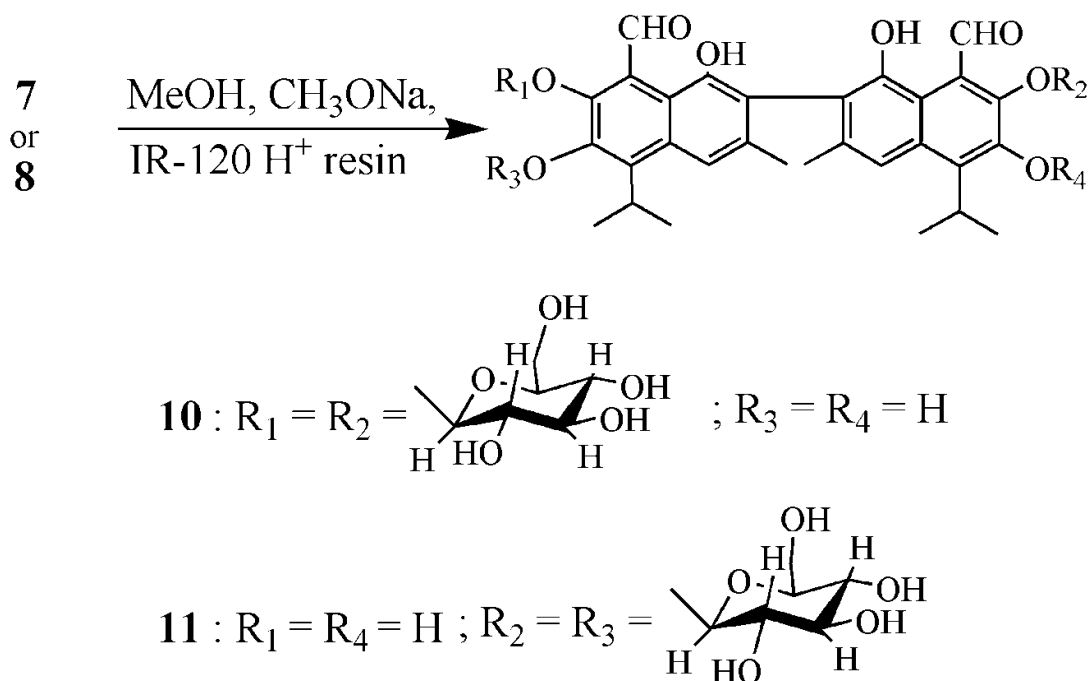di-glucosidic tetraacetate **8** in 24% yield (0.24g) and trace amount of gossypol

Figure 3.4 Hydrolysis of compounds **7** and **8**
(**10** or **GS1'**:7, 7'-gosspol di-glucoside
11 or **GS2'**:6, 7'-gosspol di-glucoside)

mono-glucosidic tetraacetate **9**. The gossypol glucosidic tetraacetates could be converted into gossypol glucosides quantitatively in dry methanol (10 mL) and sodium methoxide. The deacetylation reaction (**Figure 3.4**) was monitored via TLC. At the end of the reaction (30 min), the solution was neutralized by the addition of freshly regenerated IR-120 H+ resin.

All structures of glycosylated gossypol derivatives were fully characterized via rigorous structure determination through multiple spectral experiments such as 1D NMR (^{1}H NMR, ^{13}C NMR, DEPT and 1D NOE), 2D NMR (HMBC, HMQC), UV spectroscopy, HRMS as well as HPLC technique.

3.4.4 Experimental results and discussion

The negative-ion mode HR-nano-ESI Q-TOF MS/MS spectrum of **7** showed the molecular ion peak of $C_{58}H_{66}O_{26}$ at *m/z* 1177.4166 (intensity 100%) and two other major peaks at *m/z* 847.2607 (intensity 35%) and 516.1364 (intensity 20%) corresponding to the fragments from **7** which lost one and two glycosyl groups respectively (see **Figure 3.5)**. The fragment structure in blue bracket is corresponding to the mass peak from which the arrow in blue pointed, the same to the red ones). Similar MS/MS spectra of **8** showed the molecular ion peak of $C_{58}H_{66}O_{26}$ at *m/z* 1177.4055 and two fragment peaks at m/z 847.2491 and 516.1309 as shown in **Figure 3.6**. The compound **9** showed the molecular ion peak of $C_{44}H_{48}O_{17}$ at *m/z* 847.2687 corresponding to the gossypol mono-glucosidic tetraacetate (**Figure 3.7**).

^{1}H NMR (300 MHz, CDCl$_3$) data of **7**: 1.52 (d, 12H, J=3Hz, -C*H*$_3$ at 12, 12', 13 and 13'), 2.21 (m, 12H, -C*H*$_3$ of -OAc groups), 2.31 (s, 6H, -C*H*$_3$ at 15 and 15'), 3.81 (m, 2H, J=3Hz, -C*H*= at 11 and 11'), 4.26 (m, 4H, -C*H*=, sp^2 protons in sugar residues), 5.16-5.52 (m, 5H, -C*H*=, sp protons in sugar residues), 6.34(-O*H*), 7.06(d, 2H, J=2Hz, -C*H*=, sp protons at 14 and 14'), 7.42(s, 2H, sp protons at 4 and 4').

^{1}H NMR (300 MHz, CDCl$_3$) data of **8**: 1.52 (t, 12H, J=3Hz, -C*H*$_3$ at 12, 12', 13 and 13'), 2.16 (m, 12H, -C*H*$_3$ of -OAc groups), 2.28 (s, 6H, -C*H*$_3$ at 15 and 15'), 3.79 (m, 2H, J=3Hz, -C*H*= at 11 and 11'), 4.15 (m, 4H, -C*H*=, sp^2 protons in sugar residues), 4.25-5.52 (m, 5H, -C*H*=, sp protons in sugar residues), 5.18(-O*H*),
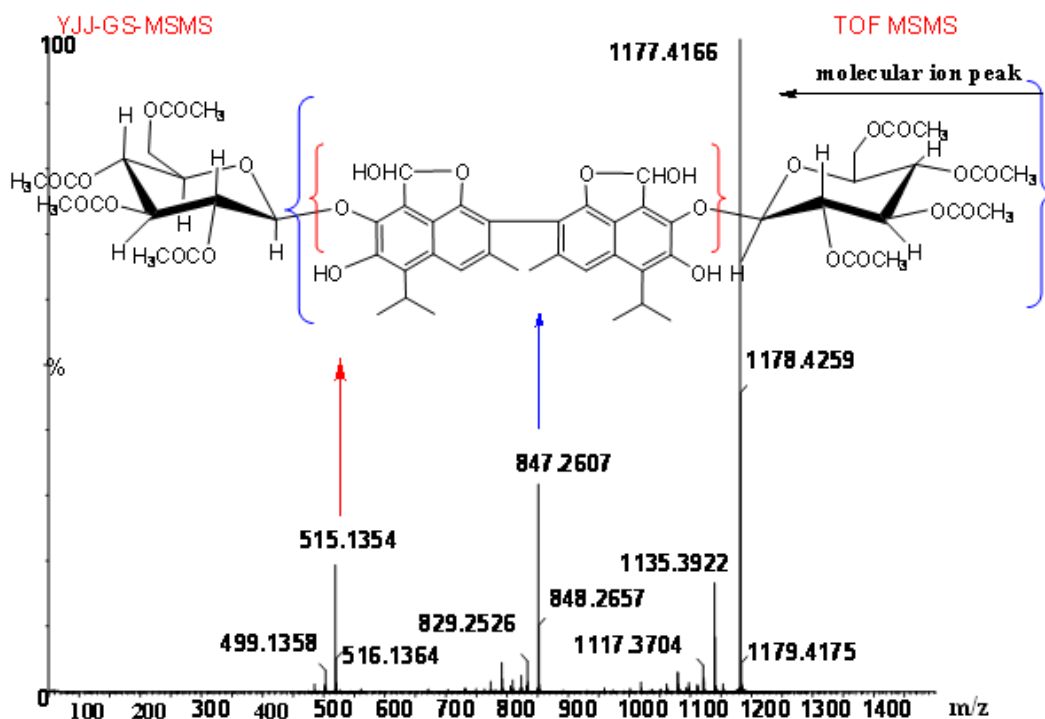

Figure 3.5 The ESI- Q-TOF MS/MS spectrum of **7**

78

6.36(-O*H*), 7.08(s, 2H, -C*H*=, sp protons at 14 and 14'), 7.39(s, 2H, sp protons at 4 and 4').

^{13}C NMR data of **7** (75MHz, CDCl$_3$): 20.54, 20.61, 20.75, 20.96, 21.33, 26.97, 30.90, 61.65, 66.77, 69.47, 70.17, 70.80, 76.61, 77.03, 77.23, 77.45, 100.67, 102.87, 109.24, 114.15, 117.88, 120.17, 126.62, 127.60, 138.25, 138.59, 146.01, 155.12, 169.99, 170.20, 170.92, 171.52.
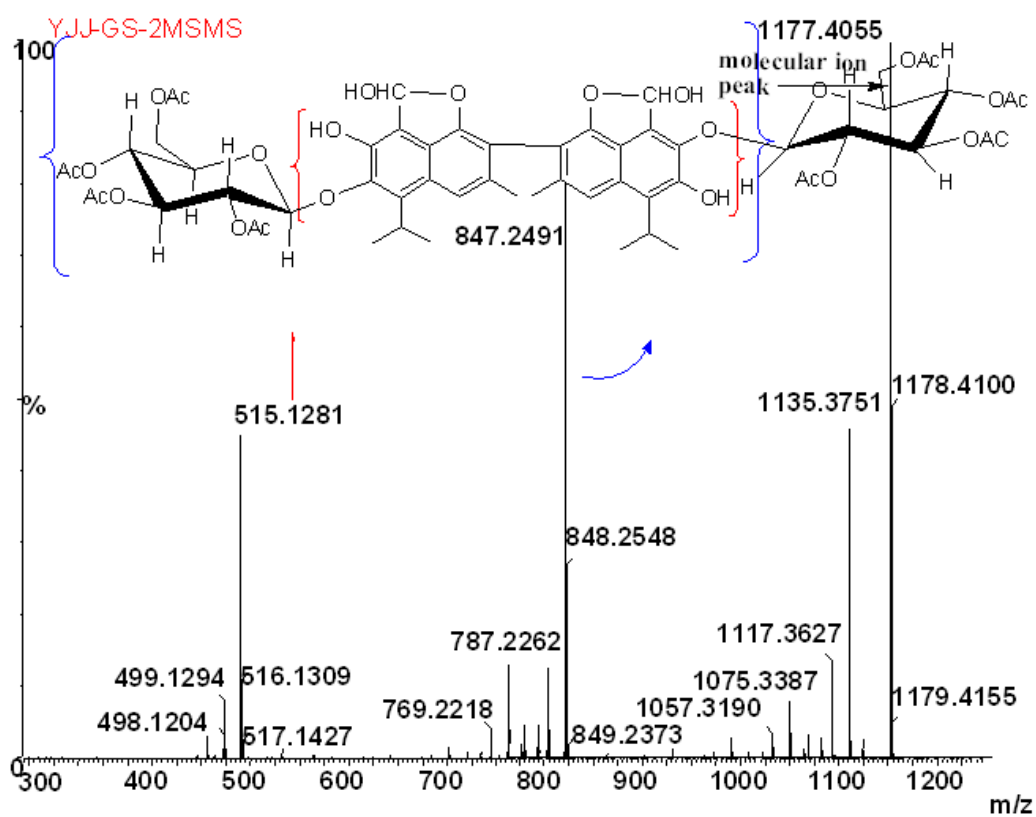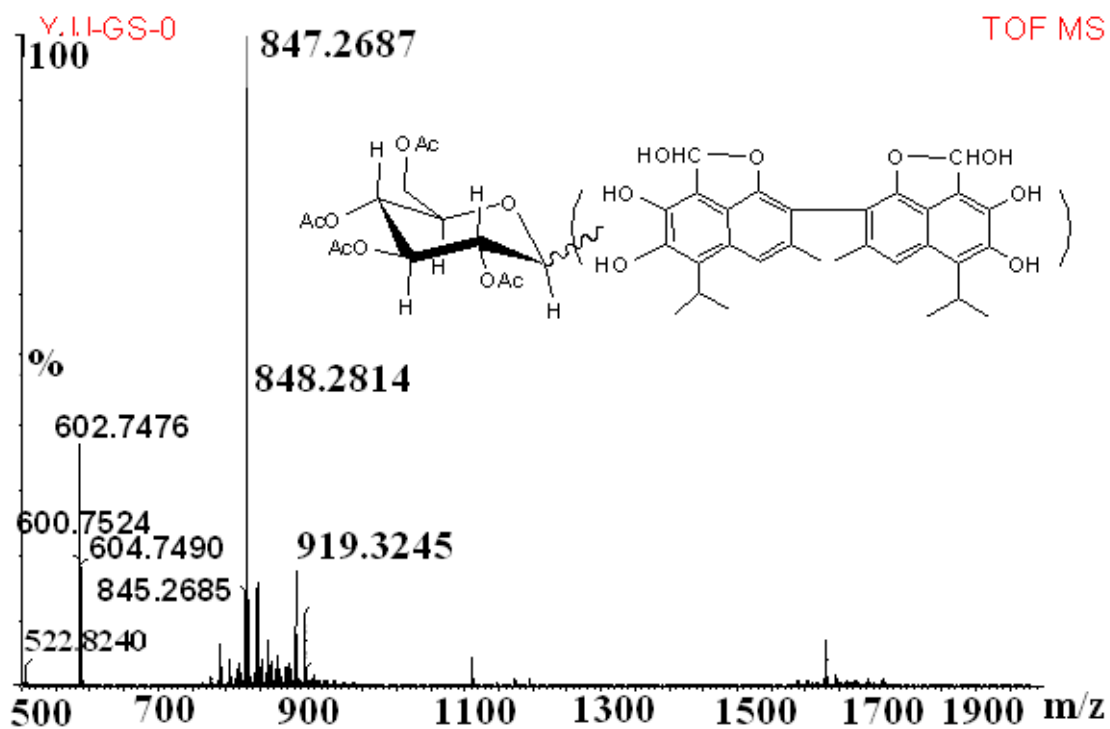

Figure 3.6 The ESI- Q-TOF MS/MS spectrum of **8**

Figure 3.7 ESI- Q-TOF MS spectrum of **9**

^{13}C NMR data of **8** (75MHz, CDCl$_3$): 20.53, 20.61, 21.04, 21.24, 21.33, 26.94, 30.92, 62.06, 67.03, 69.41, 70.07, 71.02, 76.60, 77.02, 77.22, 77.45, 99.90, 103.08, 109.29, 114.09, 117.70, 119.95, 126.35, 127.45, 137.96, 138.22, 145.93, 154.94, 170.00, 170.28, 170.65, 171.45.

The ^{1}H NMR spectrum of **7** clearly showed one set of doublet proton resonance (methyl groups at 12, 13 and 12′, 13′ position) at 1.52ppm (**Figure 3.9**) while the ^{1}H
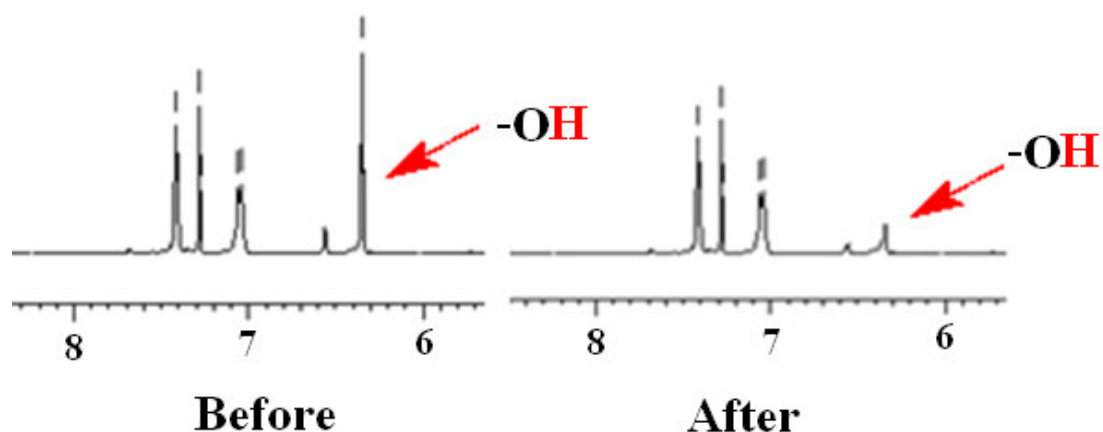
Figure 3.8 The change of the signal at 6.3ppm in ^{1}H NMR spectra of **7** after CD$_3$OD were added

NMR of **8** showed two sets of doublet proton resonance signals at 1.52ppm for the methyl groups at the same position (triplet at 500MHz, doublet of doublets at 300MHz, J=3Hz). The signal at 6.3ppm in both ^{1}H NMR spectra of **7** and **8** became less intense after a few drops of CD$_3$OD added into the sample tube (**Figure 3.8**) indicating that one of the OH groups left in gossypol framework of gossypol. The identification of hydroxyl group in gossypol framework (left: before adding CD$_3$OD; right: after adding CD$_3$OD). glucosidic molecule gave rise to the signal at 6.3ppm for both **7** and **8**. The protons attached to carbon 14′ were demonstrated to be in a hemiacetal form according to the appearance of the signal at 7.02ppm and absence of aldehyde signal at 11ppm.

The ^{13}C NMR and DEPT spectra of **7** (in CDCl$_3$) (See AddendixII, **Figure**

A3.1, **A3.2, A3.14**) located a set of CH$_2$ peaks from glucoside moiety at 61.96ppm, a set of CH peaks at 27.01ppm for methine group at position 11 and 11′, four sets of tertiary carbon peaks from glucoside moiety at 66.99, 69.28, 70.01, 71.25 ppm respectively, the other three sets of tertiary carbon peaks from the carbon in the hemiactal structure of gossypol, the anomeric carbon of glucoside moiety and the tertiary carbon of benzene at 100.66, 102.88, 114.15ppm respectively. The compound **8** possesses ^{13}C NMR and DEPT spectra similar to that of **7** but some of the signals split and have more fine signals.
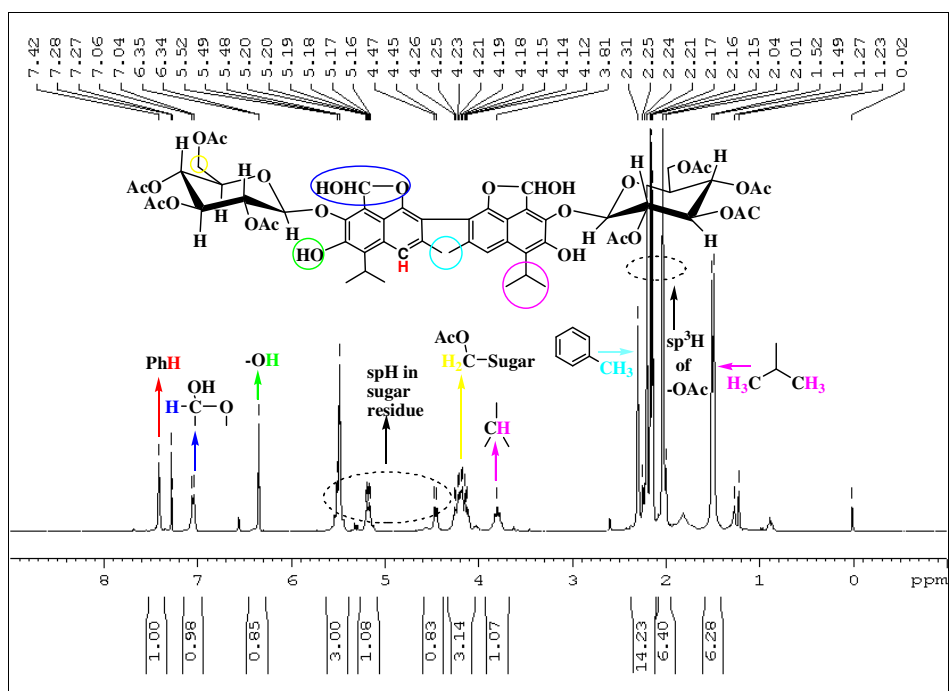

Figure 3.9 The ^{1}H NMR spectrum of **7** (in CDCl$_3$, 300 MHz)

In addition, the ultraviolet absorption spectra (**Figure 3.10**) of gossypol diglucosidic tetraacetates and gosspol diglucosides all have profound hypsochromic shift comparable to the unfunctional gossypol. Ultraviolet and visible light have sufficient energy to cause only two electronic transitions, the promotion of a nonbonding (lone-pair) electron (n) into an antibonding molecular orbital (n to π^* transition), the higher energy electronic transition is the promotion of an electron from a bonding molecular orbital into an antibonding molecular orbital (π to π^* transition). While the ultraviolet absorption spectrum of pure gossypol shows three well separated bands at 235, 288, 372 nm since it contains conjugated Pi-electron system, the strongest absorbance is at 235nm, after glycosylation, the compound **7-11** presumably due to the substitution of the two bulky glycosidic groups which could cause distortion of the naphthalene ring in the gossypol framework, besides, the conversion from the dialdehyde form to the dilactol form and substitution also affected the electron density and the conjugation system. The UV spectra showed that glycosylation of gossypol could alter the relative intensities of the main UV absorption bands. There is hyperchromic shift at 266 nm except of the hypsochromic shift for the absorption bands.

The UV-Vis of gossypol: max/nm (MeOH) 235(strongest), 288, 372; HPLC: t_R=7.94min; mobile phase: CH_3OH: H_2O=87:13 (0.1% H_3PO_4), the average pressure=1052psi, flow rate=1ml/min;

The UV-Vis of 7, 7'-gosspol diglucosidic tetraacetate (Compound **7**): max/nm (MeOH) 206, 225, 260 (strongest); HPLC: t_R=1.63min; mobile phase: pure CH_3OH, the average pressure=600psi, flow rate=1ml/min;

The UV-Vis of 6, 7'-gosspol diglucosidic tetraacetate (Compound **8**): max/nm (MeOH) 205, 225, 260 (strongest); HPLC: t_R=1.84 min; mobile phase: pure CH_3OH, the average pressure=600psi, flow rate=1ml/min;

The UV-Vis of 7, 7'-gossypol diglucoside (Compound **10**): max/nm (MeOH) 206, 226, 261 (strongest); HPLC: t_R=1.49 min; mobile phase: pure CH_3OH, the average pressure=597psi, flow rate=1ml/min;

The UV-Vis of 6, 7'-gossypol diglucoside (Compound **11**): max/nm (MeOH) 206, 227, 261 (strongest); HPLC: t_R=1.59min; mobile phase: CH_3OH: H_2O=87:13 (0.1% H_3PO_4), the average pressure=600psi, flow rate=1ml/min.
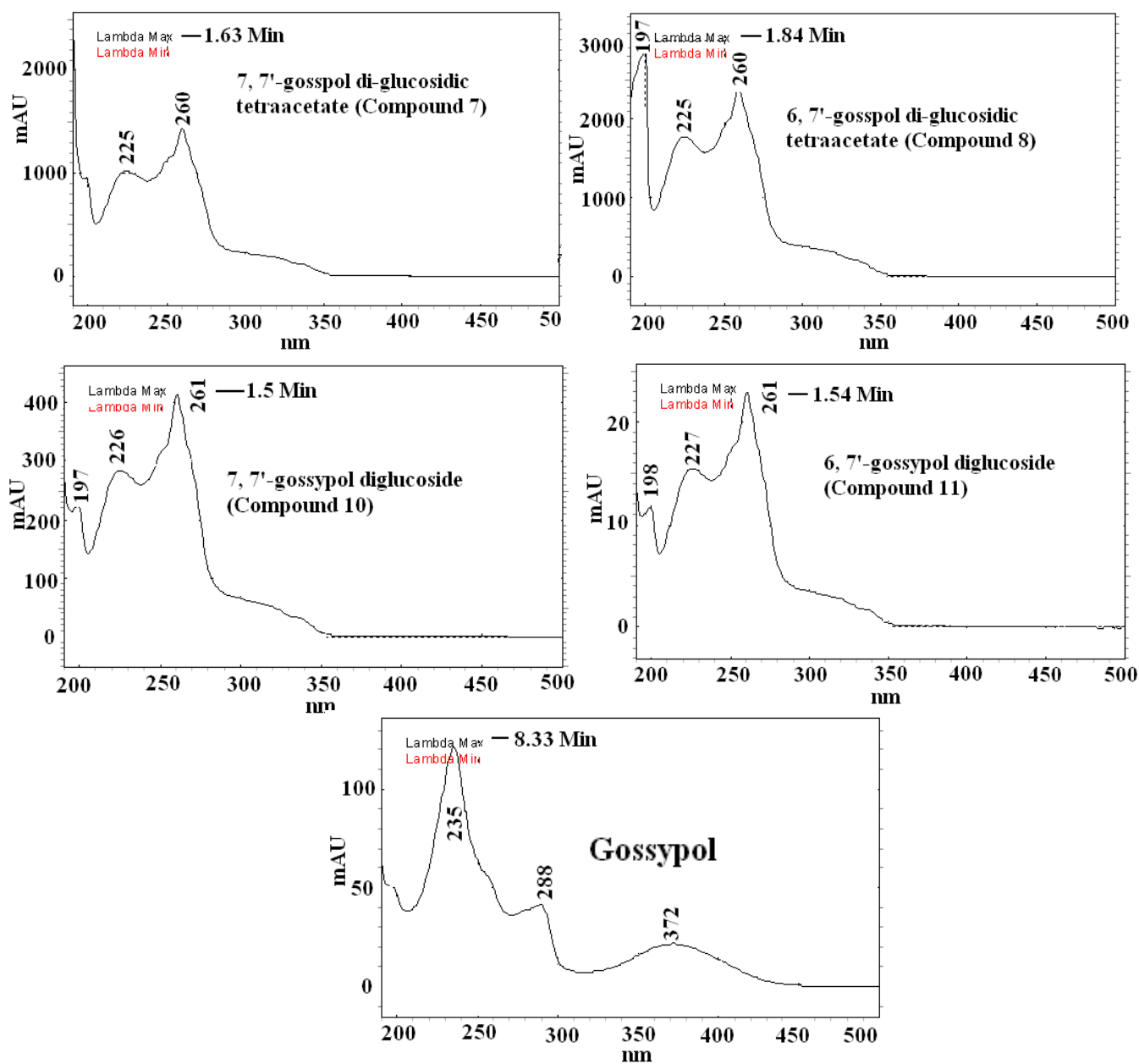
Figure 3.10 The UV/vis absorbance spectra for gossypol, gosspol diglucosidic tetraacetates, gosspol diglucosides
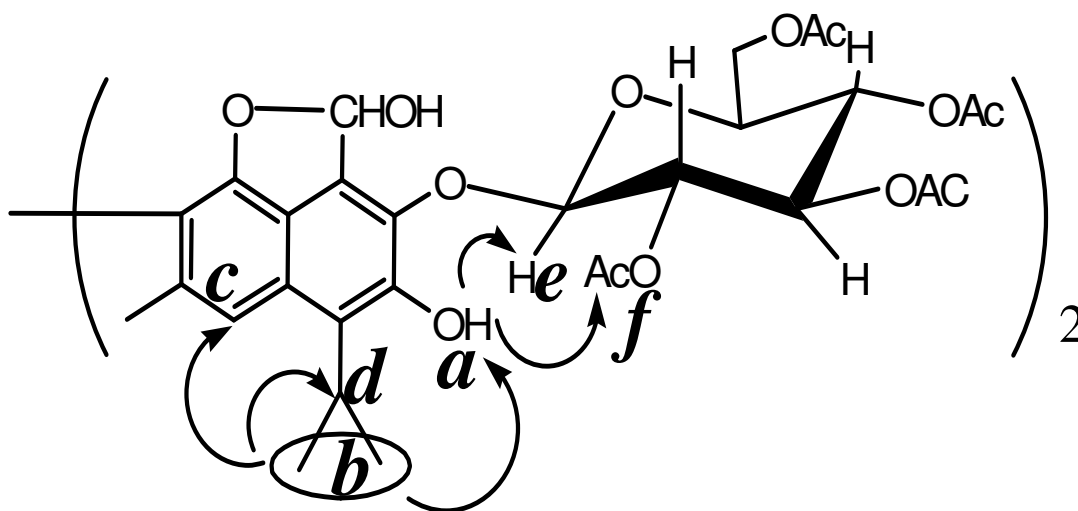
Figure 3.11 The arrow indication of the NOE correlation in the structure of compound **7**, **a-f** refer the protons at different position in the molecule

All the data indicate that the two glucose molecules in compound **7** is symmetrical, while it is unsymmetrical for compound **8**. There are two possible isomers of **1**: 6, 6′ or 7, 7′-double substitution. In order to discriminate the possible configuration, 1D NOE experiments were carried out (**Figure 3.11** and **3.12**). The arrows in (A) indicate the mutual NOE correlations. The protons at position **b** and **a** were irradiated separately, the proton signals which arise from **a**, **c** and **d** give NOE in response to the irradiation of signal **b**, while the signals of **b**, **e** and **f** give a NOE in response to the irradiation of signal **a**. The protons of the hydroxyl group left in the gossypol framework and the methyl groups at position **b** are spatially
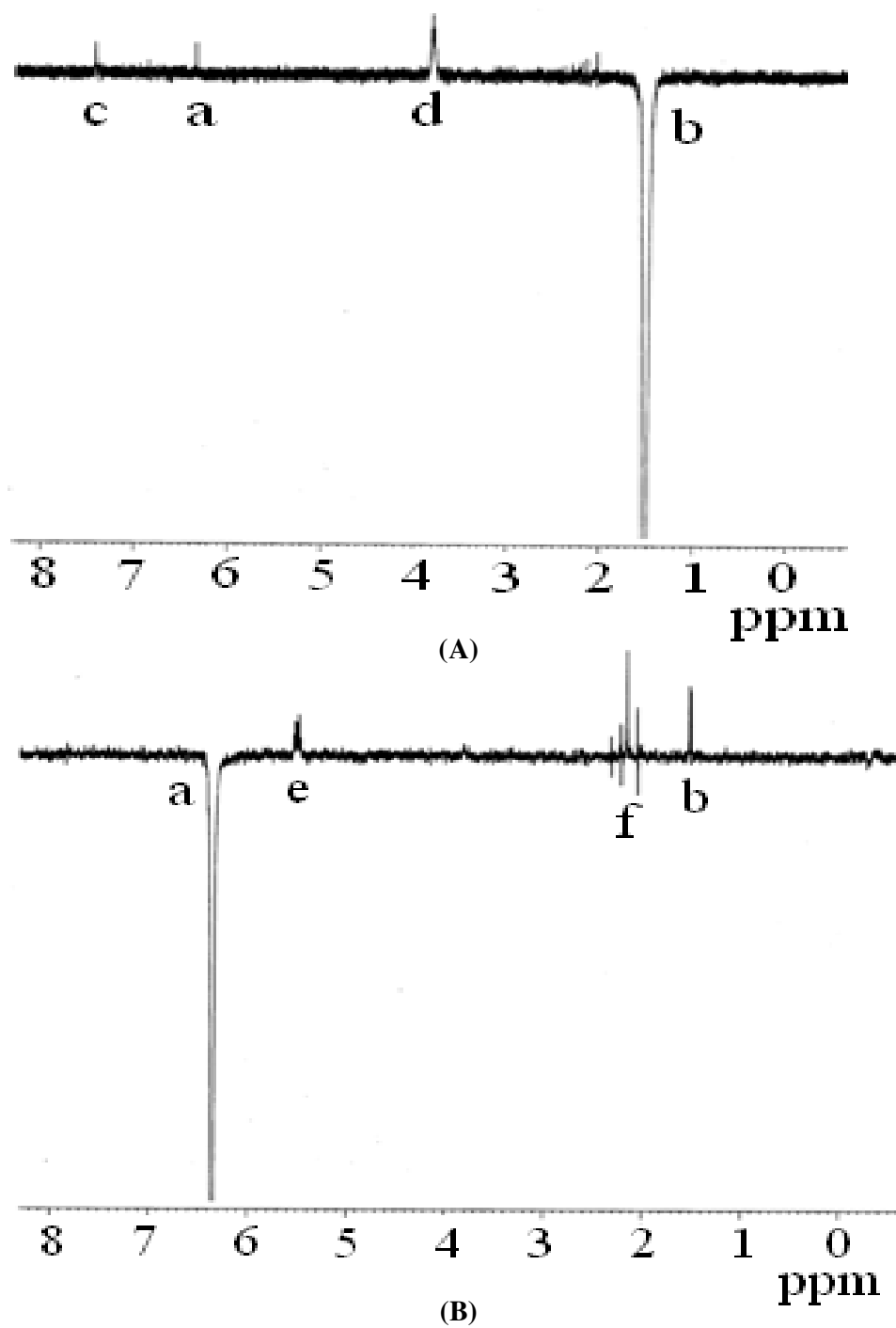
Figure 3.12 1D NOE spectra of isomer **7** (500MHz),
(A) Irradiating proton signal at **b** position
(B) Irradiating proton signal at **a** position.
Position refers to **Figure 3.11**.

close enough to elicit an NOE response which gives an evidence of compound **7** to be 7,7′-substitution. Interestingly, the hydrolyzed products of **10** and **11** exist as dialdehyde form according to the reappearance of proton signal at 11.1ppm in the ^{1}H NMR spectra. The new gosspol glucosidic tetraacetates are relatively stable in air. While stocking in methanol, they would undergo hydrolysis slowly possibly due to larger proton activity and less 3D hydrogen bonded structure as well as higher solubility of gossypol glucosidic tetraacetates in methanol than the other solvents.

Let me disscuse the FT-IR spectra of gossypol and glycosylated gossypols (**Figure 3.13-15**). The starting material, gossypol acetic acid is a complex which consists of one gossypol molecule and one acetic acid molecule through hydrogen bonding, there are no additional hydro-gen bonds between these complexes, gossypol crystal structure is stabilized by Van der Waals interactions only. The functional group region of 4000-1400 cm^{-1} an IR spectrum is where most of the functional groups show absorption bands; the finger print region of 1400-600 cm^{-1} is characteristic of the compound as a whole. In the functional region of the FT-IR spectrum of unmodified gossypol, two clear bands at 3503.37 and 3425.63 cm^{-1} assigned to different types of hydroxyl groups involved in the hydrogen bonds of different strength are observed, in contrast, the rest O-H groups after gossypol glycosylation show stretches at 3502.34 cm^{-1} for the compound **8** and 3481.20 cm^{-1} for the compound **7** which is the only difference at absorption frequency for these

two isomers, and it also give a further evidence to indicate that the O-H groups exist in different chemical environment further. Also, the FT-IR spectrum shows the stretching vibration mode of C=O of the ester group in eight acetyl groups of the gosspol diglucosidic tetraacetates show the strongest absorption band at the frequency of 1754.79 cm^{-1} for both Compound **7** and **8,** while the FT-IR spectrum of unglycosylated gossypol show absorption at 1712.01 cm^{-1} with medium intensity for the stretching vibration of C=O in the aldehyde groups. The frequency occurs at around 2961.07 cm^{-1} reflect sp^3 C-H scissoring vibration mode for both glycosylated gossypol and pure gossypol. In addition, the increased C-O bonds of both Compound **7** and **8** show strong stretches at 1223 cm^{-1} in the fingerprint region.
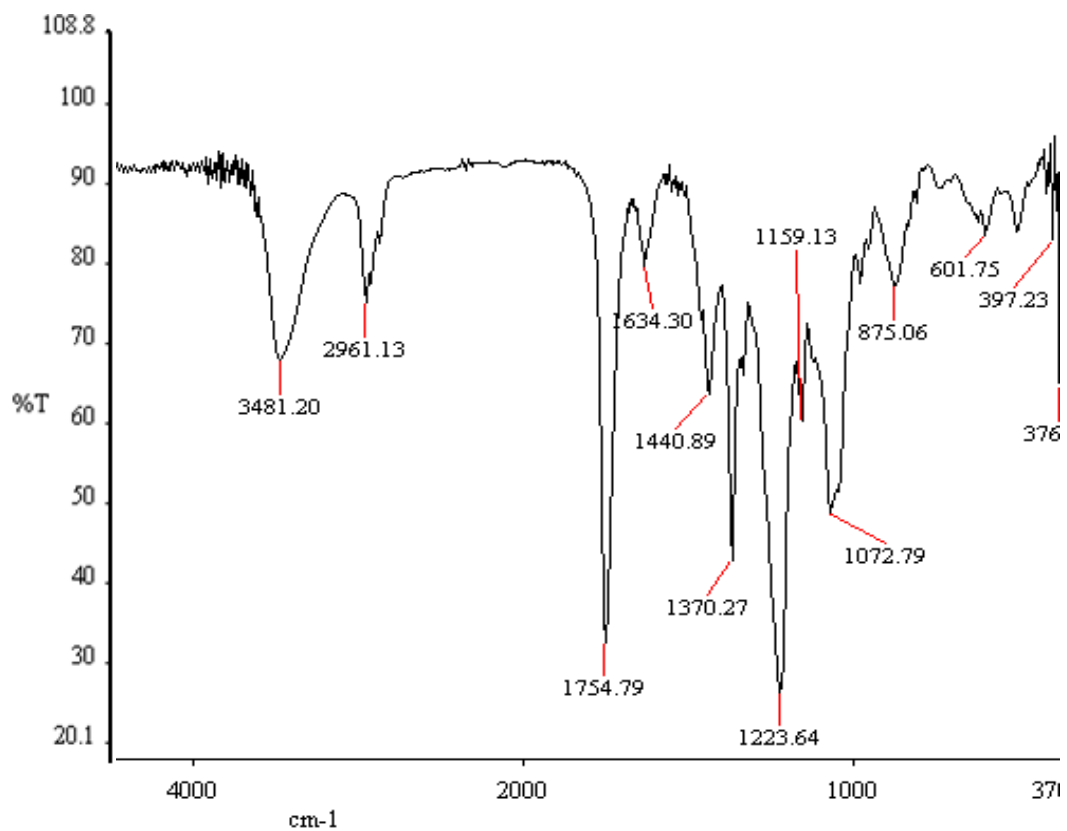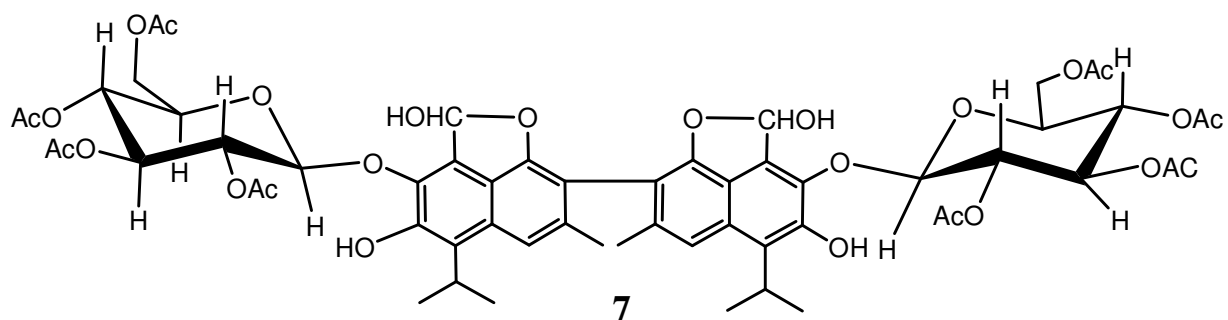
Figure 3.13 The FT-IR spectrum of 7, 7'-gosspol diglucosidic tetraacetate (Compound **7**) in KBr pellet in the range 4000–370 cm^{-1}

[IR ν/cm^{-1} (KBr) of 7, 7'-gosspol diglucosidic tetraacetate (Compound **7**): 3481.20, 2961.13, 1754.79, 1634.30, 1440.89, 1370.27, 1223.64, 1159.13, 1072.79, 875.06, 601.75, 397.23, 376]
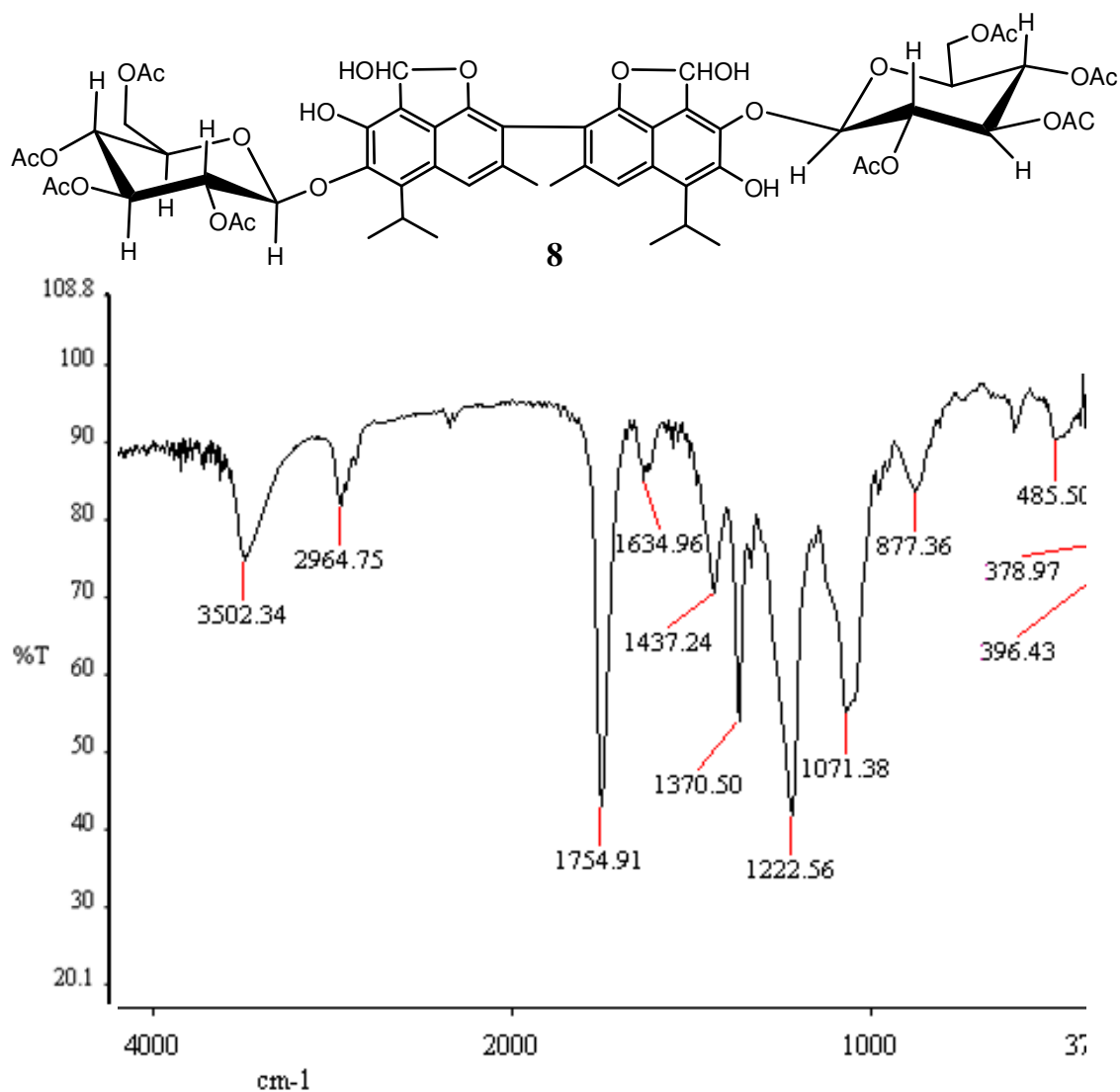
Figure 3.14 The FT-IR spectrum of 6, 7'-gosspol diglucosidic tetraacetate
(Compound **8)** in KBr pellet in the range 4000–370 cm^{-1}

[IR ν/cm^{-1} (KBr) of 6, 7'-gosspol diglucosidic tetraacetate (Compound **8**): 3503.37,

3425.63, 1961.07, 1712.01, 1577.13, 1613.81, 1441.09, 1381.10, 1339.22, 1297.84,

1179.01, 1123.59, 1053.13, 966.65, 912.80, 772.49, 611.99, 542.43, 478.40, 394.83,
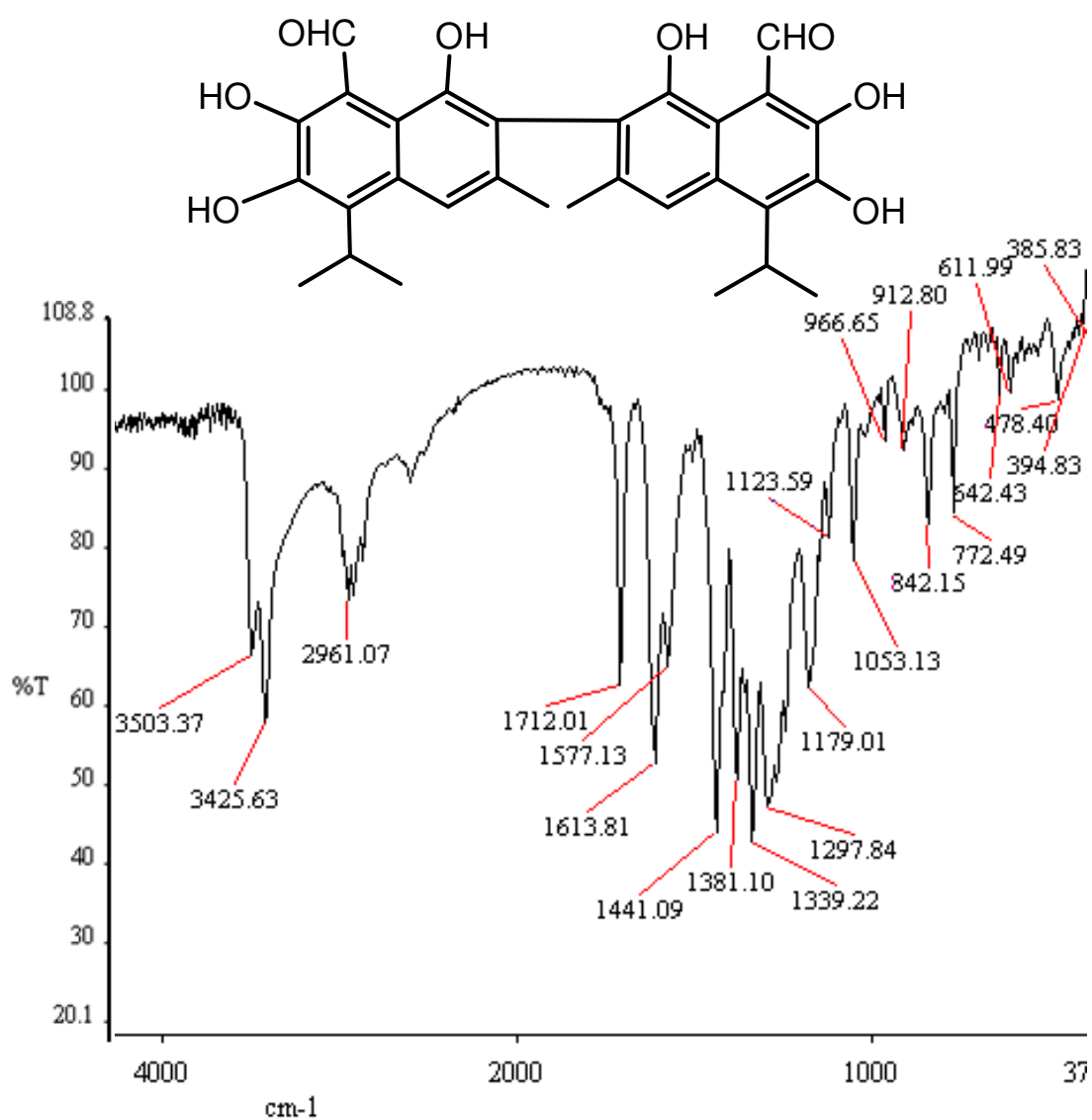
385.83]

Figure 3.15 The FT-IR spectrum of gosspol in KBr pellet in the range 4000–370 cm^{-1}

[IR ν/cm[-1] (KBr) of gossypol: 3503.37, 3425.63, 2961.07, 1712.01, 1613.81, 1577.13, 1441.09, 1381.10, 1339.22, 1297.84, 1179.01, 1123.59, 1053.13, 966.65, 912.80, 842.15, 772.49, 642.43, 611.99, 478.40, 394.83, 385.83]

The anticancer activities of gossypol, 7, 7′-gosspol diglucosidic tetraacetate, 6, 7′-gosspol diglucosidic tetraacetate, 7, 7′-gosspol diglucoside and 6, 7′-gosspol diglucoside were investigated by using an MTT (3-(4, 5-dimethyl- thiazole-2yl)-2, 5-diphenyl tetrazolium bromide) assay on human colon adenocarcinoma HT-29 and breast adenocarcinoma MCF-7 human cancer cell lines, the results are presented in **Figure 3.16**. When the growing cancer cell cultures achieved 80-90% confluence, they were incubated for another 24 hours right after chemical treatment. The result was recorded on a universal EL800 Bio-Tek microplate reader at 490nm. A mitochondrial enzyme in living cells, succinate dehydrogenase, cleaves the tetrazolium ring and converts the MTT into an insoluble purple formazan and the amount of formazan produced is directly proportional to the number of viable cells. The cytotoxicity of gossypol, 7, 7′-gosspol diglucosidic tetraacetate, 6, 7′-gosspol diglucosidic tetraacetate, 7, 7′-gosspol diglucoside and 6, 7′-gosspol diglucoside to 3T3L1 adipocytes evaluated with an LDH (lactate dehydrogenase) assay were shown in **Figure 3.17**. The cells were incubated for 4 hours after chemical treatment, cell death in the cultures was assessed by determining release of lactate dehydrogenase from the cells into the culture medium. Results from two assays (MTT and LDH) to cancer cell lines and adipocytes showed that the cytotoxicity of compound 7, 7′-gosspol diglucosidic tetraacetate, 7, 7′-gosspol diglucoside and 6, 7′-gosspol diglucosidic tetraacetate, were significantly lower than gossypol and 6, 7′-gosspol diglucoside at $P < 0.05$.
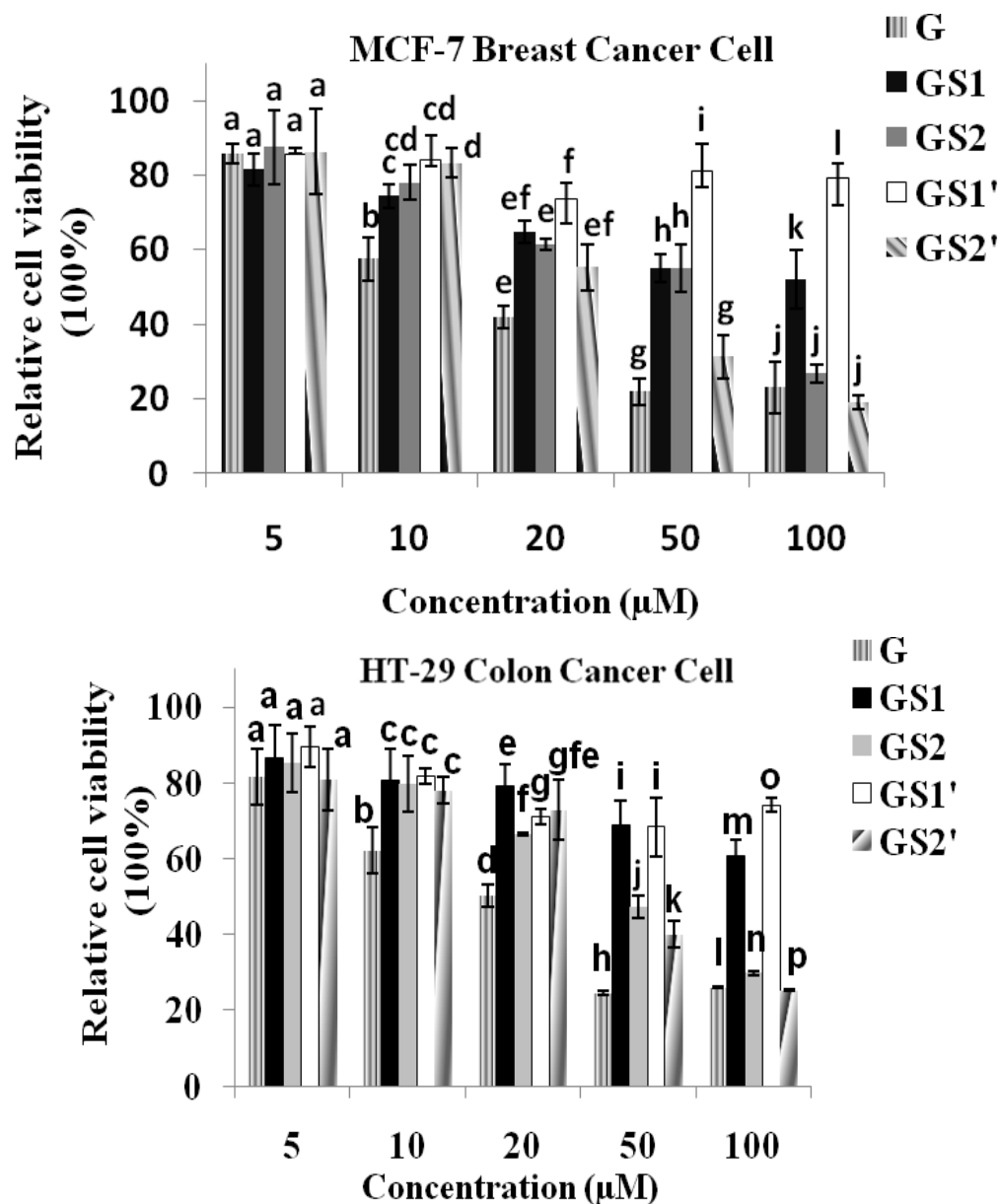
Figure 3.16 Growth inhibition of human breast MCF-7 cancer cell line (top) and human breast HT-29 colon cell line (bottom) incubated with gossypol, gossypol diglycosidic tetraacetates (compound **7** and **8**), gossypol diglycosides (compound **10** and **11**) for 24 hrs. Error bars represent standard deviations of six experiments, and different letters represent significant difference at $P > 0.05$. **G** stands for Gossypol, **GS1** for **7**, **GS2** for **8**, **GS1'** for **10**, **GS2'** for **11**, see **Figure 3.3** and **3.4** about the numbering

The relative cytotoxicity at concentration of 50µM are 57.99%, 22.11%, 23.27%, 23.22%, and 71.05% for gossypol, 7, 7′-gosspol diglucosidic tetraacetate, 6, 7′-gosspol diglucosidic tetraacetate, 7, 7′-gosspol diglucoside and 6, 7′-gosspol diglucoside respectively, while the anti-proliferation activity for cancer cell lines (eg. HT-29 colon cancer cell) at 50µM of those five glycosidic gossypols are 24.57%, 68.85%, 47.26%, 68.29% and 39.95% respectively which give hints that the 6, 7′ isomer-gossypol diglycosidic tetraacetate (compound **8**), targetedly inhibits cancer cell growth with reduced cytotoxic effect to normal cells comparable to un-functionalized gossypol.
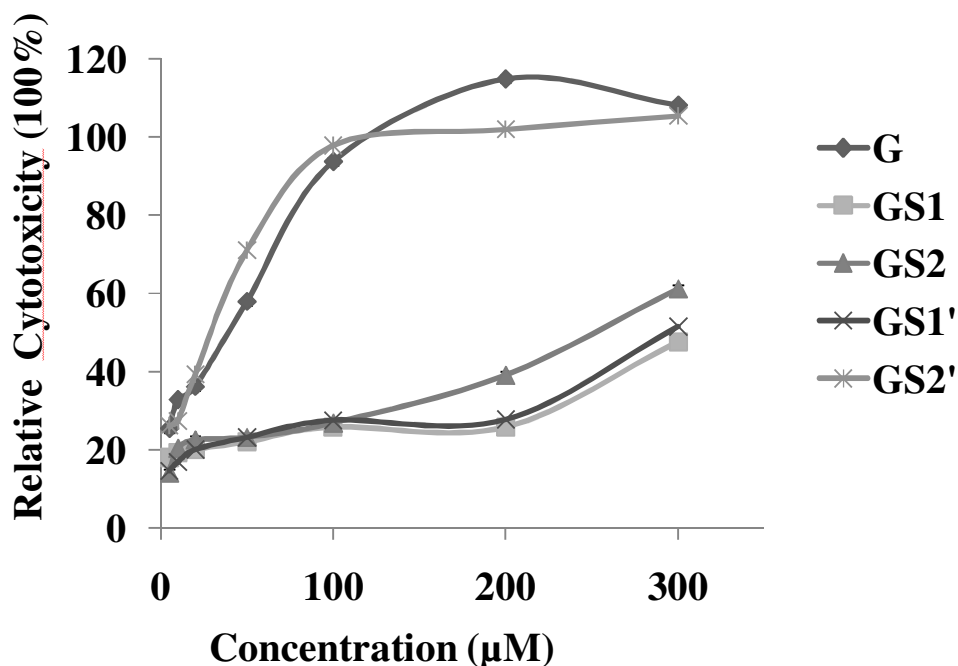

Figure 3.17 The cytotoxicity of gossypol and its glycosidic analogues, data is means of three or more determinations, SD were within 5%. **G** stands for Gossypol, **GS1** for **7**, **GS2** for **8**, **GS1'** for **10**, **GS2'** for **11**, see **Figure 3.3** and **3.4** about the numbering

The naphthalene-based compound gossypol has long been known to exhibit antimalarial and other biological activities. Previous studies have indicated that compounds of this type target plasmodium falciparum lactate dehydrogenase (pfLDH), an essential enzyme for energy generation within the parasite. Crystal structures of the complexes formed by binding of to their target enzyme have been used to delineate the molecular features likely to form the gossypol binding site. Although this core pharmacophore-like molecule only exhibits low levels of inhibitory activity, these molecular snapshots provide a rational basis for renewed structure-based development of naphthalene-based compounds as anti-malarial agents. The impact of the new gossypol glycosides on trypanosoma brucei parasites has also been explored. Gossypol has been reported to inhibit certain oxidoreductases, such as R-hydroxy acid and malate dehydrogenases in trypanosoma. Brucei, and Kaminsky et al. reported that the EC_{50} value of gossypol in 24 hrs growth inhibition test for three separate *T. brucei* strains was over 10 ppm (Kaminsky et al., 1989). In our study, diglycosidic tetraacetates (compound **7**&**8**) have been shown to be most effective against trypanosome brucei with significantly lower LD_{50}s values (2.21 µM and 2.44µM respectively) compared with unmodified gossypol and gossypol diglycosides **10** and **11**(**Table 1** & **Figure 3.18**). The fact that the hemiacetal form in **7** and **8** might probably block themselves from the Schiff base formation with proteins maybe contribute to their potent inhibition effect on trypanosoma brucei cell growth,

	Gossypol	7	8	10	11
LD_{50}	36.90	2.21	2.44	>100	72.60
±SD	10.24	0.09	0.21	------	1.04

Table I. LD_{50} (µM) values of gossypol (**G**), gossypol diglycosidic tetraacetate (**7**&**8**), gossypol diglycoside (**10**&**11**) to trypanosoma brucei cells
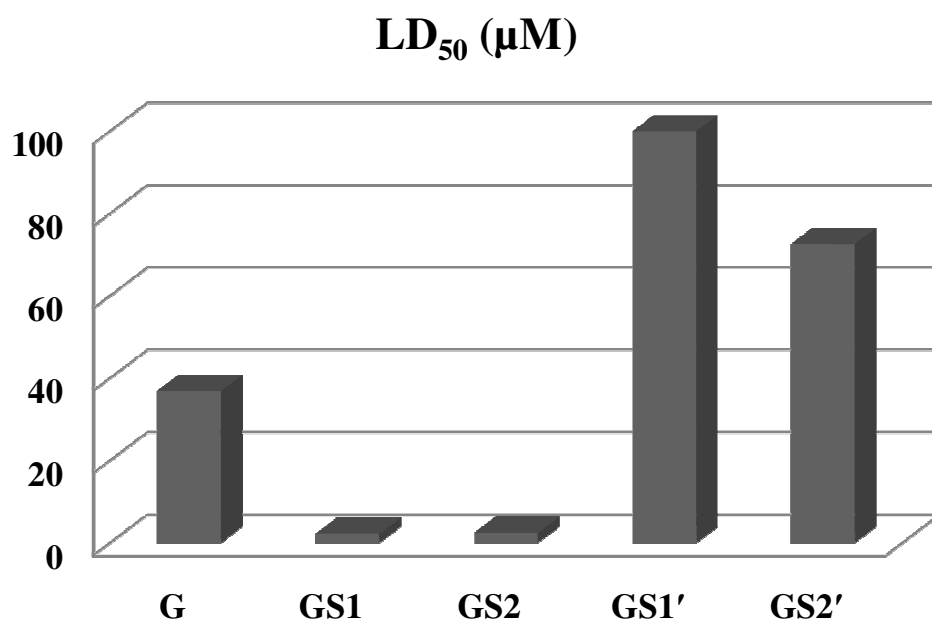
LD_{50} (µM)

Figure 3.18 .The LD_{50} (µM) values of gossypol, gossypol diglycosidic tetraacetates, gossypol diglycosides to trypanosoma brucei cells. **G** stands for Gossypol, **GS1** for **7**, **GS2** for **8**, **GS1'** for **10**, **GS2'** for **11**, see **Figure 3.3** and **3.4** about the numbering

The attenuation of gossypol's impact against trypanosomes is possible partially due to the gossypol protein interactions. In addition, acetyl residues have also been proved to play an essential role in the anti-trypanosomal activity from our results, the non-acetyl gossypol diglycosides (**10**&**11**) which are present as dialdehyde form yield weaker inhibition comparable to unmodified gossypol (72.6μM and >100μM), which is consistent with our hypothesis. Flitter et al. also reported that some specific vaccines containing acetyl residues could elicit reverse biological response (Moe et al., 2009).

3.5 Conclusion

In conclusion, novel glycosidic gossypol analogues were obtained and fully characterized for the first time. The studies of inhibition of cancer cell lines and the cytotoxic effect indicated that the gossypol diglycosidic tetraacetate **8** possessed the lowest cytotoxic effect compared to other gossypol glycosides. Moreover, **8** exhibited strong anticancer as well as anti-trypanosomal activity. It shows that the diglycosidic tetraacetate **8** can be possibly developed as a potential anticancer agent or anti-trypanosomal agent. Further investigation is being carried out in our lab to identify the mechanism of structure activity relationship responsible for the biological activities.

3.6 Reference

Adams, R., and Geissman, T. A. (1938). Structure of gossypol. VII. Gossypol dimethyl ethers. *J. Am. Chem. Soc*. **60**, 2163-2166.

Brzezinski, B. (2009). Synthesis, crystal structures and antibacterial activity studies of aza-derivatives of phytoalexin from cotton plant–gossypol. *Eur. J. Med. Chem*. **44**, 4393-4403.

Clark, E. P. (1927). Studies on gossypol. I. The preparation, purification, and some of the properties of gossypol, the toxic principle of cottonseed. *J. Biol. Chem*. **75**, 725-739.

Dodou, K., Anderson, R. J., Lough, W.J., Small, D. A. P., Shelley, M. D., and Groundwater, P. W. (2005). Synthesis of gossypol atropisomers and derivatives and evaluation of their anti-proliferative and antioxidant activity, *Bioorg. Med. Chem*. **13**, 4228-4237.

Duffey, S. S. (1980). Sequestration of Plant Natural Products by Insects. *Annu. Rev. Entomol*. **25**, 447-477

Fischer, H. E., and Armstrong, E. F. (1901). Ueber die isomeren Acetohalogen derivate des traubenzuckers und die synthese der glucoside. *Ber. Dtsch. Chem. Ges.*, **34**, 2885–2900.

Gallup, W. D. (1931). Studies on the toxicity of gossypol. I. The response of rats to gossypol administration during avitaminosis. *J. Biol. Chem*, **93**, 381-405.

Haas, R. H., and Shirley, D. A. (1965). The oxidation of gossypol II. formation of gossypolone with ferric chloride. *J. Org. Chem*. **30**, 4111-4113.

Jacobsson, M., Malmberg, J., and Ellervik, U. (2006). Aromatic O-glycosylation. *Carbohydr. Res*. **341**, 1266-1281.

Kaminsky, R., and Zweygarth, E. (1989). Feeder layer-free in vitro assay for screening antitrypanosomal compounds against *Trypanosoma brucei* and T. b. evansi. *Antimicrob. Agents Chemother*. **33**, 881-885.

Koenigs, W., and Knorr, E. (1901). Ueber einige Derivate des Traubenzuckers und der Galactose . *Berichte der deutschen chemischen Gesellschaft*. **34**, 957–981.

Liang, X. S., Rogers, A. J., Webber, C. L., Ormsby, T. J., Tiritan, M. E., Matlin, S. A., and Benz, C. C. (1995). Developing gossypol derivatives with enhanced antitumor activity*Invest. New Drug*. **13**, 181-186.

Majak, W. (1992). Mammalian metabolism of toxic glycosides from plants. *Toxin Reviews.* **11**, 1-40.

Meltzer, P. C., Bickford, P. H., and Lambert, G. (1985). A regioselective route to gossypol analogues: the synthesis of gossypol and 5, 5′-didesisopropyl-5, 5′-diethylgossypol. *J. Org. Chem.* **50**, 3121-3124.

Moe, G. R. Bhandari, T. S., and Flitter, B. A. (2009). De-*N*-acetyl-gangliosides in humans. *J. Immunol.* **182**, 6610-6617.

Moon, D. O., Kim, M. O., Lee, J. D., and Kim, G. Y. (2008) Gossypol suppresses NF-kappaB activity and NF-kappaB-related gene exp ression in human leukemia U937 cells. *Cancer. Lett.* **264**, 192-200.

Morris, R. C., and Adams, R. (1937). Structure of gossypol. III. Gossypol ethers. *J. Am. Chem. Soc.* **59**, 1731-1735.

Porat, O. (1990), Effects *of* gossypol on the motility *of* mammalian spermatozoa. *Mol. Reprod. Dev.* **25**, 400-408.

Przybylski, P., Huczynski, A., Pyta, K., Brzezinski, B., and Bartl, F. (2009a). Biological properties of Schiff bases and azo derivatives of phenols. *Curr. Org. Chem.* **13***, 124-148.

Przybylski, P., Pyta, K., Remlein, D., Schroeder, G., Brzezinski, B., and Bartl, F. (2009b). Antifungal activity of alkyl and heterocyclic aza-derivatives of gossypol as well as their complexes with $NaClO_4$ against Fusarium oxysporum *f. sp. lupini. Bioorg. Med. Chem. Lett.* **19**, 1996-2000.

Przybylski, P., Pyta, K., Stefanska, J., Sitarz, M. R., Katrusiak, A., Huczynski, A., and Brzezinski, B. (2009c). Synthesis, crystal structures and antibacterial activity studies of aza-derivatives of phytoalexin from cotton plant--gossypol. *Eur. J. Med. Chem.* **44**, 4393-4403.

Radloff, R. J., Deck, L. M., Royer, R. E., Vander, J., and David, L. (1986). Antiviral activities of gossypol and its derivatives against herpes simplex virus type II. *Pharmacol. Res. Comm.* **18**, 1063-1073.

Razakantoanina, V., Phung, N. K. P., and Jaureguiberry, G. (2000). Antimalarial activity of new gossypol derivatives. *Parasitol. Res.* **86**, 665-668.

Rezhepov, K. Zh., Ziyaev, Kh. L., Baram, N. I., Ismailov, A. I., Kamaev, F. G., and Saiitkulov, A. M. (2002). Synthesis and interferon-inducing activity of azo-derivatives of gossypol and its imines. *Chem. Nat. Compd.* **38**, 319-322.

Royer, R. E., Mills, R. G., Young, S. A., and Vander Jagt, D. L. (1995). Comparison of the antiviral activities of 3'-azido-3'-deoxythymidine (AZT) and gossylic iminolactone (GIL) against clinical isolates of HIV-1. *Pharmacol. Res.* **31**, 49-52.

Shelley, M. D., Hartley, L., Groundwater, P. W., and Fish, R. G. (2000). Structure activity studies on gossypol in tumor cell lines. *Anti-Cancer Drug.* **11**, 209-216.

Talipov, S. A., and Ibragimov, B.T. (1999). X-Ray crystal structure of four inclusion complexes of the novel host gossindane: an oxidation product of gossypol. *J. Inclusion Phenom. Macrocyclic Chem.* **31**, 27-38.

Zhu, G. D., Chen, D. H., Huang, J. H., and Chi, C. S. (1992). Regioselective bromination and fluorination of apogossypol hexamethyl ether. *J. Org. Chem.* **57**, 2316-2320.
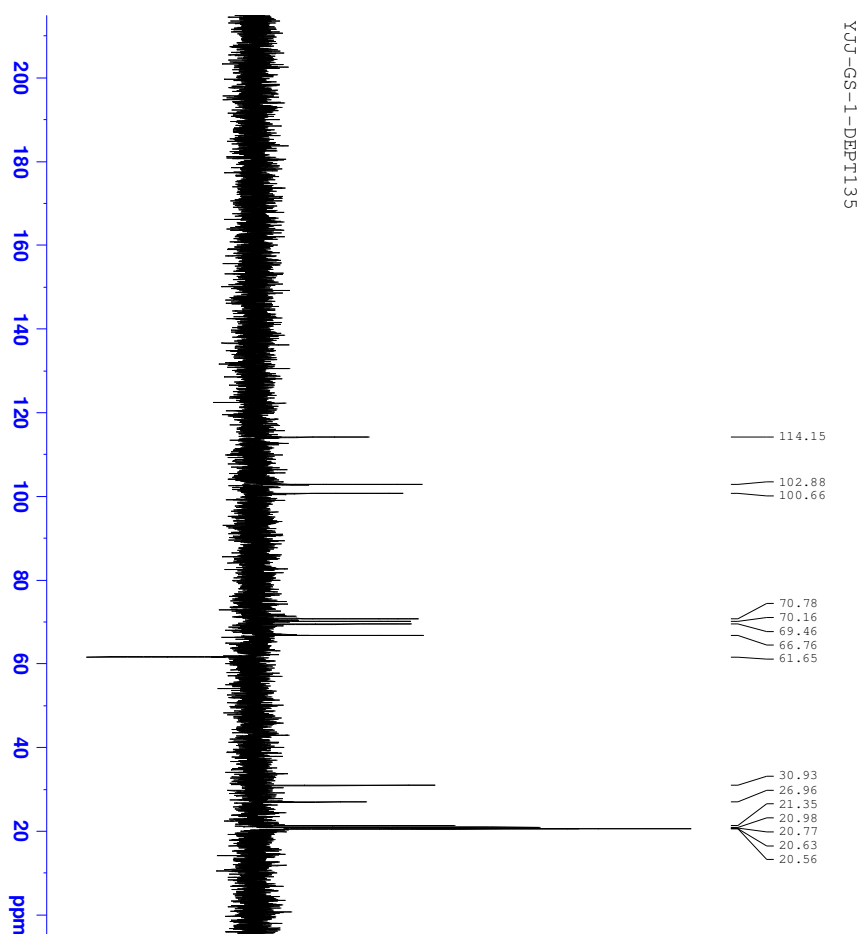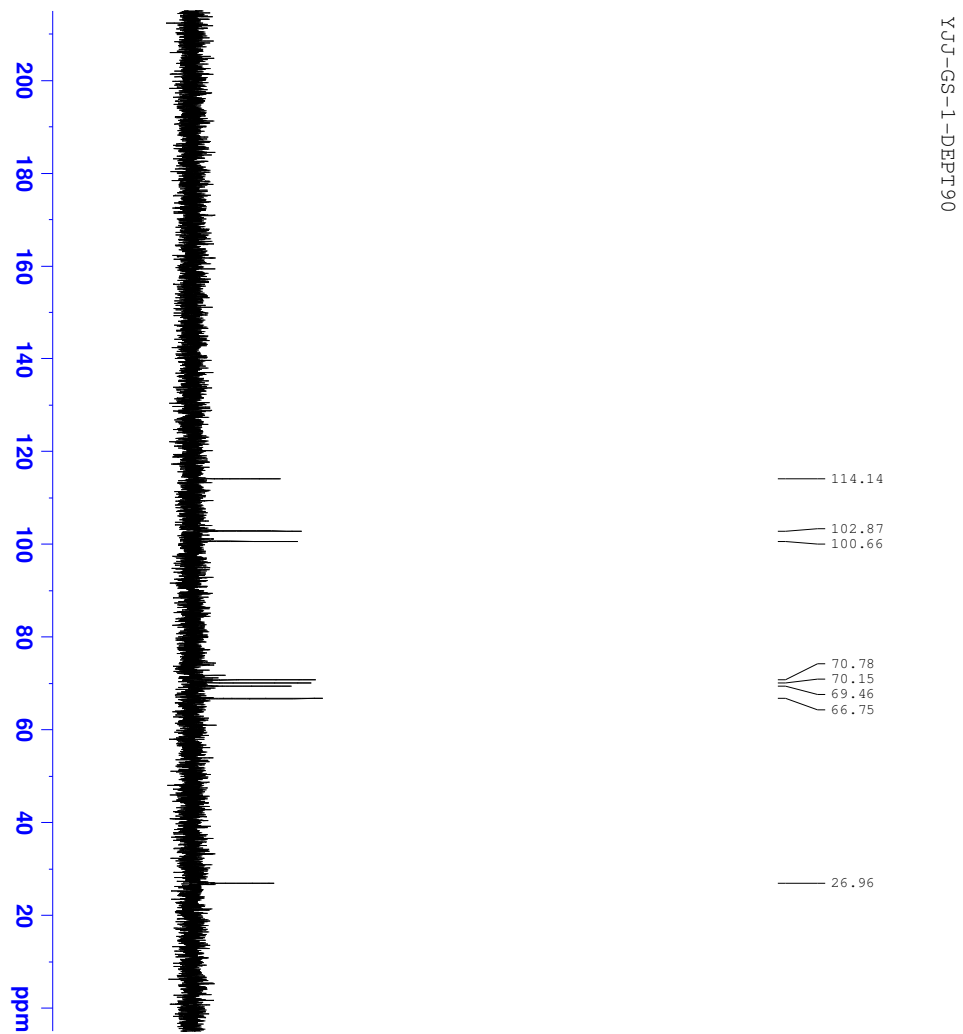
Figure A3. 1 The DEPT 135^0 spectra of **7**
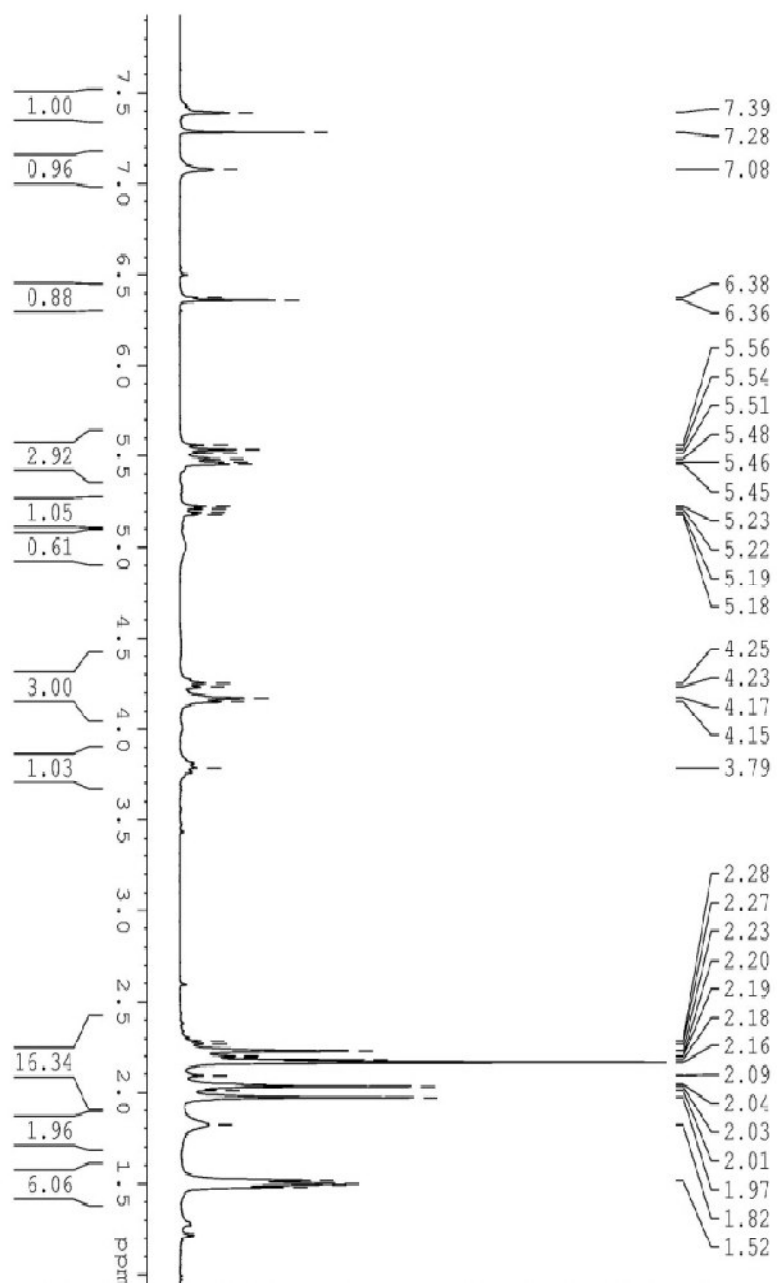
Figure A3.2 The DEPT 90^0 spectra of **7**

Figure A3.3 ^{1}H NMR spectra of **8**
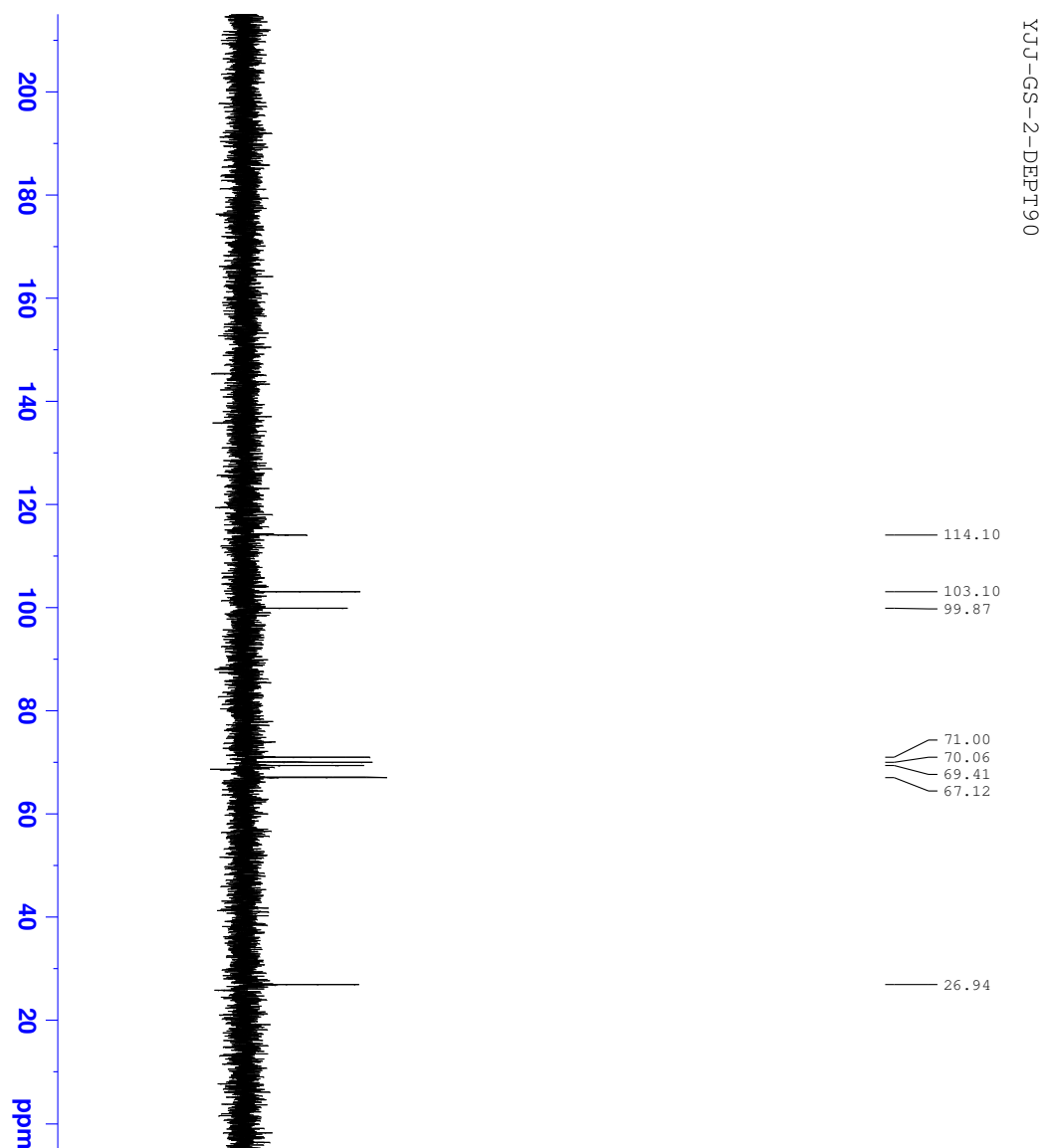
Figure A3.4 The DEPT 90^0 spectra of **8**

YJJ-GS-2-DEPT135

200 180 160 140 120 100 80 60 40 20 ppm

114.10
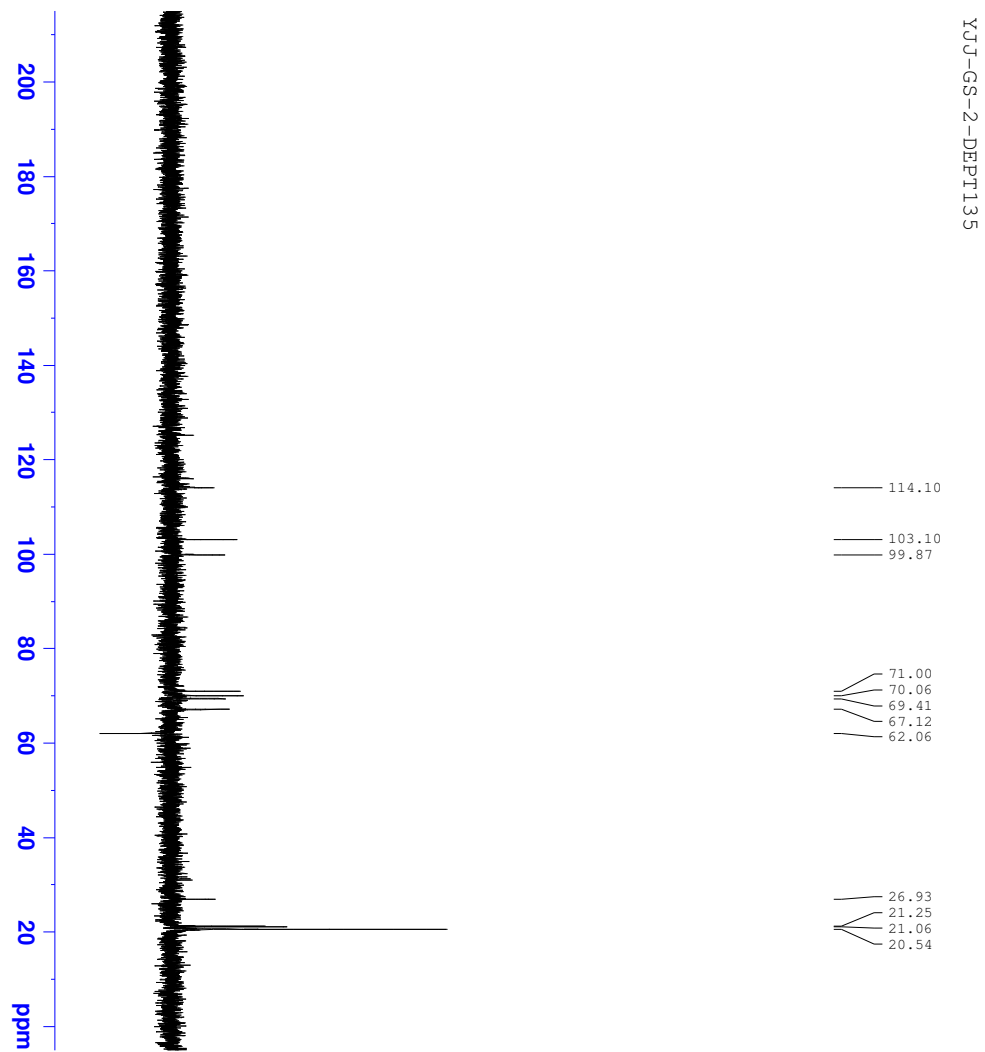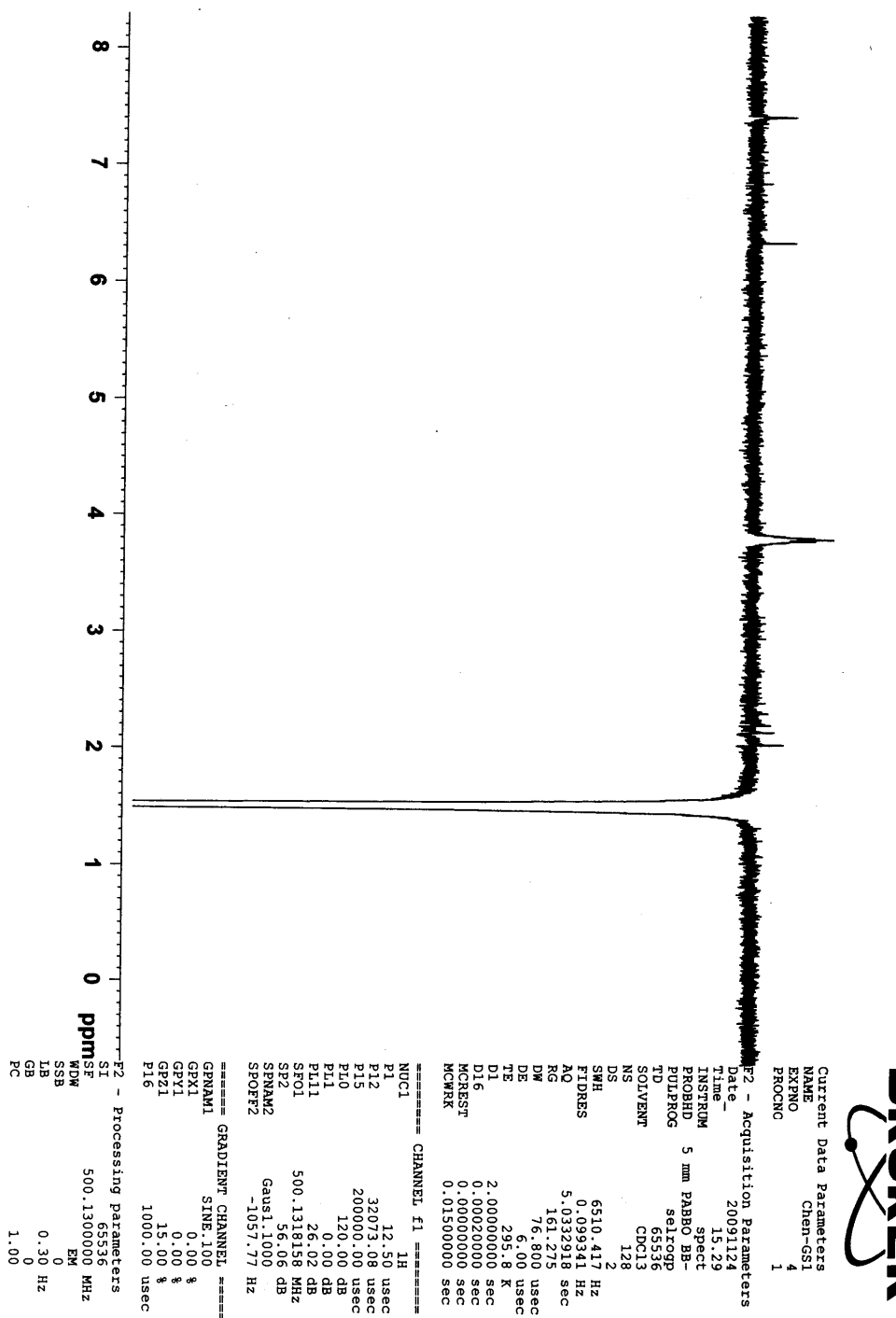
103.10
99.87

71.00
70.06
69.41
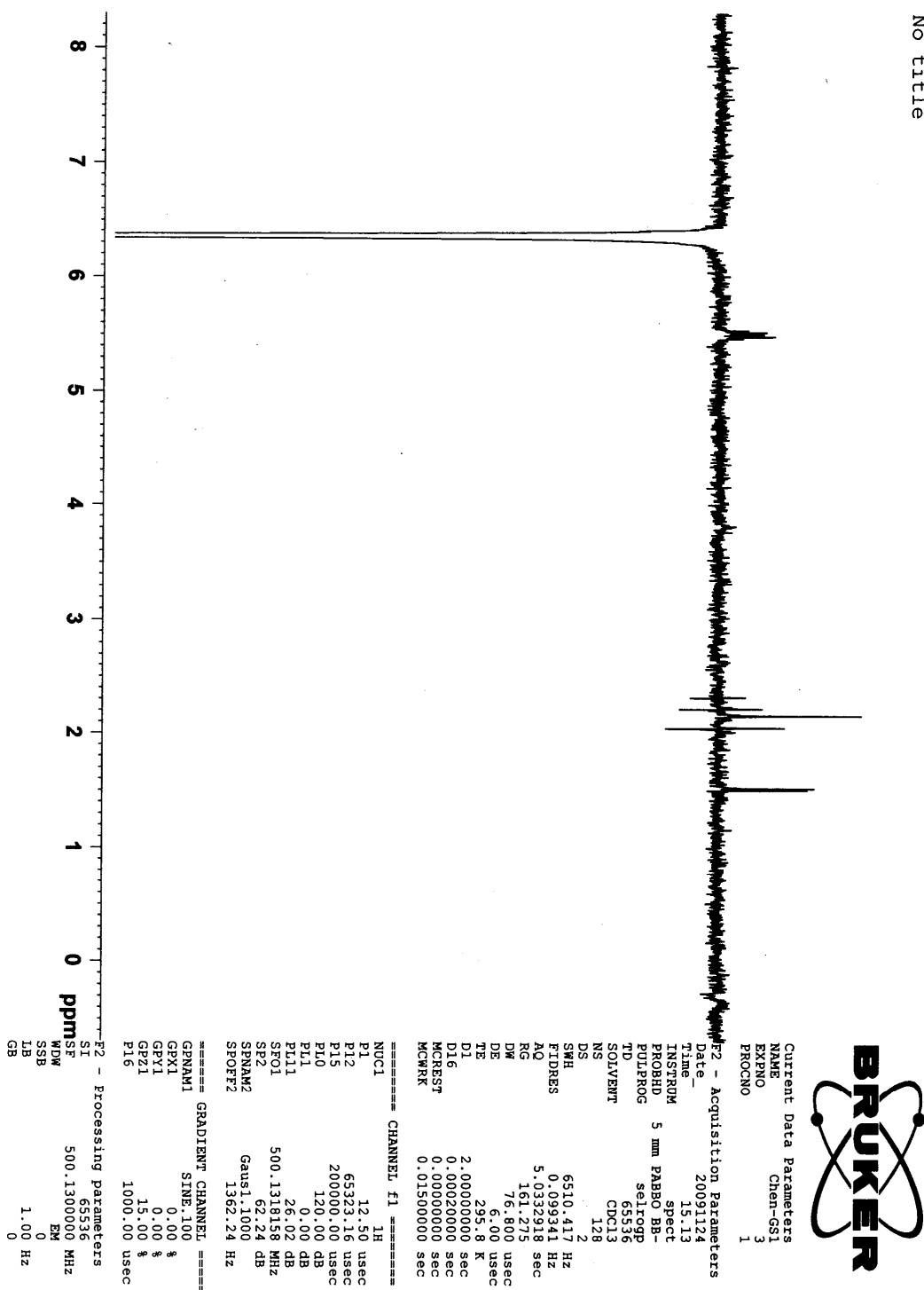67.12
62.06

26.93
21.25
21.06
20.54

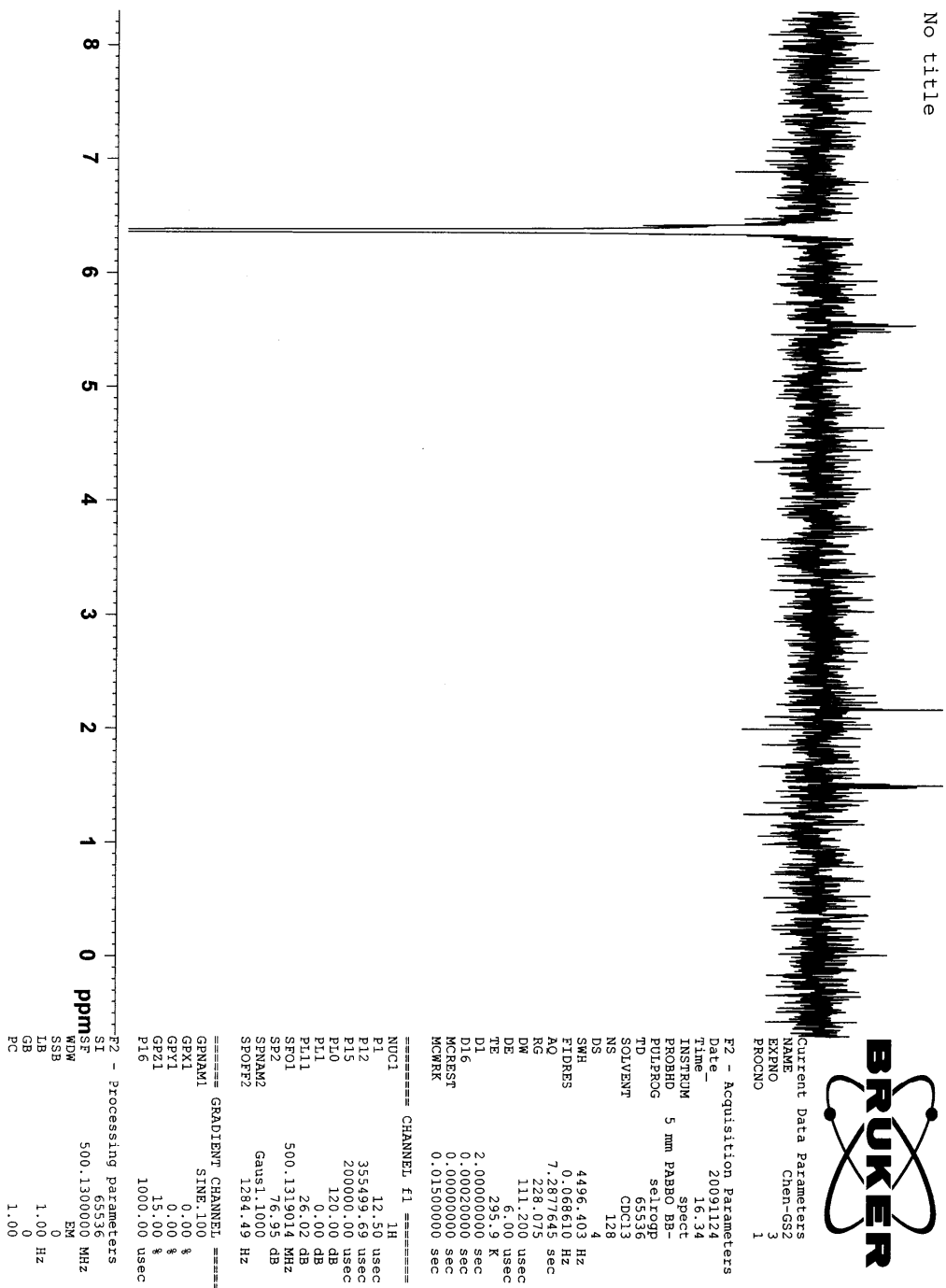**Figure A3.5** The DEPT 135^0 spectra of **8**
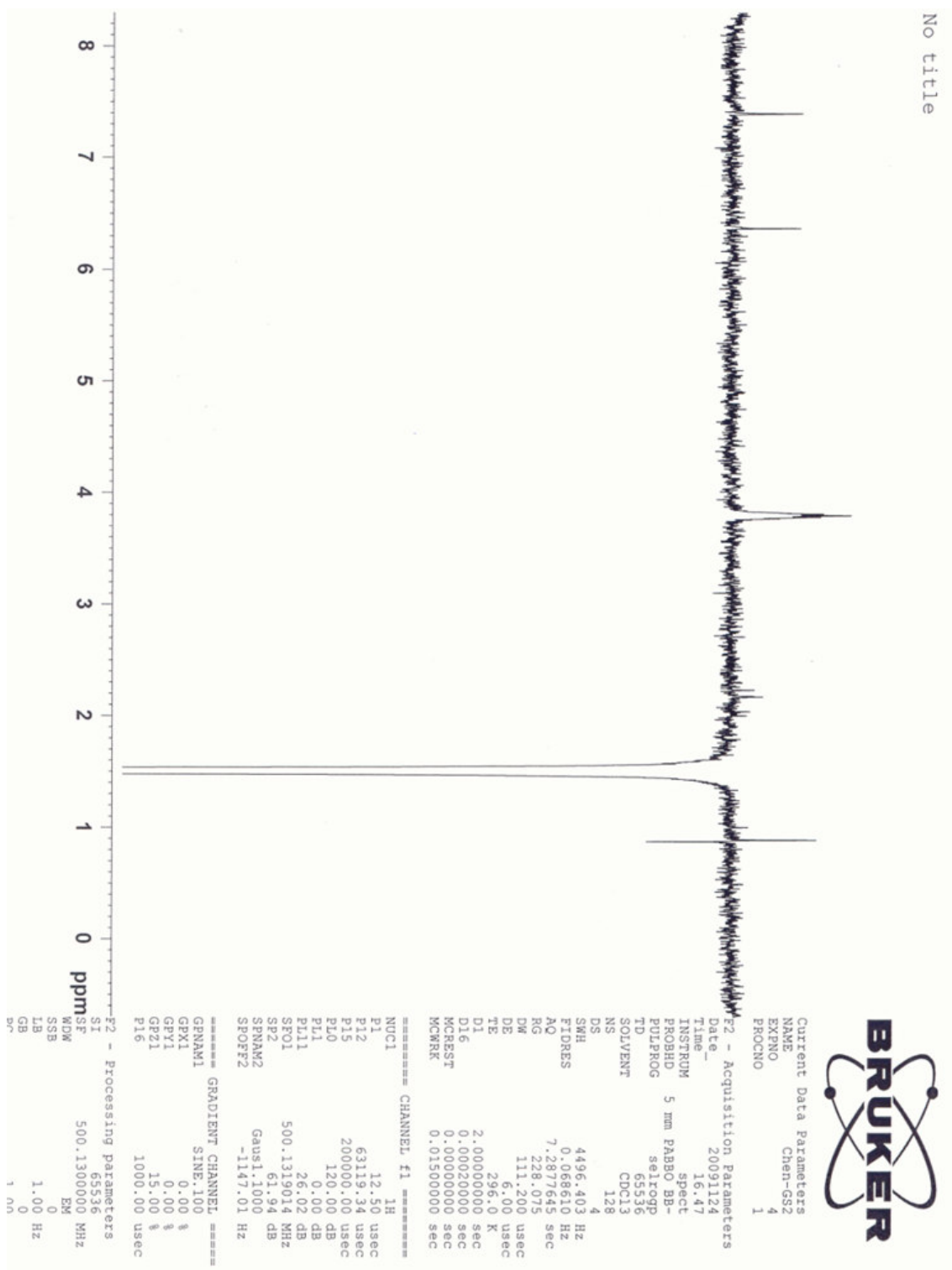
(Figure A3.6-1)

(Figure A3.6-2)

Figure A3.6 The 1D NOE spectra of **7** (A, B)

(Figure A3.7-1)

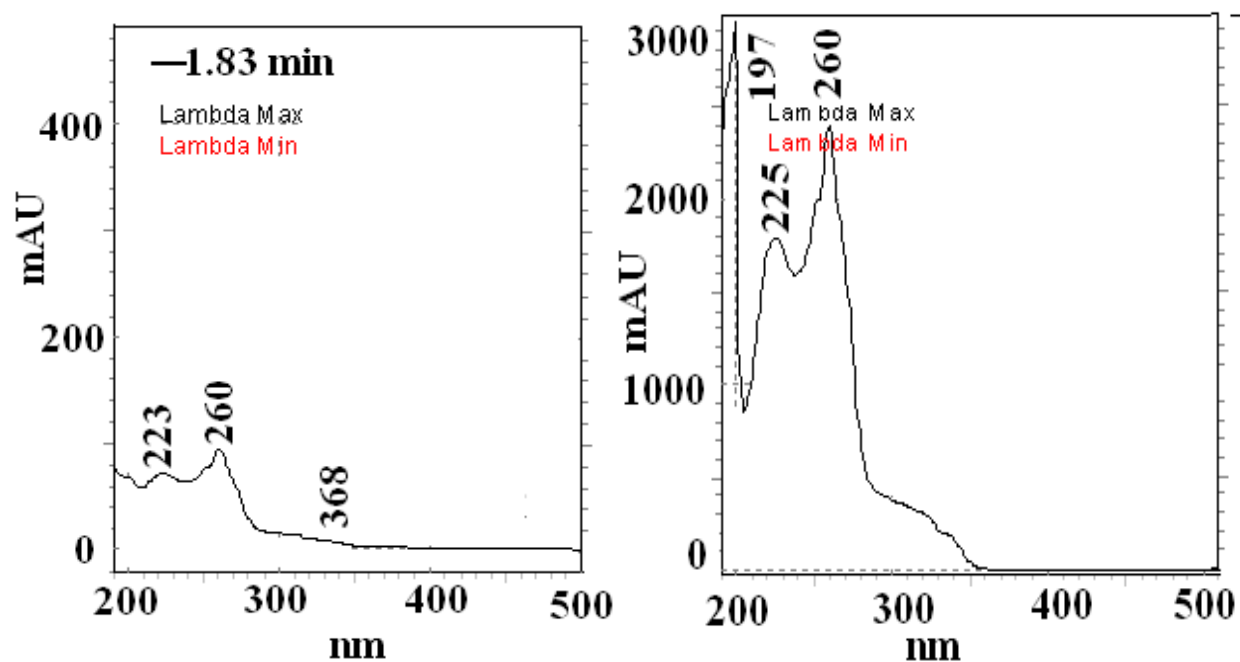(**Figure A3.7-2**)

Figure A3.7 The 1D NOE spectra of **8**

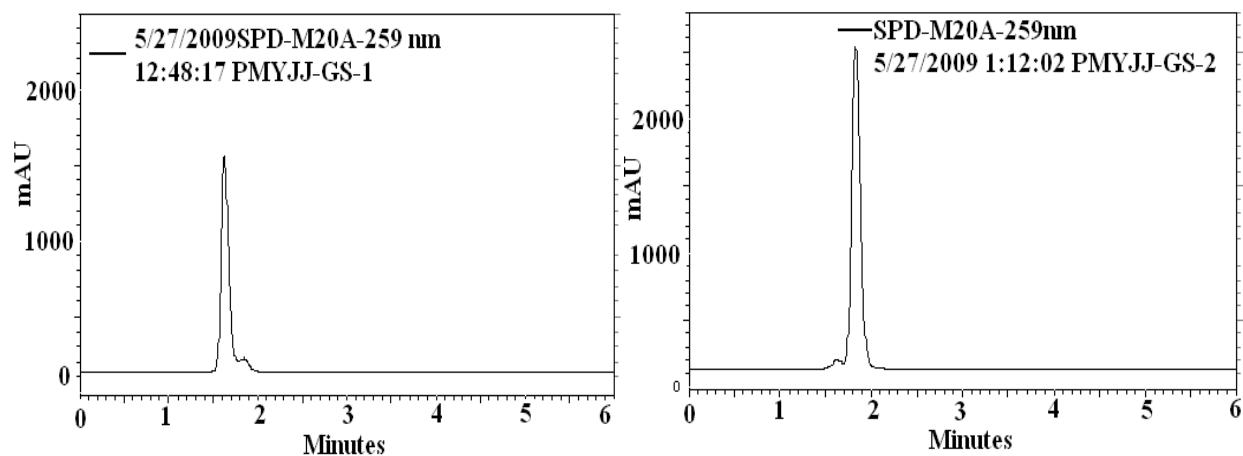**Figure A3.8** The UV spectra of **7** (left) and **8** (right)

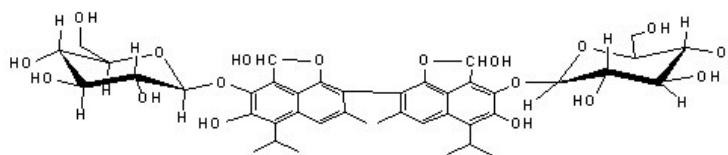**Figure A3.9** The HPLC spectra of **7**(left) and **8** (right)

*MSD1 SPC, time=0.213 of C:\CHEM32\1\DATA\YJJ\GS10H00002.D
ES-API, POS, Scan,Frag:140, "Scan 100-850"

Max: 138112
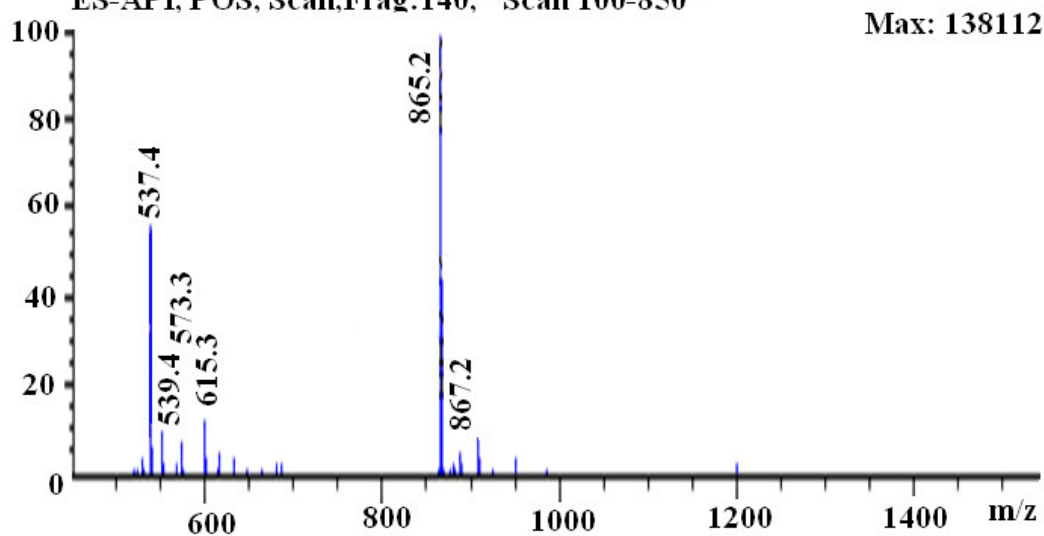
*MSD1 SPC, time=0.211 of C:\CHEM32\1\DATA\JulieJ\1000009.D
ES-API, NEG, Scan,Frag:140, "Scan 100-850"

Max:357736
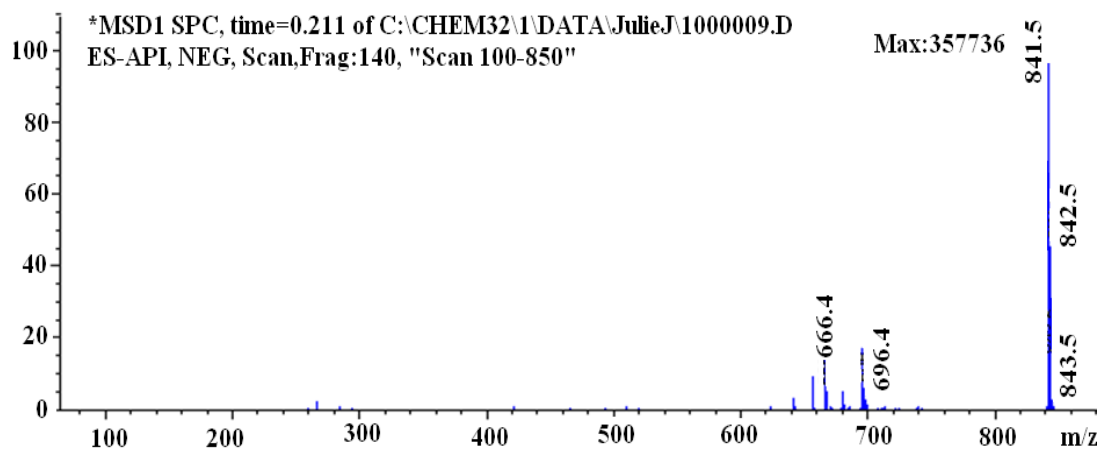
Figure A3.10 The MS spectra of **10**, m/z=[M+Na]$^+$=865.2(Positive mode: top), m/z=[M-H]$^-$=841.5(Negative mode: bottom)
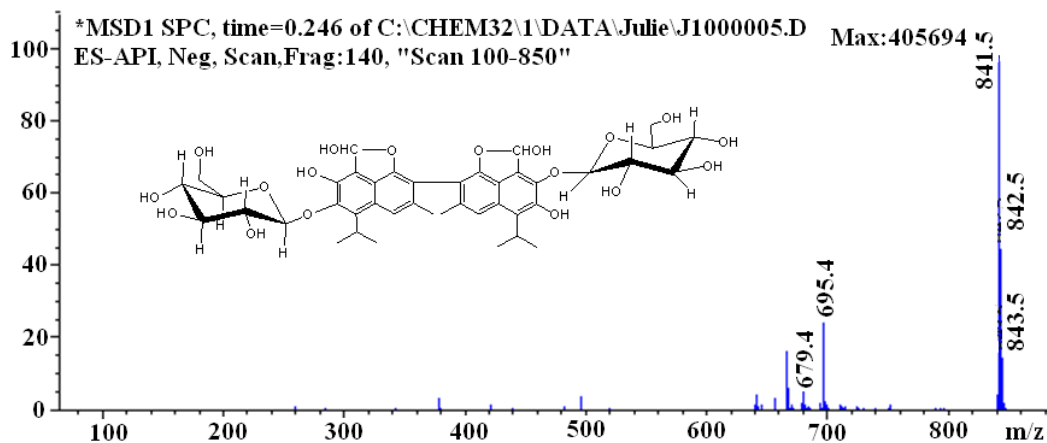
Figure A3.11 The MS spectra of **11**, m/z = [M-H]$^-$=841.5(Negative mode)
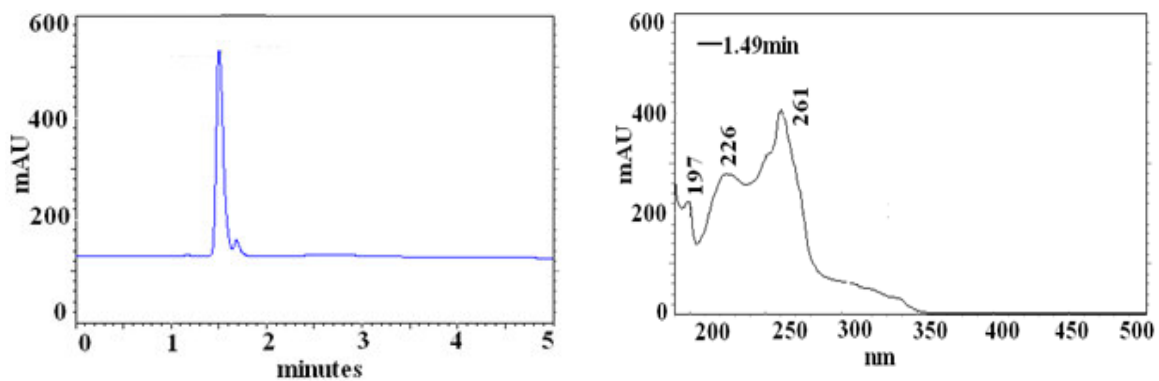
Figure A3.12 The HPLC and UV spectra of **10**
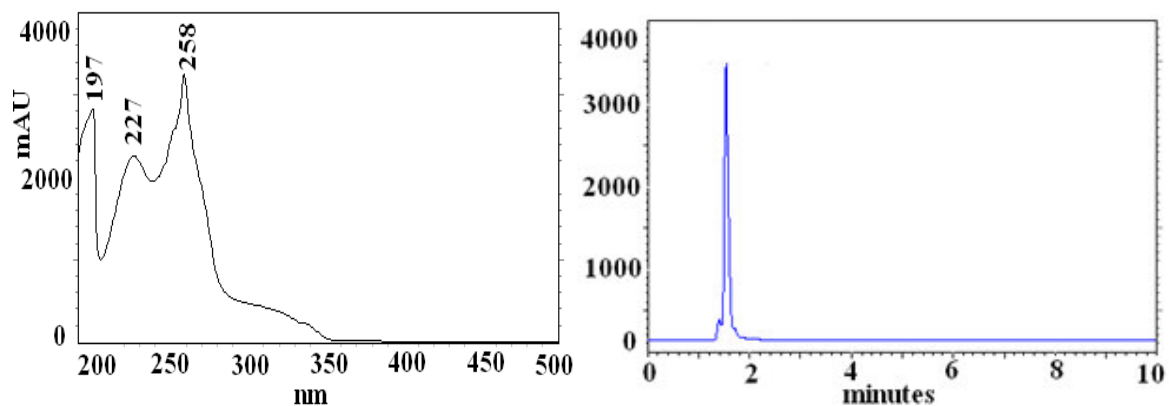
Figure A3.13 The HPLC and UV spectra of **11**
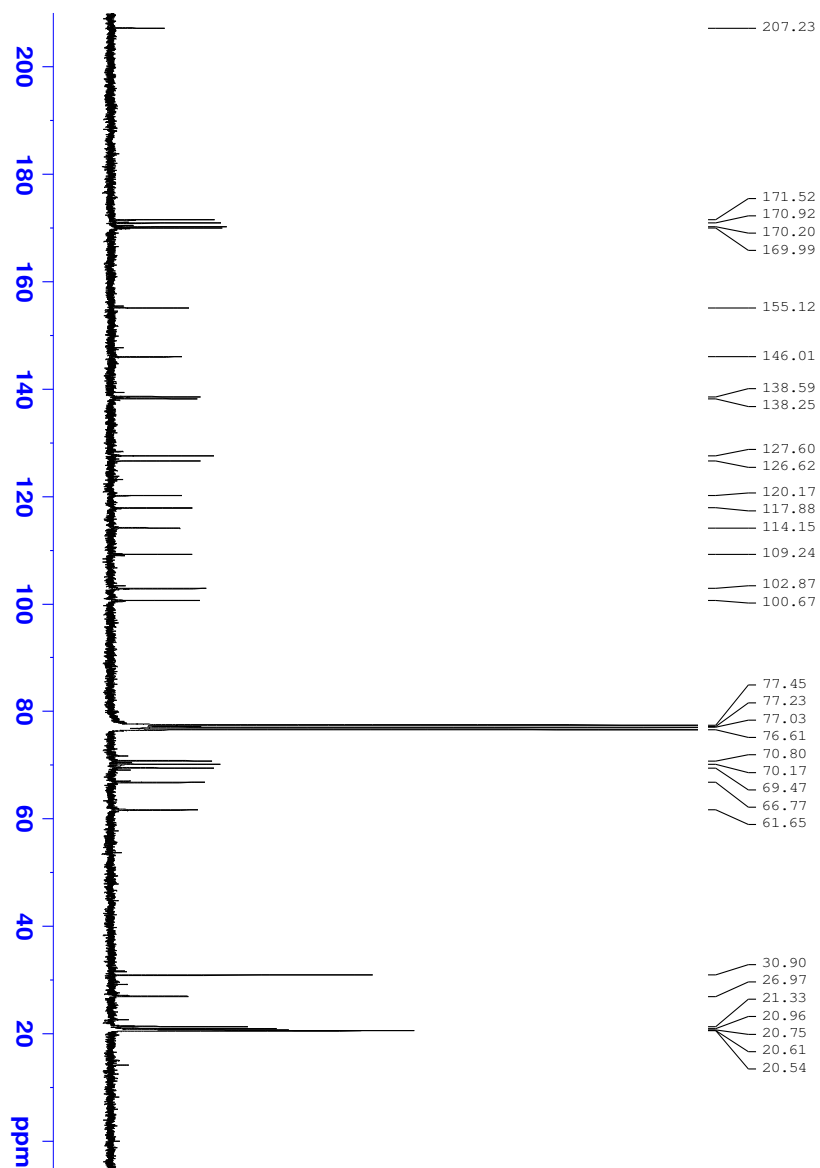
Figure A3.14 The ^{13}C NMR spectrum of **7**

207.23

171.52
170.92
170.20
169.99

155.12

146.01

138.59
138.25

127.60
126.62

120.17
117.88
114.15

109.24

102.87
100.67

77.45
77.23
77.03
76.61
70.80
70.17
69.47
66.77
61.65

30.90
26.97
21.33
20.96
20.75
20.61
20.54
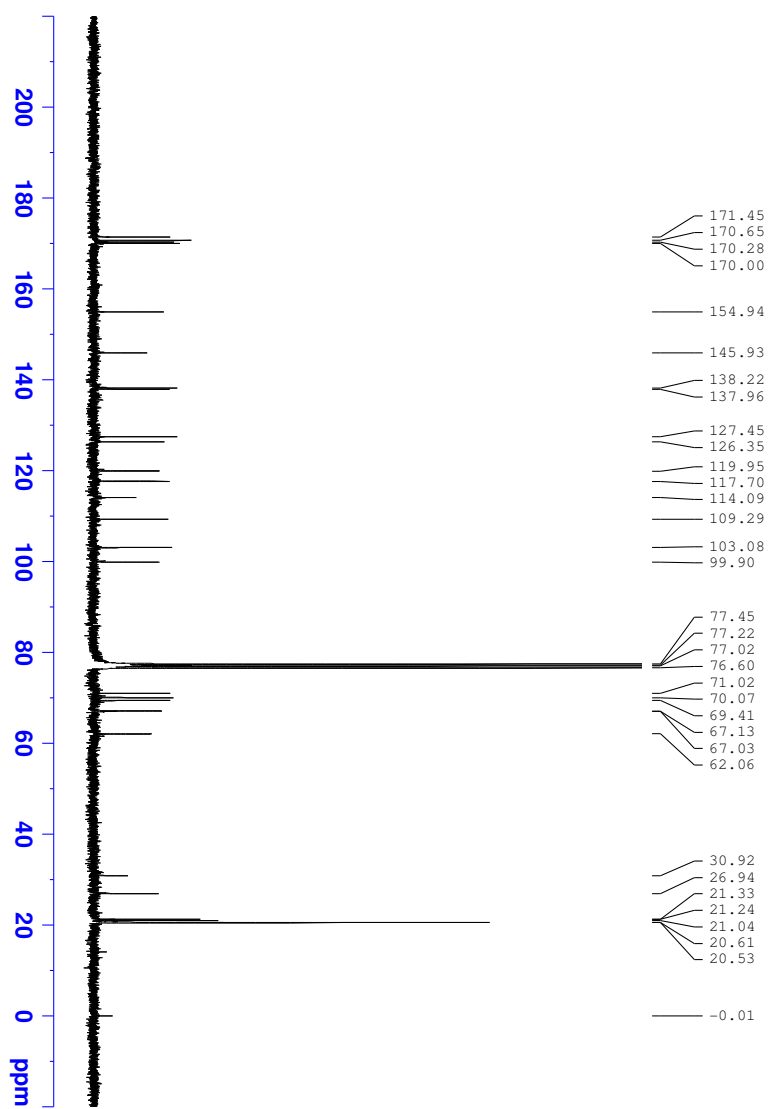
Figure A3.15 The ^{13}C NMR spectrum of **8**

171.45
170.65
170.28
170.00

154.94

145.93

138.22
137.96

127.45
126.35
119.95
117.70
114.09
109.29
103.08
99.90

77.45
77.22
77.02
76.60
71.02
70.07
69.41
67.13
67.03
62.06

30.92
26.94
21.33
21.24
21.04
20.61
20.53

-0.01

CHAPTER 4

UNEXPECTED FORMATION OF N-METHYLFULLEROPYRROLIDINES BY THE REACTION OF FULLERENE AND GOSSYPOL AND THEIR BIOACTIVITIES

4.1 Abstract

Fullerene [60] reacted with 2, 2′-bis-(formyl-1, 6, 7 trihydroxy-5-isopropyl-3-methylnaphthalene) (gossypol) in the presence of sarcosine through the Prato reaction, this reaction resulted in some unexpected N-methylfulleropyrrolidines, and different products in variable yield were obtained when choosing toluene or chlorobenzene as reaction medium. These fulleropyrrolidines were fully characterized via rigorous structure determination through multiple spectral experiments, which included 1D NMR (^{1}H NMR, ^{13}C NMR, the DEPT), 2D NMR (HMQC, HMBC), UV, FT-IR, HRMS, HPLC and X-ray crystallography. During the reaction, gossypol decomposed into benzaldehyde which was successfully detected as a new intermediate through GC–MS spectra, although the polyphenolic gossypol undergoes decomposition under drastic conditions such as heat and high pressure and the detailed composition have been studied, this new intermediate has never been detected and reported.

Besides, in an in vitro assay of NO radical induced apoptosis in 3T3L1 cells for the N-methylfulleropyrrolidines and pure fullerene, N-methylfulleropyrrolidine (the

compound **7**) and N-methyl-2, 2-dimethylfullerpyrrolidine (the compound **8**) showed dose dependent and stronger radical scavenging activities than the parent fullerene.

The study in this chapter enriched the chemistry of gossypol l and gave a hint to illustrate the mechanism during the decomposition f gossypol.

4.2 Introduction

Buckminster fullerene also called bucky ball is a distinct state of carbon. They were reported by Kroto *et al.* (1985; 1991) in the form of C60 molecules. Since then there have been various studies for the utilization of this physically stable but chemically reactive molecule. Applications of C60 in areas such as optical devices, semiconductors, chemical sensors, catalysis and in the medical field have been explored (Yadav et al., 2008). While among various potential properties of the parent fullerene and fullerene derivatives, biomedicinal function might be one of the most promising utilities (Hirsch et al., 1994; Jensen et al., 1996; Daros et al., 1999; Bolskar et al., 2003; Zhou et al., 2001). The capability of C60 and its derivatives to scavenge

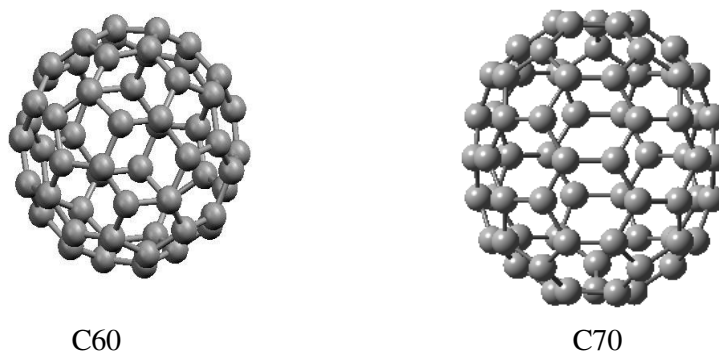C60   C70

Figure 4.1 The molecule structures of fullerene [60], fullerene [70]

free radicals enables them to be a potentially useful source of new chemotherapeutic agents in the prevention or treatment of some chronic diseases, such as AIDS (HIV-1 protease inhibition) (Marcorin et al., 2000; Friedman et al., 1998; Zhu et al., 2003), malignant tumors (Mashino et al., 2003), osteoporosis (Gonzalez et al., 2002; Mirakyan et al., 2002; Yin et al., 2005; Yin et al., 2006) etc, fullerene and its derivatives also possess neuroprotective, antibacterial and gene transfection properties(Susanna et al., 2003). Moreover, it has been recognized that fullerenes are one of the key building blocks for nanoscale materials, C60 has been considered as interesting candidate for constructing nanoparticulate drug delivery systems that are able to be loaded with various biofunctional agents for providing different bioactivities (Maggini et al., 1993; Georgakilas et al., 2002).

Nanoparticle based drug delivery systems have considerable potential for treatment of some certain diseases. The important technological advantages of nanoparticles used as drug carriers are high stability, high carrier capacity, feasibility of incorporation of both hydrophilic and hydrophobic substances, and feasibility of variable routes of administration. Nanoparticles can also be designed to allow controlled (sustained) drug release from the matrix. These properties of nanoparticles enable improvement of drug bioavailability and reduction of the dosing frequency, Nanoparticles for the purpose of drug delivery are defined as submicron colloidal particles. This definition includes monolithic nanoparticles or nanospheres in which the drug is adsorbed, dissolved, or dispersed throughout the matrix and nanocapsules

in which the drug is confined to an aqueous or oily core surrounded by a shell-like wall. Alternatively, the drug can be covalently attached to the surface or into the matrix (Gelperina et al., 2005).

In our study, the original purpose is to synthesize a covalent bonded fullerene gossypol conjugate through 1, 3-dipolar cycloaddition as the following **Figure 4.2** and **4.3** shows.

The Prato reaction or 1, 3-dipolar cycloaddition which is the most versatile and wildly used method to functionalize fullerene, there need an aldehyde group bearing molecule, and an α-terminal amino acid and unsaturated compound, the pyrrolidine
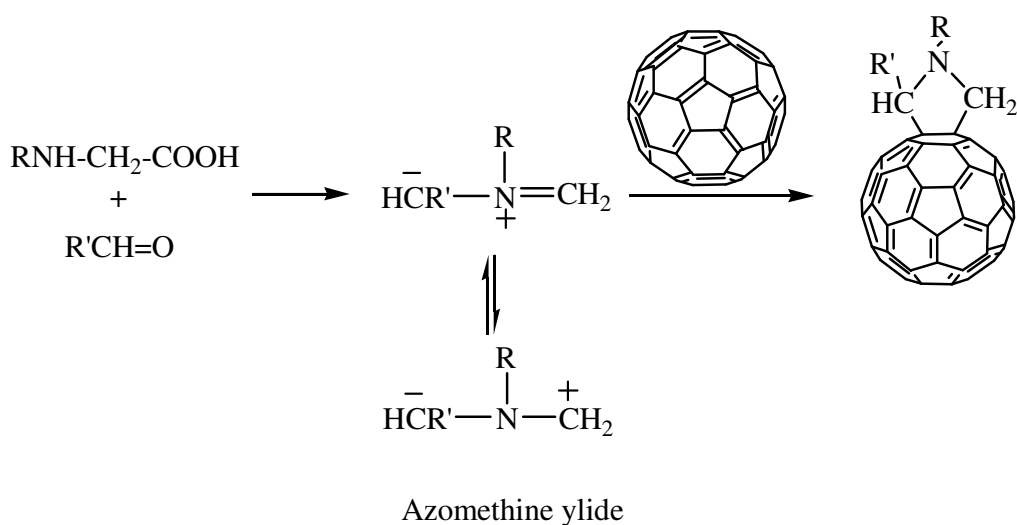

Azomethine ylide

Figure 4.2 The reaction of C60 with azomethine ylide through the Prato reaction
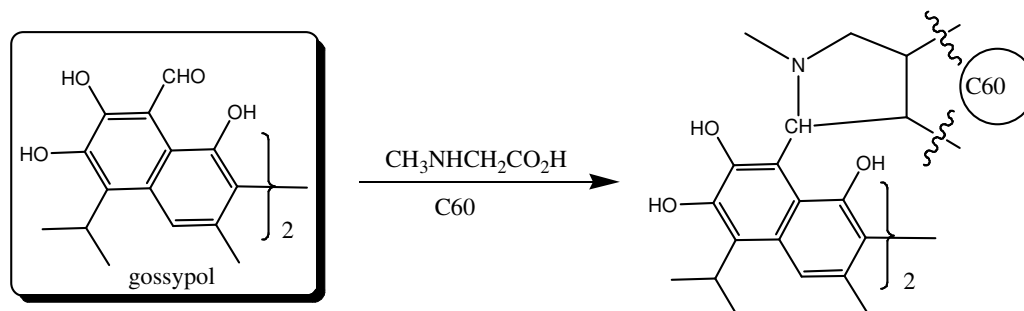
Figure 4.3 The reaction between gossypol and C60

like derivatives were obtained though a azomethine ylide as intermediate (Maggini et al., 1993).

Some pioneering work has been initiated to make various functional fullero-pyrrolidines, which are regarded as versatile building blocks for fullerene containing functional molecules. As we mentioned before, gossypol, which is a polyphenolic compound widely existing in members of the Malvaceae family and particularly rich in cottonseed, has two aldehyde groups and possesses a wide spectrum of biological activities such as contraceptive, antiviral, antiamoebic and antiprotozoan effects. While gossypol displays toxicity to a few of system in mammals as we introduced in the review in Chapter1, and gossypol is hydrophobic compound which to some extent limit the bioavailability of gossypol. Some researchers reported that the aldehyde

group could bind to proteins when it is consumed by human or animals. If the fullerene based gossypol could be obtained through the 1, 3-cycloaddition and the reactive aldehyde groups would be blocked and the lower toxicity was expected. In addition, the fullerene residue is more lipophilic, so the designed nano-based gossypol could become more lipophilic and maybe affect the way of administration and the process of absorption, distribution, metabolism, and excretion. Gossypol is considered suitable for making nanoparticlebased drug for its multiple bioactivities and chemical reactivity of gossypol.

In this context, an attempt to synthesize a fullerene–gossypol hybrid was conducted by 1, 3-dipolar addition, the Prato reaction. However, fulleropyrrolidines rather than the expected fullerene–gossypol hybrid were formed. These fulleropyrrolidines were fully characterized via rigorous structure determination through multiple spectral experiments such as 1D NMR (^{1}H NMR, ^{13}C NMR, DEPT), 2D NMR (HMQC, HMBC), UV, FT-IR, HRMS, HPLC and X-ray crystallography. In the course of synthesis and with the aid of gas chromatography–mass spectrometry (GC–MS), we found that benzaldehyde was formed as a new reaction intermediate from gossypol degradation upon heating in toluene. In 1930s, Adams and his coworkers (1938; 1939) found that, under heating conditions, gossypol ethers degraded into a reaction intermediate termed gossic acid, which had roughly half molecule of gossypol. In addition, Clark and his coworkers (1928) found that formic acid, acetic acid, n-butyric acid, as well as iso-butyric acid were formed as

decomposition products during the reaction between gossypol and potassium permanganate in sodium hydroxide solution. In the present study, benzaldehyde was found for the first time to be an intermediate for gossypol reactions.

4.3 Experimental

4.3.1 Materials

Fullerene [60] (99.5%) was purchased from SES Research, Houston, TX, USA. All organic solvents (HPLC grade) were distilled in vacuum in order to reduce the content of dissolved oxygen or filtrated by 0.2micro PVDF membrane filter. Toluene, chlorobenzene were purchase from Fisher Scientific, Pittsburgh, PA, USA. The solvents were dehydrated by distillation in the presence of CaH_2. 1, 2-dichlorobenzene-d4 and chloroform-d was from Cambridge Isotope Laboratories, Inc., MA, USA. Carbon disulfide (CS_2, MW=76.14). Sarcosine (*N*-methylglycine, $C_3H_7NO_2$, MW=89.09) was from Alfa Company, MA, USA. Gossypol acetic acid was isolated by Soxhlet extraction, 6-methoxygossypol and 6, 6-dimethoxygossypol were provided by USDA-SRRC. Both methoxygossypol derivatives were 1:1 M solvates of acetic acid. Like gossypol acetic acid (1:1), both methylated gossypols are racemic. Sodium nitroprusside (SNP, $Na_2 [Fe(CN)_5NO]\cdot2H_2O$, MW= 261.92) was from Sigma–Aldrich (Atlanta, GA). Heat-inactivated fetal bovine serum, fetal bovine serum, and newborn calf serum were purchased from Hyclone Laboratories, Inc. (Logan, UT). 3T3L1 fat cells were purchased from the American Type Culture

Collection (ATCC) (Rockville, MD). The CellTiter96 Aqueous assay kitwas purchased fromPromega, Madison, WI.

4.3.2 Instruments

4.3.2.1. X-ray analysis

The X-ray diffraction data were collected with graphite-monochromated Cu Ka radiation (k = 0.71073 A°) on a Rigaku AFC8S diffractometer with a Mercury CCD detector at 193 K. The structure was solved by direct methods, and refined using full-matrix least-squares techniques with the program SHELXTL.

4.3.2.2 NMR experimental

1D and 2D NMR spectra were acquired using a Bruker AV-500 spectrometer or JEOL operating at 300 MHz (for 1H NMR). Data processing was carried out by the Bruker XWINNMR 3.50 program. (See Chapter2 for detail)

4.3.2.3 FT-IR analysis

The transmission FT-IR spectra were obtained using a Perkin Elmer 2000 FT-IR spectrometer. (See Chapter2 for detail)

4.3.2.4 Mass spectral analysis

Mass spectra were acquired on Q-Tof micro (Waters) with direct injection through capLC to nanospray in negative ion mode. MassLynx software drives the LC

and autosamplerand permits data collection in MS and MS/MS modes. The ProteinLynx Globe Server 2.1.5 (PLGS) software performed the data analysis. (See Chapter2 for detail)

4.3.3 Synthesis of fulleropyrrolidines

4.3.3.1 Extraction of gossypol from cottonseed

Dry the Soxhlet apparatus at 105°C to constant weight, add the crushed cotton seed (1.5kg) to the cloth container and seal to prevent sample loss during the extraction. Place several boiling chips into a clean, dry receiving flask (5L container). Pour 3L solvent into the dry receiving flask and insert the cloth container and install the apparatus as Figure4.5 shown. Heat at reflux for 48hrs, periodically check the
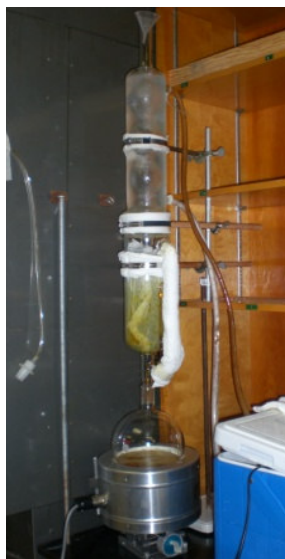

Figure 4.4 The gossypol extraction apparatus

reflux rate and adjust the heating rate to give solvent exchanges every three hours, we use petroleum ether to remove fatty acid and proteins and use acetone to extract gossypol. When the extraction time is complete, place the receiver flask on the rotary evaporator and remove the solvent under vacuum. Pure gossypol (22.5g, yield: 1.5%) which was confirmed by NMR spectra was obtained by repeated recrystallization from acetone solution by adding 50% glacial acetic acid.

4.3.3.2 Synthesis and spectral data of N-methyl-2-phenylfulleropyrrolidine (compound **12**) and N-methylfulleropyrrolidine (compound **13**)

A sample of C60 (100 mg, 0.139 mmol) was dissolved in dry toluene (30 ml) and then the solution of gossypol (80.36 mg, 0.139 mmol) in DMSO (3 ml) as well as an equivalent amount of sarcosine (12.37 mg, 0.139 mmol) were added. After 5 min of nitrogen flushing, the mixture was heated at 110 ^{o}C for 18 hrs (**Figure 4.5**). The product of N-methyl-2-phenylfulleropyrrolidine (**12**, 32.4 mg, 27.3%) was purified

Figure 4.5 The reaction apparatus

by flash chromatography (chlorobenzene/hexane, 5/3). The subsequent elution with chlorobenzene/ methanol (100/1) afforded N-methylfulleropyrrolidine (**13**, 8.6 mg, 7.3%). Noticeably, 43% amount of C60 was recovered in this reaction.

Spectral data of **12**: 1H NMR (300 MHz, ODCB-d4) 2.76 (s, 3H, N–CH$_3$), 4.14 (d, 1H, one of proton of CH$_2$ in pyrrolic structure), 4.86 (d, 1H, the other proton of CH$_2$ in pyrrolic structure), 4.88 (s, 1H, CH in pyrrolic structure), 7.30 (m, 1H, Ph-H), 7.42 (t, 2H, Ph-H), 7.86 (s, 2H, Ph-H); 13C NMR (75 MHz, ODCB-d4) 39.68, (N–CH$_3$), 69.05 (sp^3 C of C60), 69.95 (CH$_2$ in pyrrolic structure), 77.22 (sp^3 C of C60), 83.52 (CH in pyrrolic structure), 135.72, 135.91, 136.51, 136.80, 137.37, 139.28, 139.72, 139.99, 140.02, 141.30, 141.51, 141.71, 141.75, 141.84, 141.86, 141.94, 142.00, 142.14, 142.17, 142.31, 142.35, 142.47, 142.78, 142.92, 144.18, 144.25, 144.37, 144.53, 144.92, 145.01, 145.06, 145.11, 145.17, 145.33, 145.37, 145.40, 145.56, 145.72, 145.89, 145.98, 146.02, 146.05, 146.07, 146.35, 146.66, 147.08, 153.37, 153.55, 153.96, 156.35;

IR m/cm$^-$1 (KBr):   3437, 2921, 2779, 1637, 1429, 1182, 1107, 699, 575, 526;

ESI m/z: 854 [M+1] $^+$. Anal. calcd for C69H11N: C, 97.06%; H, 1.30%; N, 1.64%. Found: C, 97.46%; H, 1.29%; N, 1.50%.

Spectral data of **13**: 1H NMR (300 MHz, CDCl$_3$) 3.04 (s, 3H, N–CH$_3$), 4.44 (s, 4H, four proton of CH$_2$ in pyrrolic structure), 13C NMR (75 MHz, ODCB-d4) 41.12 (N–CH$_3$), 69.98 (two CH$_2$ in pyrrolic structure), 71.22 (two sp^3 C of C60), 131.98,

132.84, 136.19, 139.95, 141.66, 141.87, 142.09, 142.39, 142.87, 144.37, 145.06, 145.21, 145.51, 145.84, 145.95, 146.03, 147.09, 154.97;

IR m/cm⁻1 (KBr): 3447, 2851, 1384, 1338, 1229, 1158, 1069, 797, 737, 596, 573, 552, 525.

4.3.3.3 Synthesis and spectral data of N-methyl-2, 2-dimethylfulleropyrrolidine (compound **14**)

A sample of C60 (60 mg, 0.0834 mmol) was dissolved in dry chlorobenzene (30 ml) and then the solution of gossypol (48 mg, 0.0834 mmol) in DMSO (3 ml) as well as two equivalents amount of sarcosine (24.74 mg, 0.167 mmol) were added. After 5 min of nitrogen flushing, the mixture was heated at 120 ^{o}C for 18 h. The reaction products were purified by flash chromatography (chlorobenzene/methanol, 100/1, vol) to afford the compounds **14** (11.3 mg, 27.3%) and 2 (7.4 mg, 18.5%).

Spectra data of **14**: ^{1}H NMR (300 MHz, CS2–CDCl3) 1.95 (s, 6H, C–(CH$_3$)$_2$), 2.87 (s, 3H, N–CH$_3$), 4.56 (d, 2H, CH$_2$ in pyrrolic structure), 13C NMR (75 MHz, CS$_2$–CDCl$_3$) 22.85, (two carbons of C–(CH$_3$)$_2$), 34.20 (N–CH$_3$), 65.73 (CH$_2$ in pyrrolic structure), 68.89 (quartary carbon attached to N), 69.59 (sp^3 C of C60), 77.73 (sp^3 C of C60), 136.26, 136.71, 139.92, 140.34, 141.84, 141.99, 142.09, 142.23, 142.32, 142.54, 142.77, 144.67, 144.72, 145.35, 145.41, 145.52, 145.80, 146.16, 146.35, 146.39, 146.65, 154.61, 156.33;

IR m/cm^{-1} (KBr): 3434.81, 2924.88, 2963.09, 1384.90, 1157.13, 1097.91, 1021.96, 990.75, 802.95, 736.43, 640.90, 573.80, 554.15, 525.76;

HRMS (ESI) m/z calcd for C65H11N, 805.09; found, 806.09 [M+1] $^{+}$.

4.3.4 Bioactivity assay

In the selected in vitro assay of NO radical induced apoptosis in 3T3L1 cells, the 3T3L1 preadipose cells in RPMI supple-mented with 5% fetal bovine serum (FBS) were seeded into a 96-well tissue culture plate (10^5 cells/well, 80 µl/well), prior to chemical treatment. They were allowed to attach for 24 h. After that, 10 µl SNP (0.3 mg/ml) in medium was added into each well except the control group. In this test, the cell viability in 0.3 mg/ml SNP solution was 63.46% compared to the blank. The cells were then treated with a defined concentration (0–100 µg/ml) of the test compounds (C60, **12**, **13**, **14**), which were finely dispersed in medium for another 24 hrs. Then 20 µl /well of combined MTS/PMS solution were added. After keeping in an incubator in a humidified, 5% CO2 atmosphere at 37 ^{o}C for 3 hrs, the supernatant (80 µl /well) was transferred to another 96-well tissue culture plate, which was recorded under the absorbance at 490 nm using an EL800 Bio-Tek microplate reader. Each treatment was measured in three replicates to give the value in the mean ± SD.

4.4 Results and discussion

C60 reacts with gossypol in the presence of sarcosine in toluene to produce N-methyl-2-phenylfulleropyrrolidine (**12**) and N-methylfulleropyrrolidine (**13**) in 27% and 7.3% yield, respectively (**Figure 4.6**). Their structures were determined by MS, FT-IR, 1H, 13C NMR, DEPT (distortionless enhancement by polarization transfer) and HMQC spectroscopy [(1H-detected) heteronuclear multiple-bond quantum coherence correlation]. The 1H NMR spectrum of **12** showed that it was not a simple hybrid of fullerene and gossypol because of the missing proton signals of $-OH$, $-CH_3$ and $-CH(CH_3)_2$ groups of gossypol and unexpected appearance of proton signals in the aromatic area. The 13C NMR spectrum of compound **12** (see Appendix III) shows five signals in saturated carbon area. The HMQC spectra showed that the proton resonance at 2.76 ppm correlated to the carbon resonance at 39.68 ppm and the proton resonance at 4.14 ppm as well as 4.86 ppm correlated to the same carbon resonance at 69.95 ppm. At the same time, the proton signal at 4.88 ppm correlated to the carbon resonance at 83.52 ppm. Its 13C NMR and DEPT spectra demonstrated two sp^3 carbons of fullerene (69.05 ppm, 77.22 ppm), one secondary carbon (69.95 ppm), one tertiary carbon (83.52 ppm), and a methyl group attached to the nitrogen atom (39.68 ppm). Noticeably, fifty signals in the unsaturated carbon area indicated that **12** had C_1 symmetry. Compound **12** was finally figured out as N-methyl-2-phenylfulleropyrrolidine which was further confirmed by its X-ray crystallographic structure (**Figure 4.8**), the method of single crystal culture and the detailed data of the its X-ray crystallographic structure of compound **12** refer the

Appenda III in the end of this chapter. The 1H NMR spectra (300 MHz, CDCl₃) of

compound **13** showed a singlet at 3.04 ppm for the protons in the methyl group

attached to the nitrogen atom and a singlet at 4.44 ppm for the four protons of the
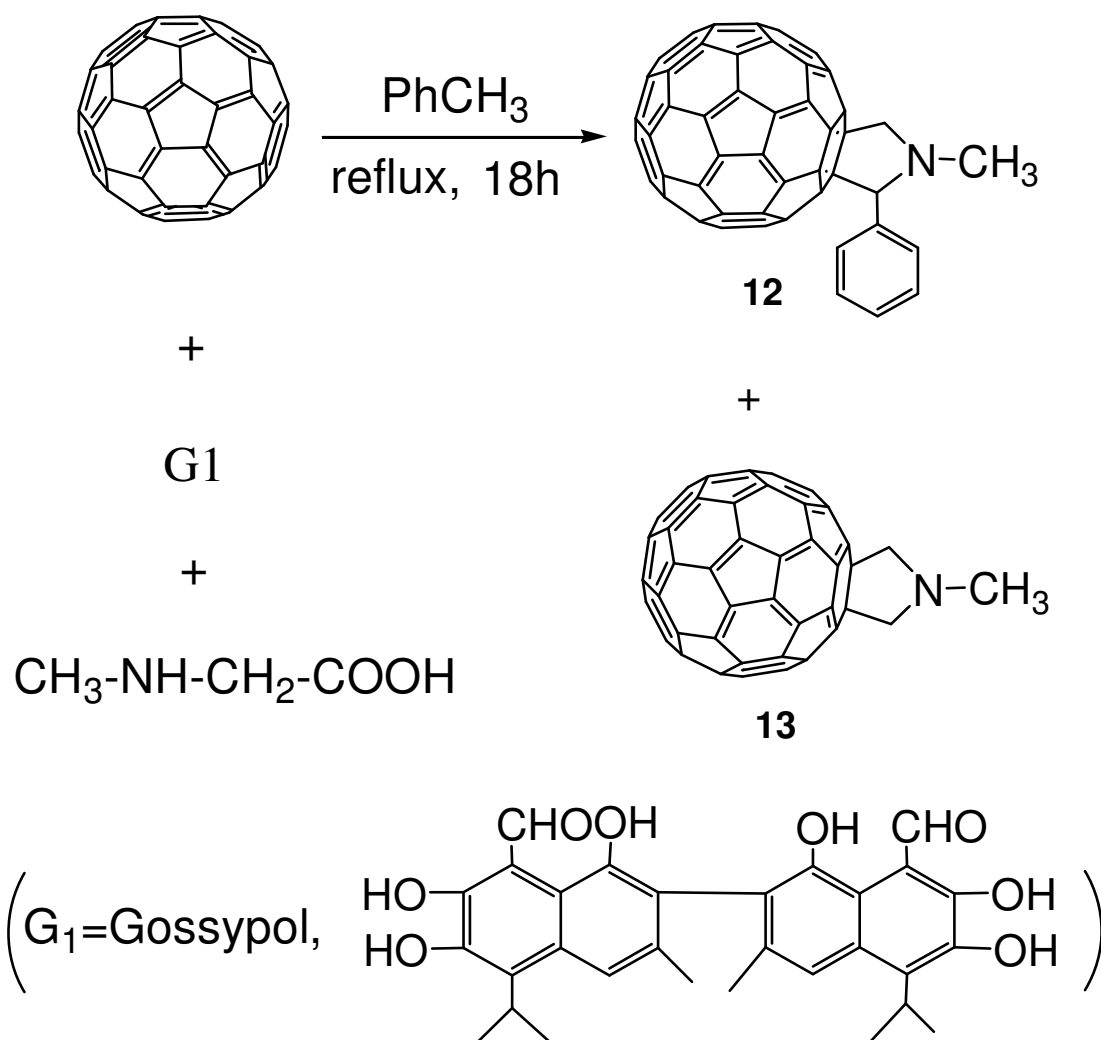

Figure 4.6 The reaction of fullerene and gossypol in toluene

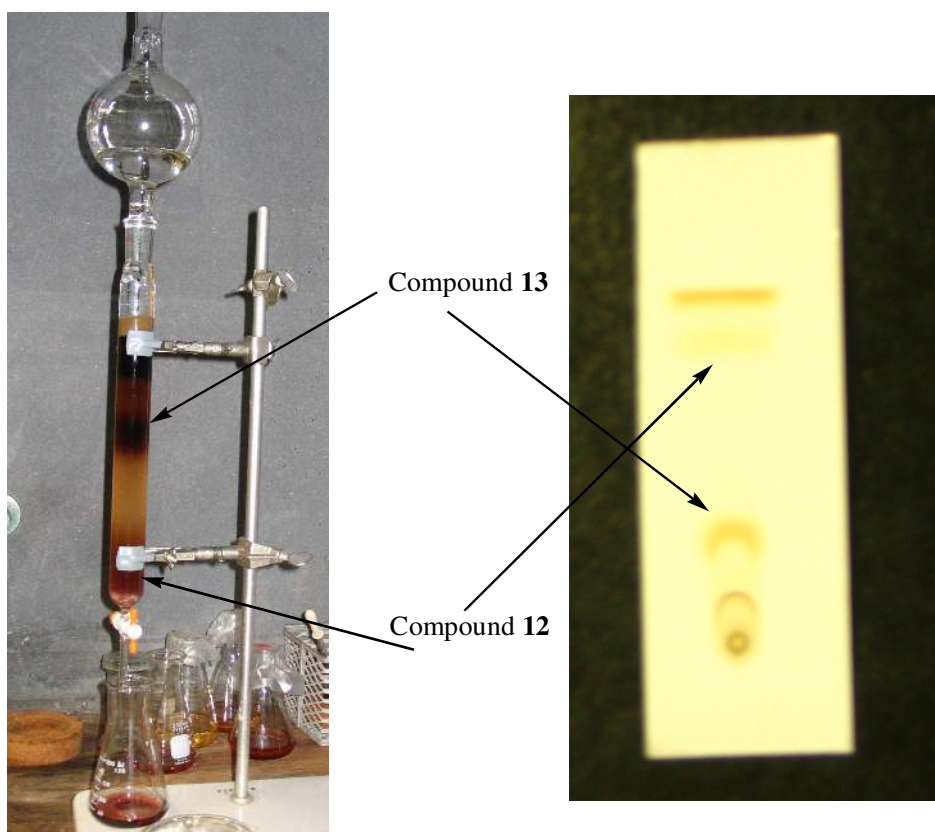Compound **13**

Compound **12**

Figure 4.7 The flash column and TLC separation of the reaction mixture, flash column chromatography (PhCl:hexane=5:3,silica gel 200-300)

methylene group in the pyrrolic structure. The 13C NMR spectra of **13** (see Appenda III) showed only 18 signals in the unsaturated carbon area, suggesting a more symmetrical C_{2v} structure. In contrast, the 1H NMR of compound **14** displayed the proton signals of methyl group attached to the nitrogen atom, two methyl groups attached to the quartary carbon as well as a methylene group in the pyrrolic structure calibrated as 3:6:2, and the 13C NMR spectra of **14** in CS_2 and $CDCl_3$ showed 6 signals in saturated area. In addition, the DEPT 90° spectra did not show any peaks, which indicated no methenyl group in the molecule of **14**. Furthermore, the spectra of DEPT 135° displayed two positive signals for the carbon of the methyl group attached to the nitrogen atom at 22.85 ppm and two equivalent carbons of the methyl groups attached to the quartary carbon in the pyrrolic ring at 34.20 ppm, respectively. Combining the mass spectra and IR data, the compound **14** was finally characterized as N-methyl-2, 2-dimethyl fulleropyrrolidine. After slow evaporation of chlorobenzene at room temperature, black single crystals of the compound **12** that were of X-ray crystallographic quality were obtained with shiny faces that were brown in transmitting light. The obtained X-ray structure (**Figure4.8**) at 273 K is in agreement with that from the NMR derived assignments.
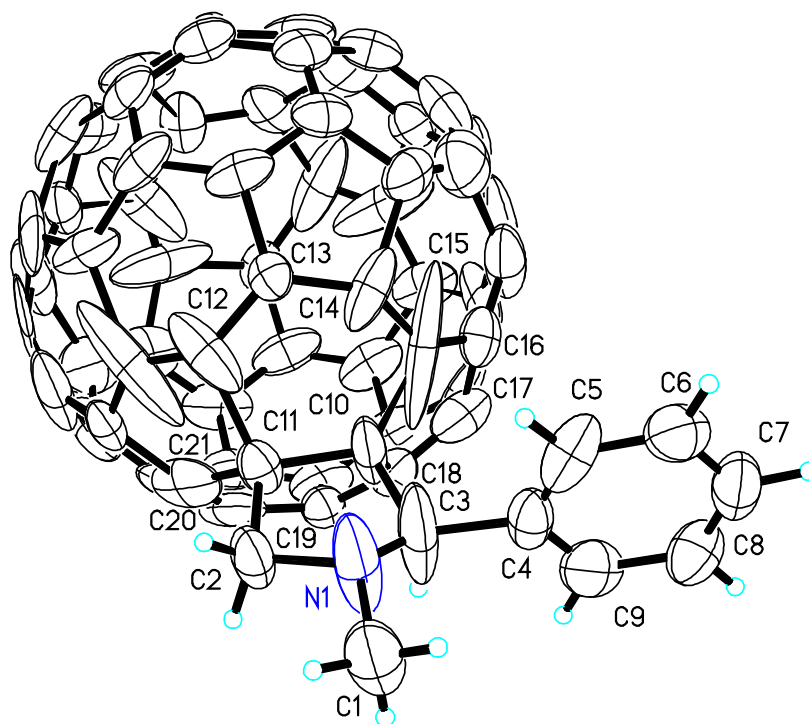
Figure 4.8 ORTEP drawing of N-methyl-2-phenylfulleropyrrolidine (**12**) with thermal ellipsoids plotted at 50% probability. Selected bond lengths (A°) and angles (deg): N(1)–C(3) 1.158(10); N(1)–C(2) 1.445(8); N(1)–C(1) 1.464(9); C(3)–C(4) 1.497(9); C(3)–C(10) 1.602(10); C(4)–C(9) 1.339(9); C(4)–C(5) 1.360(9); C(5)–C(6) .376(10); C(6)–C(7) 1.416(10); C(7)–C(8) 1.344(10); C(8)–C(9) 1.399(10); C(10)–C(11) 1.503(8); C(10)–C(18) 1.786(10); C(11)–C(21) 1.635(12); C(11)–C(12) 1.772(10); C(12)–C(13) 1.365(9); C(13)–C(14) 1.374(8); C(14)–C(15) 1.225(14).
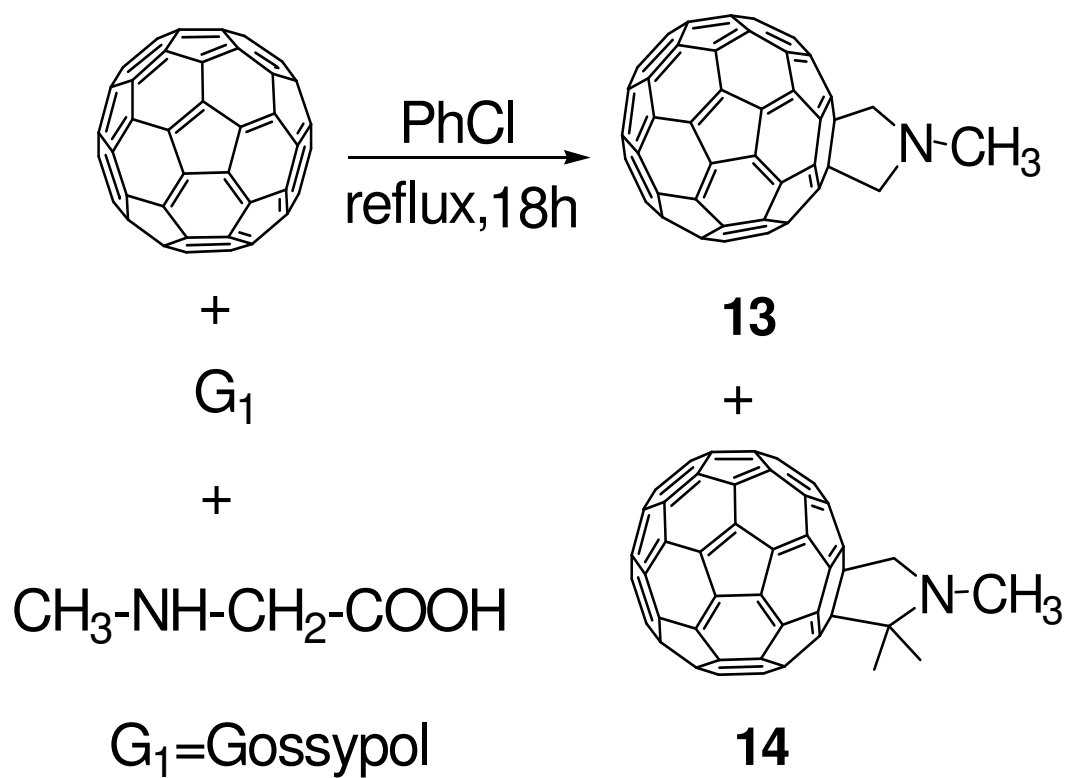
PhCl
reflux,18h

+

G₁

+

CH₃-NH-CH₂-COOH

G₁=Gossypol

13

+

14

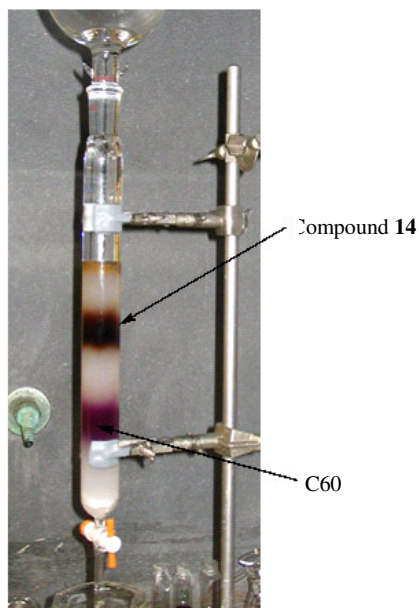**Figure 4.9** The reaction of fullerene and gossypol in chlorobenzene

Figure 4.10 The flash column separation of the reaction mixture, flash column chromatography (PhCH$_3$: methanol=5:1, silica gel 200-300)

There is no reaction at room temperature for both reactions shown in **Figures 4.6** and **4.9**, and the reactants are UV light stable too. The reactant mixture remained unchanged after being exposed to UV light irradiation at 254 nm for 17 hrs. When the reaction was carried out in toluene, compounds **12** and **13** were both the main products within 18 hrs, while the latter became the dominant product after 18 hrs. However, when using chlorobenzene, compounds **13** and **14** were obtained, but no compound **12** was detected. The mechanism of this unusual transformation is unclear by a lack of understanding of the exact nature of gossypol involved in the process. However, a plausible mechanism for this reaction in toluene was attributed to the

formation of a new reaction intermediate, benzaldehyde, which was derived from gossypol. The intermediate benzaldehyde from gossypol reacted with fullerene under such reaction conditions resulting in these fulleropyrrolidines, just like a common 1,3-dipolar addition reaction in the presence of amino acid. The formation of benzaldehyde from gossypol degradation was only detected in toluene, but not in chlorobenzene. In order to gain a deeper insight of the reaction process and elucidate the reaction mechanism, gossypol was heated without C60 in different solvents (toluene and chlorobenzene). Two portions of 10 ml gossypol solution (dissolved in toluene and chlorobenzene, respectively) at same concentration (1 mg/ml) were added into two vials which were sealed and then heated at 110 ^{o}C for 12 hrs. After the thermal treatment, the gossypol solution using toluene as solvent displayed a deep orange color that was significantly different from its original yellow color, while the gossypol chlorobenzene solution remained the same bright yellow color as before, which demonstrated that the reaction mechanism: the reaction results tell us there exist intermediate product benzaldehyde during degration of gossypol using toluene as solvent. Gossypol had undergone a much more dramatic decomposition in toluene than in chlorobenzene. Additionally, benzaldehyde was detected by GC–MS (**Figure 4.12**) in the toluene solution but not in the chlorobenzene solution. The possibility that the intermediate aldehyde derived from toluene was eliminated since it was not detected in pure toluene under the same heating condition.
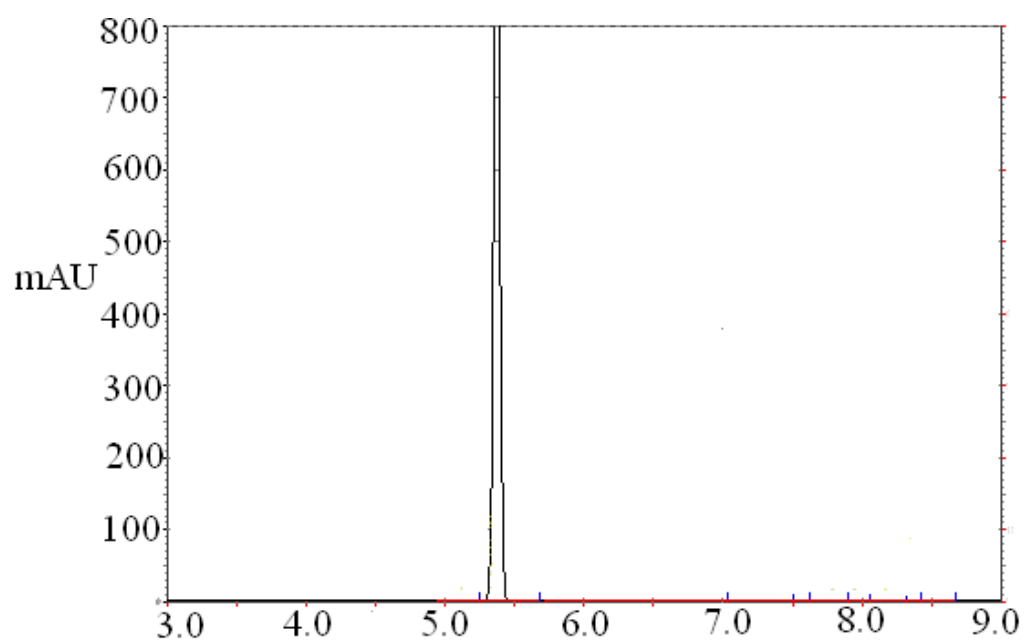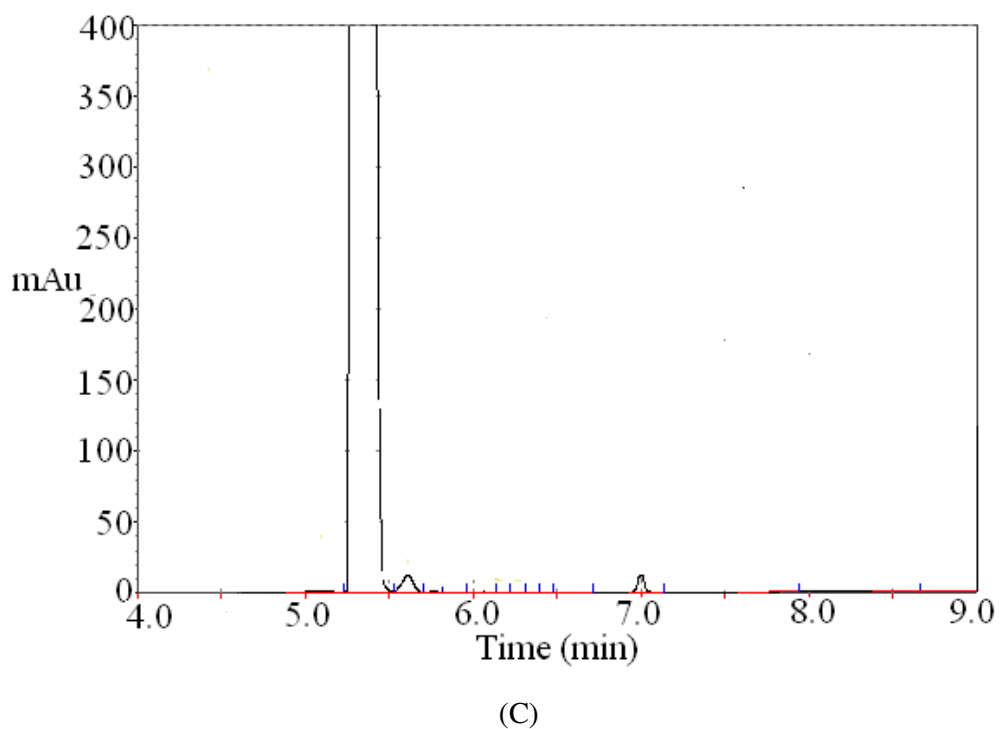
(A) (continued)

(B) (Continued)

(C)
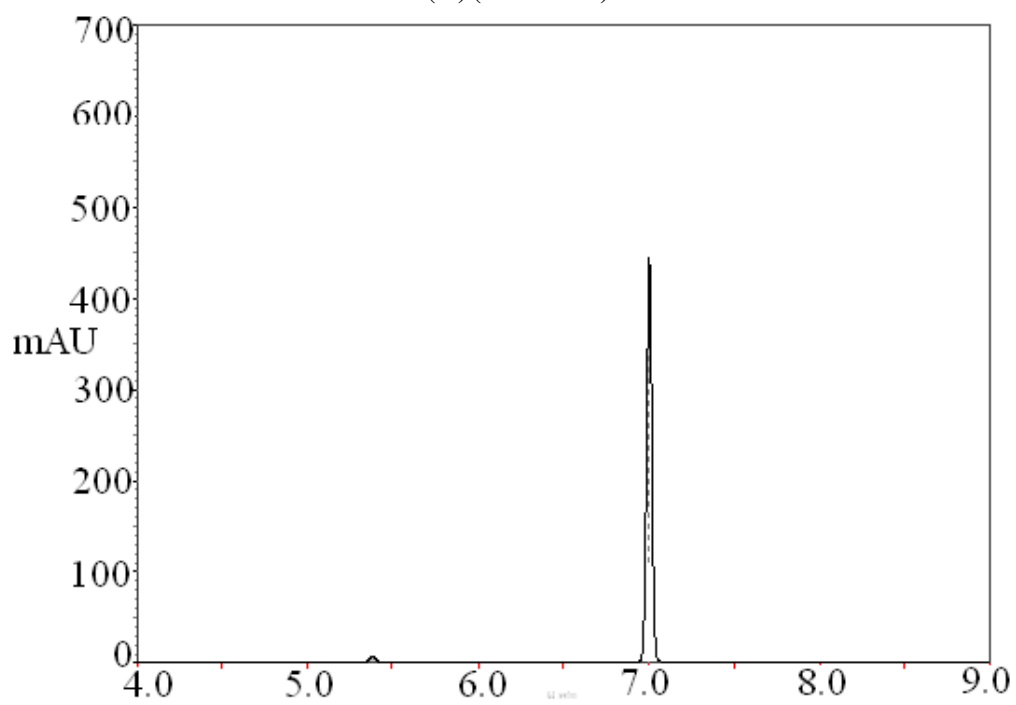
Figure 4.11 (A) The HPLC chromatography of toluene: Rt= 5.3 min; (B) The HPLC chromatography of benzaldehyde: Rt=7.0 min; (C) The HPLC chromatography of the reaction mixture of toluene and gossypol after refluxing overnight

In addition, when gossypolone which was prepared by the Shirley's method (1965), 6-methoxygossypol and 6, 6-dimethoxy-gossypol reacted with C60 under the same conditions, only compound **13** was obtained (**Figure 4.13**). Further bioassay showed that these N-methylfulleropyrrolidines exhibited dose-dependent growth protection from nitric oxide (NO) radical induced apoptosis to 3T3L1 cells (**Figure 4.14**). Sodium nitroprusside (SNP) is usually considered to be a precursor of nitric
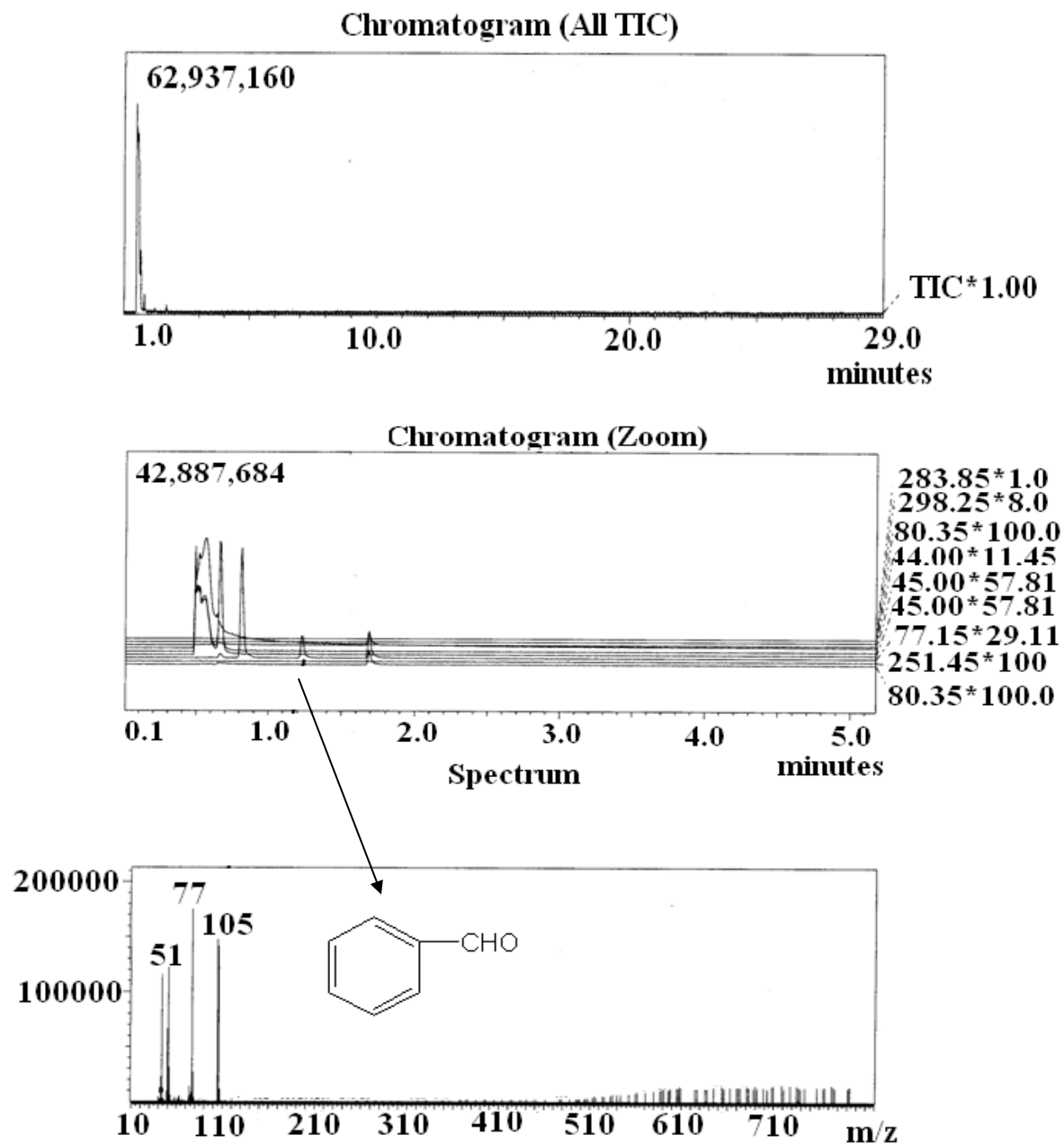
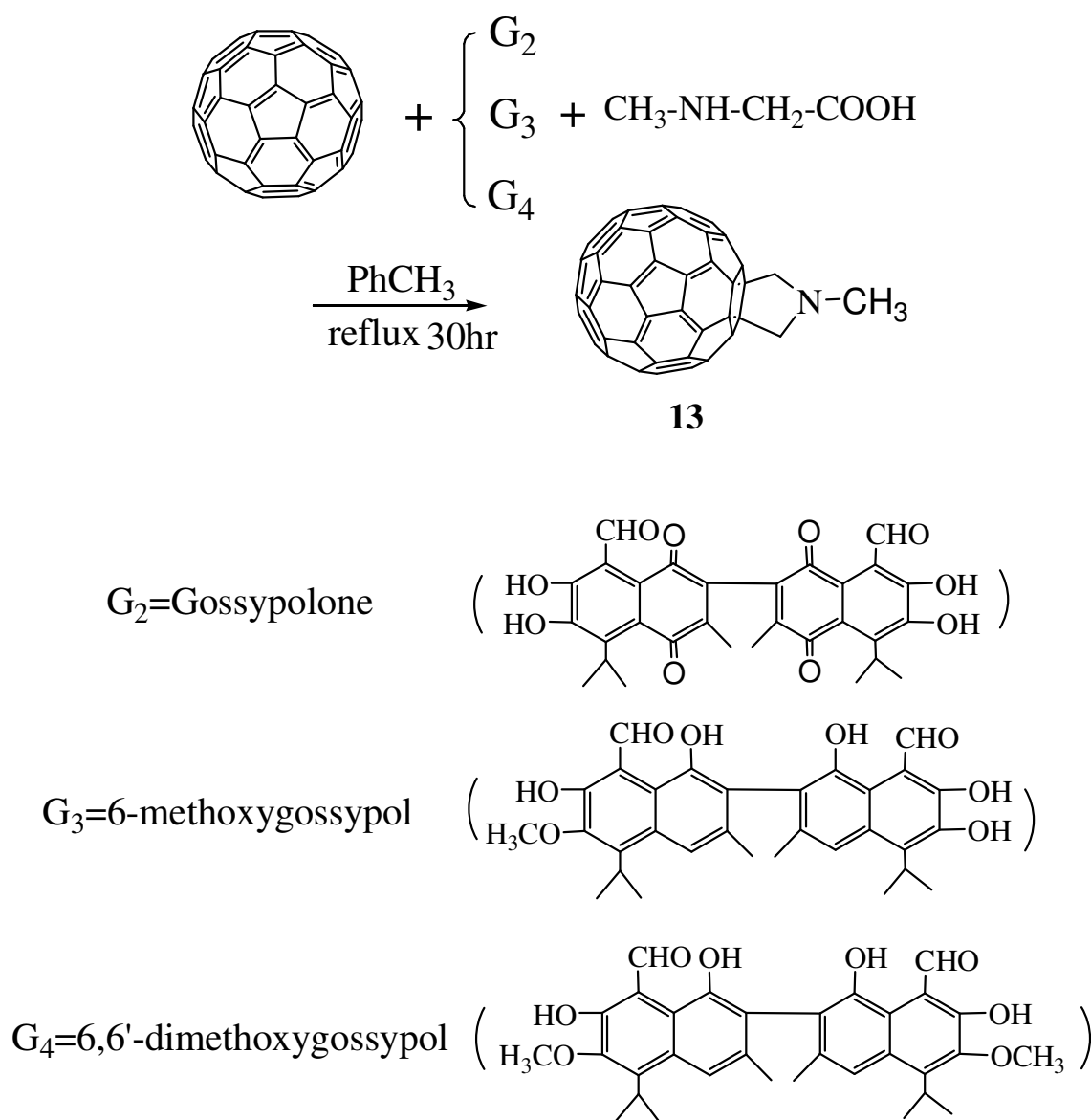**Figure 4.12** The GC-MS spectra for mixture of toluene and gossypol after refluxing overnight

Figure 4.13 The reaction of gossypol and gossypolone, 6-methoxy gossypol and 6, 6′-dimethoxygossypol respectively in toluene

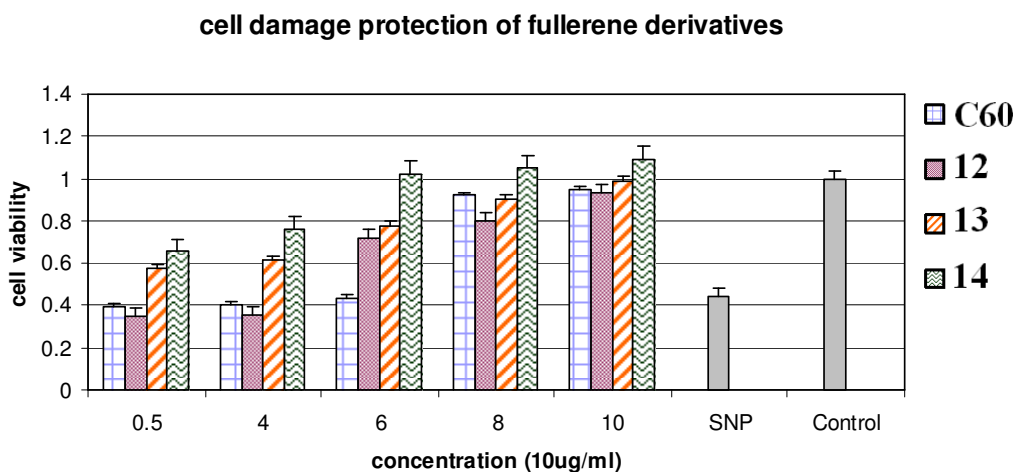## cell damage protection of fullerene derivatives

Figure 4.14 Cell damage induced by NO free radical protection of C60, and compounds **12**, **13**, **14**

oxide radical, which is a short-lived free radical generated endogenously, exerts influence on a number of functions, including vasodilation, neurotransmission, synaptic plasticity and memory in the central nervous system. Overproduction of NO can lead to toxicity, e.g. DNA fragmentation, cell damage and neuronal cell death (Dawson et al., 1992). Among the C60 and N-methylfulleropyrrolidines, compounds **13** and **14** exhibited stronger free radical scavenging activity than the parent fullerene in preventing NO induced damage, especially by the compound **14**. These results indicate that the pyrrolic structure in these fullerene derivatives has a tendency to increase the bioactivity.

4. 5 Conclusions

In conclusion, three unexpected N-methylfulleropyrrolidines were obtained from the reaction of fullerene and gossypol, and characterized by 1D, 2D NMR, FT-IR, MS and X-ray crystallography. In toluene, the N-methyl-2-phenylfulleropyrrolidine (compound **12**) and N-methylfulleropyrrolidine (compound **13**) were obtained, while the compound **13** and N-methyl-2, 2-dimethylfulleropyrrolidine (compound **14**) were formed in chlorobenzene. On the other hand, the rigorous structure characterization of these products as well as the new intermediate detection provided better understanding of gossypol's degradation reaction behavior. Moreover, the bioassay for the cell damage protection demonstrated that the pyrrolic structure in the fulleropyrrolidines might have contributed enhanced radical scavenging activity evaluated in vitro.

4.6 References

Adams, R., and Dial, W. R. (1939). Structure of gossypol. XXII. gossypol ethers and their reduction products. *J. Am. Chem. Soc*. **61**, 2077–2082.

Adams, R., Morris, R. C., and Kirkpatrick, E. C. (1938). Structure of gossypol. IX. oxidation and degradation of gossypol hexamethyl ether; gossic acid. *J. Am. Chem. Soc*. **60**, 2170–2174.

Bolskar, R. D., Benedetto, A. F., Husebo, L. O., Price, R. E., Jackson, E. F., and Wallace, S. (2003). First soluble M@C60 derivatives provide enhanced access to metallofullerenes and permit in vivo evaluation of Gd@C60[C(COOH)$_2$]$_{10}$ as a MRI contrast agent. *J. Am. Chem. Soc*. **125**, 5471–5487.

Clark, E. P. (1928). Gossypol. III. The oxidation of gossypol. *J. Biol. Chem.* **77**, 81–87.

Daros, T., and Prato, M. (1999). Medicinal chemistry with fullerenes and fullerene derivatives. *Chem. Commun*. **8**, 663–669.

Dawson, T. M., Dawson, V. L., and Snyder, S. H. (1992). Immunosuppressant FK506 enhances phosphorylation of nitric oxide synthase and protects against glutamate neurotoxicity. *Annu. Neurol.* **32**, 297–311.

Friedman, S. H., Ganapathi, P. S., Rubin, Y., and Kenyon, G. L. (1998). Optimizing the binding of fullerene inhibitors of the HIV-1 protease through predicted increases in hydrophobic desolvation. *J. Med. Chem.* **41**, 2424–2429.

Gelperina, S., Kisich, K., Iseman, M. D., and Heifets, L. (2005). The potential advantages of nanoparticle drug delivery systems in chemotherapy of tuberculosis**.** *Pulmonary Perspective*. **172**, 1487-1490

Georgakilas, V., Kordatos, K., Prato, M., Guldi, D. M., Holzinger, M., and Hirsch, A. (2002). Organic functionalization of carbon nanotubes. *J. Am. Chem. Soc.* **124**, 760–761.

Gonzalez, K. A., Wilson, L. J., Wu, W. J., and Nancollas, G. H. (2002). The differential cytotoxicity of water-soluble fullerenes. *Bioorg. Med. Chem.* **10**, 1991–1997.

Hirsch, A. (1994). The chemistry of the fullerenes. New York: Thieme Medical Publishers.

Jensen, A. W., Wilson, S. R., and Schuster, D. I. (1996). Biological applications of fullerenes. *Bioorg. Med. Chem.* **4**, 767–779.

Kroto, H. W., Allal, A. W., and Balm, S. P. (1991). C60: Buckminsterfullerene. *Chem. Rev* .**91**, 1213-1235,

Kroto, H. W., Heath, J. R., Obrien, S. C., Curl, R. F., and Smalley, R. E. (1985). C60: Buckminsterfullerene. *Nature,* **318**, 162-163.

Maggini, M., Scorrano, G., and Prato, M. (1993). Addition of azomethine ylides to C60: synthesis, characterization, and functionalization of fullerene pyrrolidines. *J. Am. Chem. Soc.* **115**, 9798–9799

Marcorin, G. L., DaRos, T., Castellano, S., Stefancich, G., Bonin, I., and Miertus, S. (2000). Design and synthesis of novel [60] fullerene derivatives as potential HIV aspartic protease inhibitors. *Org. Lett.* **2**, 3955–3958.

Mashino, T., Nishikawa, D., Takahashi, K., Usui, N., Yamori, T., and Seki, M. (2003). Antibacterial and antiproliferative activity of cationic fullerene derivatives. *Bioorg. Med. Chem. Lett.* **24**. 4395–4397.

Mirakyan, A. L., and Wilson, L. J. (2002). Functionalization of C60 with diphosphonate groups: a route to bone-vectored fullerenes. *J. Chem. Soc. Perkin. Trans.* **2**, 1173–1176.

Shirley, D. A., and Haas, R. H. (1965). Oxidation of gossypol. II. formation of gossypolone with ferric chloride. *J. Org. Chem.* **30**. 4111–4113.

Susanna, B., Daros, T., Spalluto, G., and Prato, M. (2003). Fullerene derivatives: an attractive tool for biological applications. *Eur. J. Med. Chem.* **38**, 913-923

Yadav, B. C., and Kumar, R. (2008). Structure, properties and applications of fullerenes. *Int. J. Nanotech. Appl.* **2**, 15–24.

Yin, J. J., Jin, L. M., Liu, R. L., Li, Q. N., Fan, C. H., and Li, Y. (2006). Reactions of fullerenes with reactive methylene organophosphorus reagents: efficient synthesis of organophosphorus group substituted C60 and C70 derivatives. *J. Org. Chem.* **71**, 2267–2271.

Yin, J. J., Li, Y. G., Li, B., Li, W. X., Jin, L. M., and Zhou, J. M. (2005). Facile and potent synthesis of carbon-bridged fullerene dimers (HC60–CR$_2$–C60H type). *Chem. Commun.* 3041–3043.

Zhou, S., Burger, C., Chu, B., Sawamura, M., Nagahama, N., and Toganoh, M. (2001). Spherical bilayer vesicles of fullerene-based surfactants in water: a laser light scattering study. *Science*. **291**, 1944–1947.

Zhu, W. Z., Schuster, D. I., and Tuckerman, M. E. (2003). Molecular dynamics study of the connection between flap closing and binding of fullerene-based inhibitors of the HIV-1 protease. *Biochemistry*. **42**, 1326–1333.
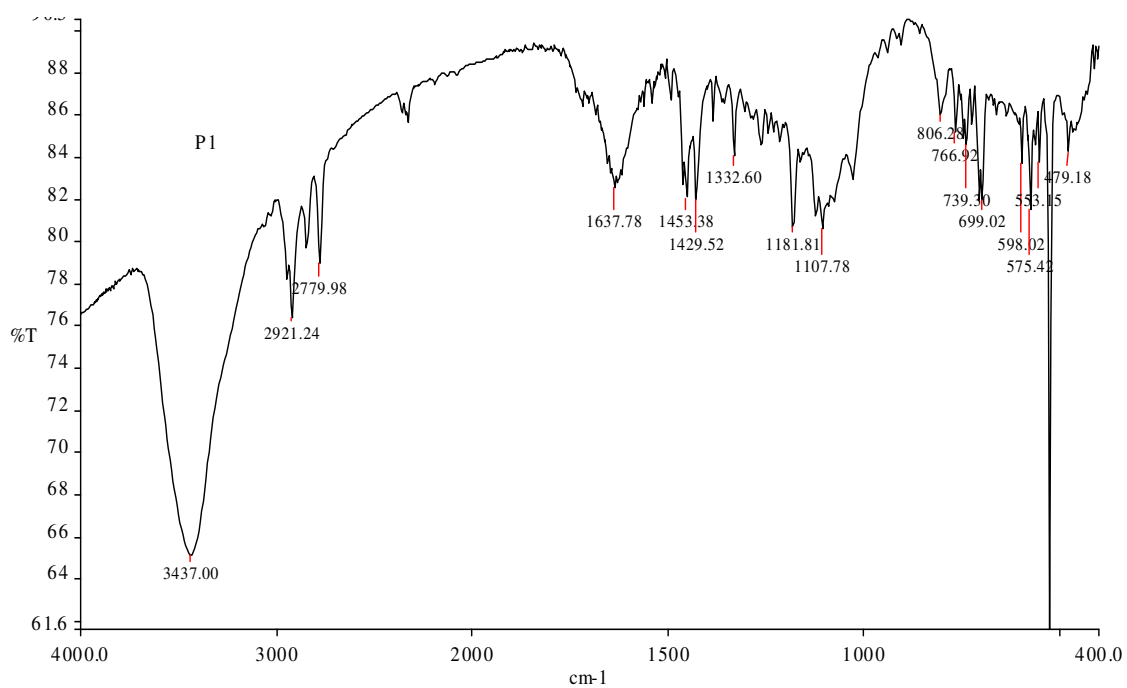
P 1

%T

3437.00

2921.24

2779.98

1637.78

1453.38

1429.52

1332.60

1181.81

1107.78

806.2

766.92

739.30

699.02

598.02

575.42

553.15

479.18

4000.0   3000   2000   1500   1000   400.0

cm-1

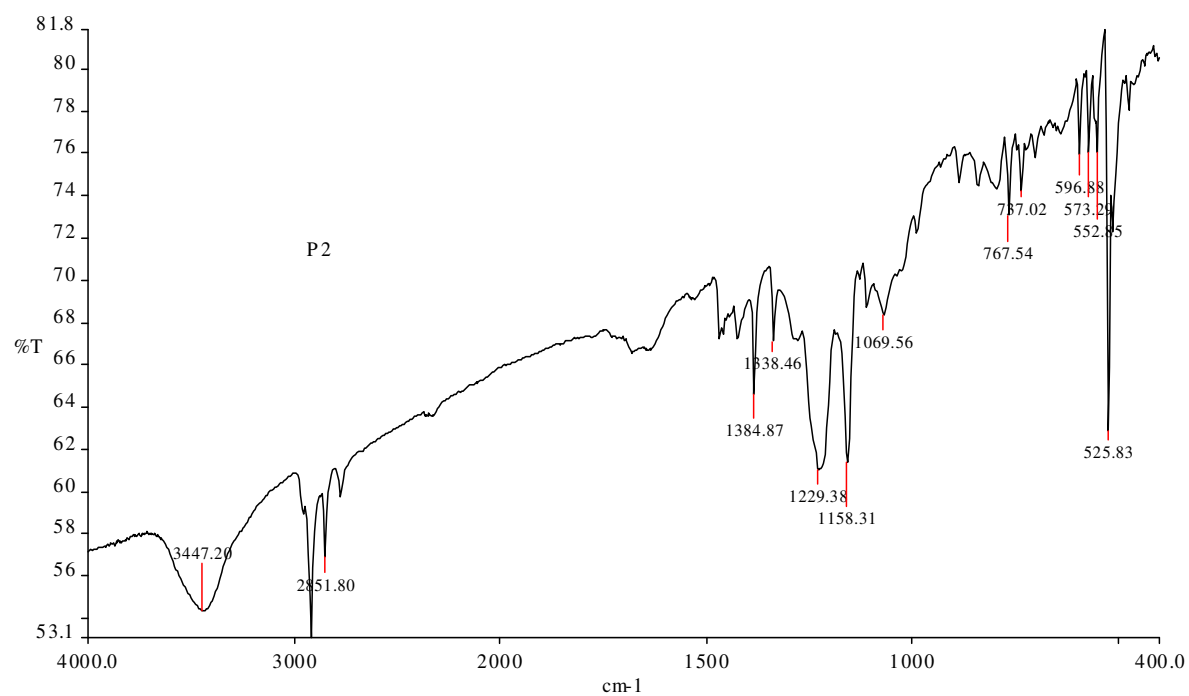**Figure A4.1** The IR spectrum of **12**
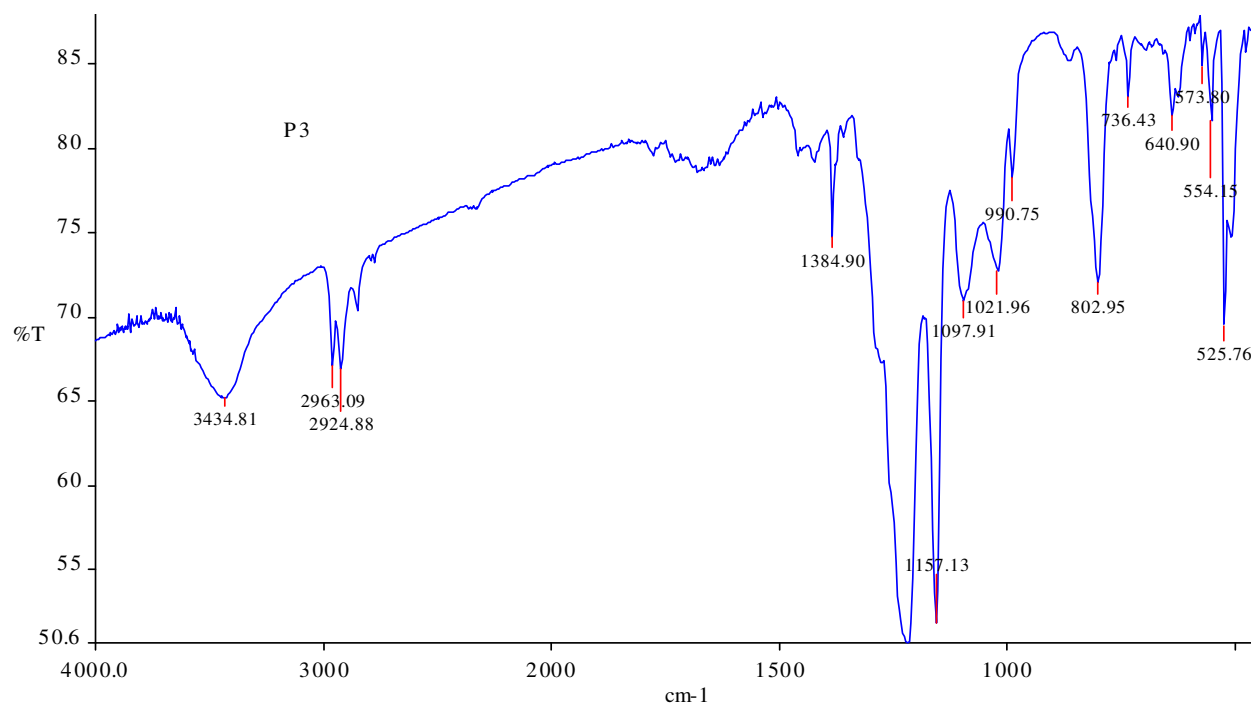
Figure A4.2 The IR spectrum of **13**

Figure A4.3 The IR spectrum of **14**
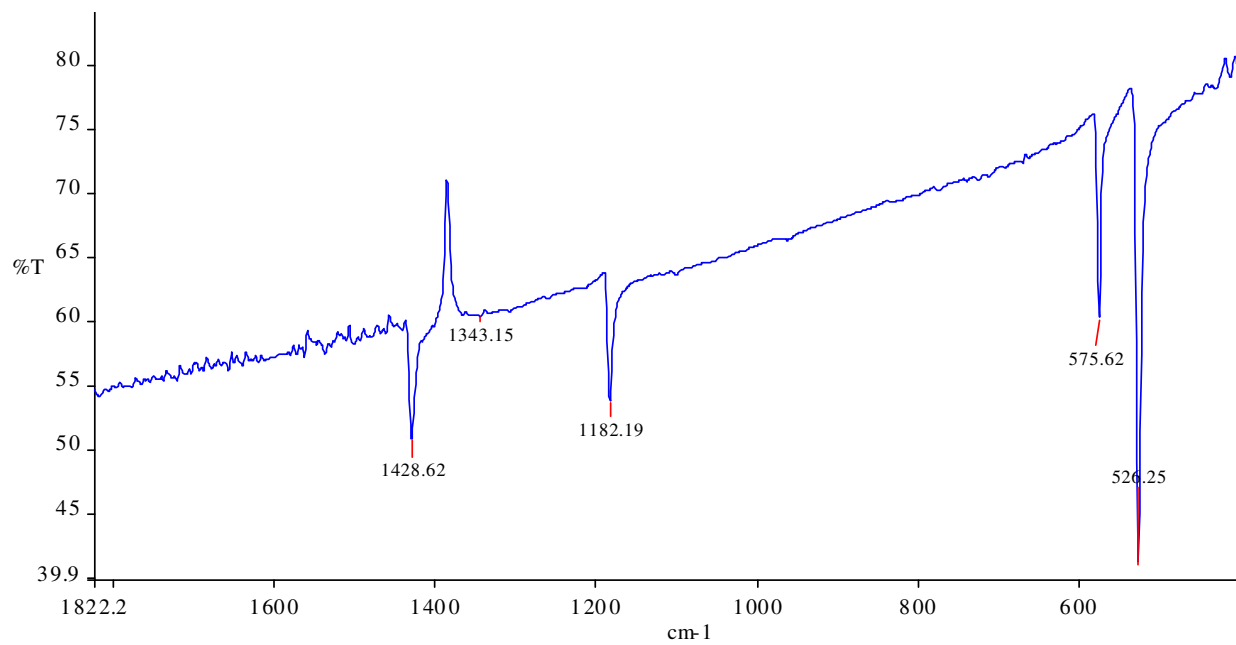
Figure A4.4 The IR spectrum of C60
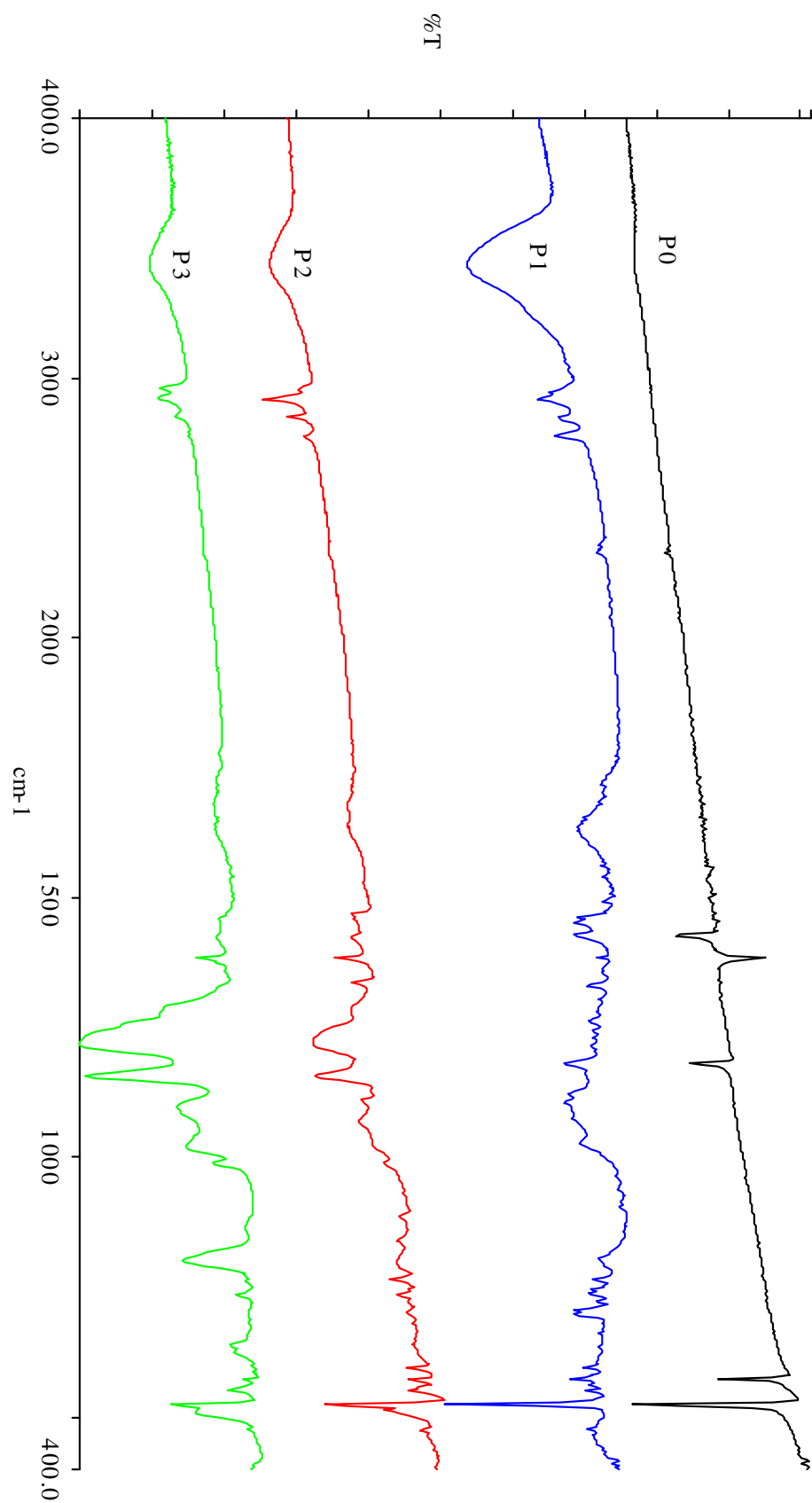
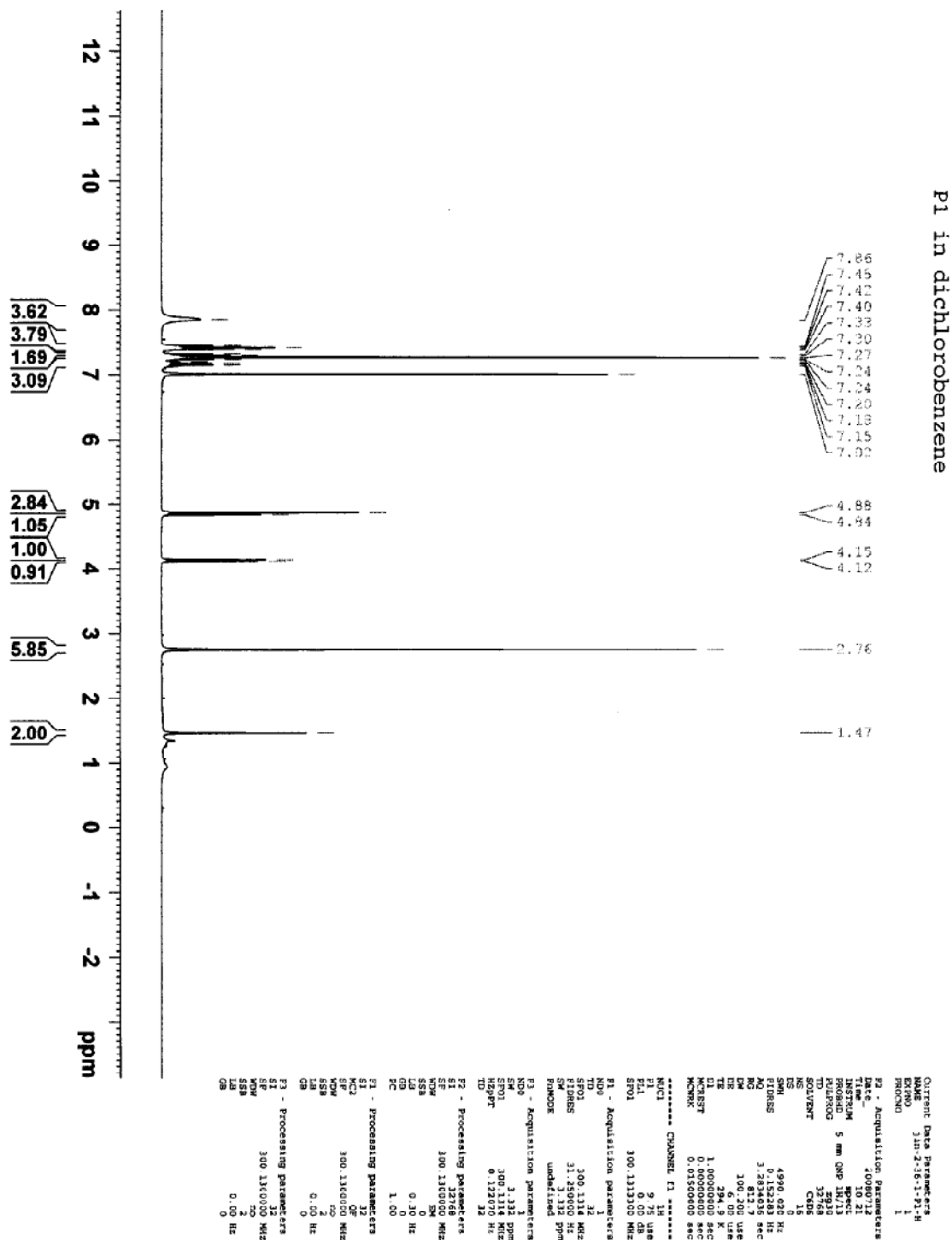**Figure A4.5** The IR spectrum of C60, **12, 13, 14**(P0:C60; P1:**12**; P2:**13**; P3:**14**)

Figure A4.6 The ^{1}HNMR spectrum of **12**(300MHz, ODCB-d$_4$)

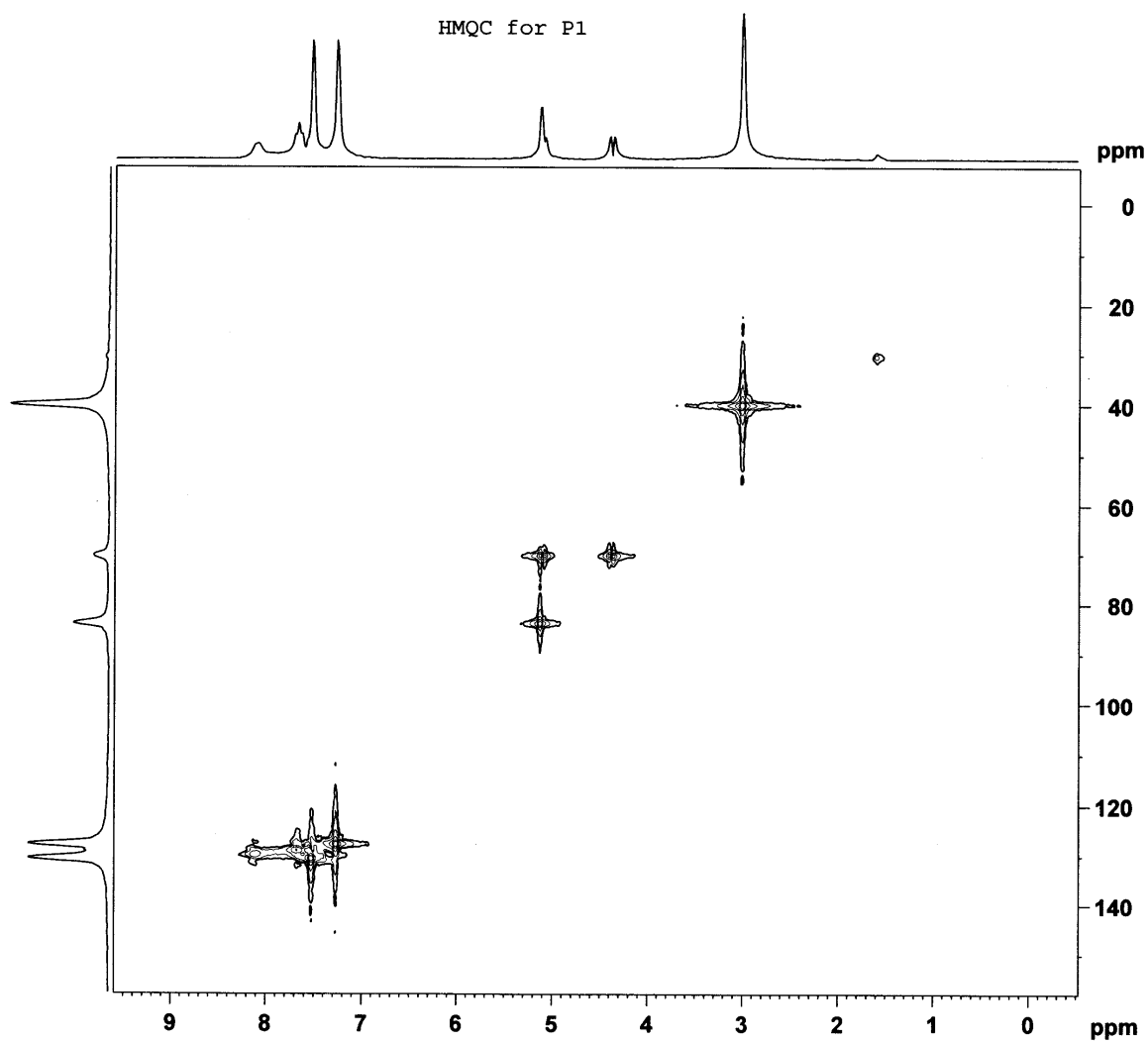**Figure A4.7** The ^{13}CNMR spectrum of **12**((75MHz, ODCB-d$_4$)

152

Figure A4.8 The HMQC spectrum for **12**(300MHz, ODCB-d₄)
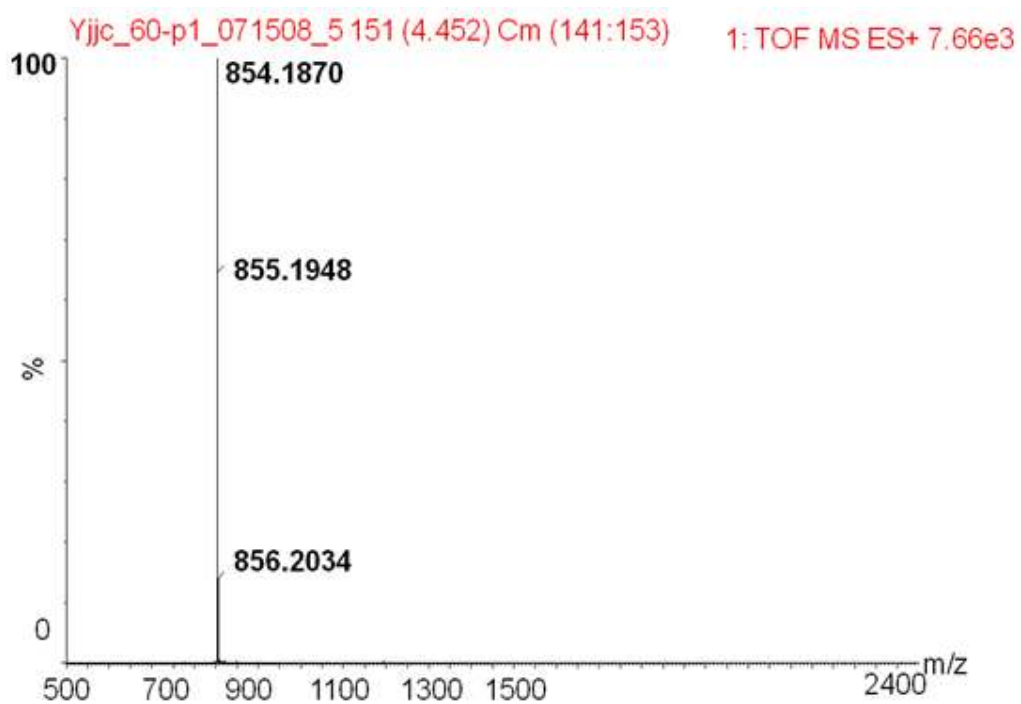
153

Figure A4.9 The ESI-MS spectrum of **12**

DEPT 90

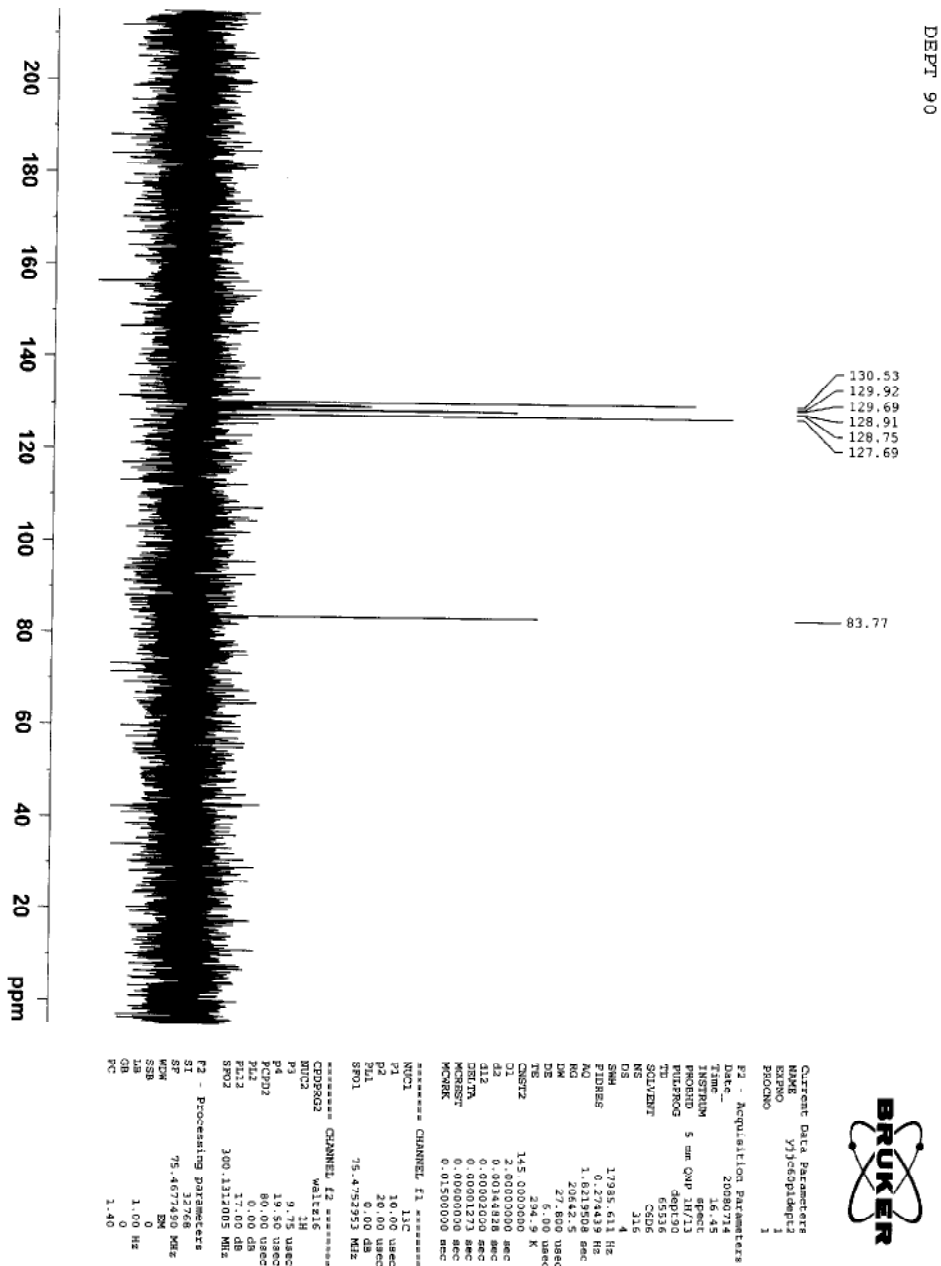Figure A4.10 The DEPT 90°spectrum for **12** (300MHz, ODCB-d₄)

155

Figure A4.11 The DEPT 135°spectrum for **12** (300MHz, ODCB-d₄)

Figure A4.12 The ^{1}HNMR spectrum of **13** (300MHz, CS$_2$-CDCl$_3$)

147.093
146.039
145.957
145.840
145.511
145.217
145.064
144.373
142.877
142.397
142.090
141.870
141.668
139.959
136.193
132.856
132.839
132.359
131.984
130.744
130.658
130.570
130.285
130.097
129.670
129.331
129.082
128.265
127.938
127.601
127.716
127.507
127.437
127.420
127.282
127.172
127.025
126.834

71.216
69.987

41.124

Figure A4.13 The ^{13}CNMR spectrum of **13**(300MHz, ODCB-d$_4$)

158

Figure A4.14 The ^{1}HNMR spectrum of **14** (300MHz, CS$_2$-CDCl$_3$)

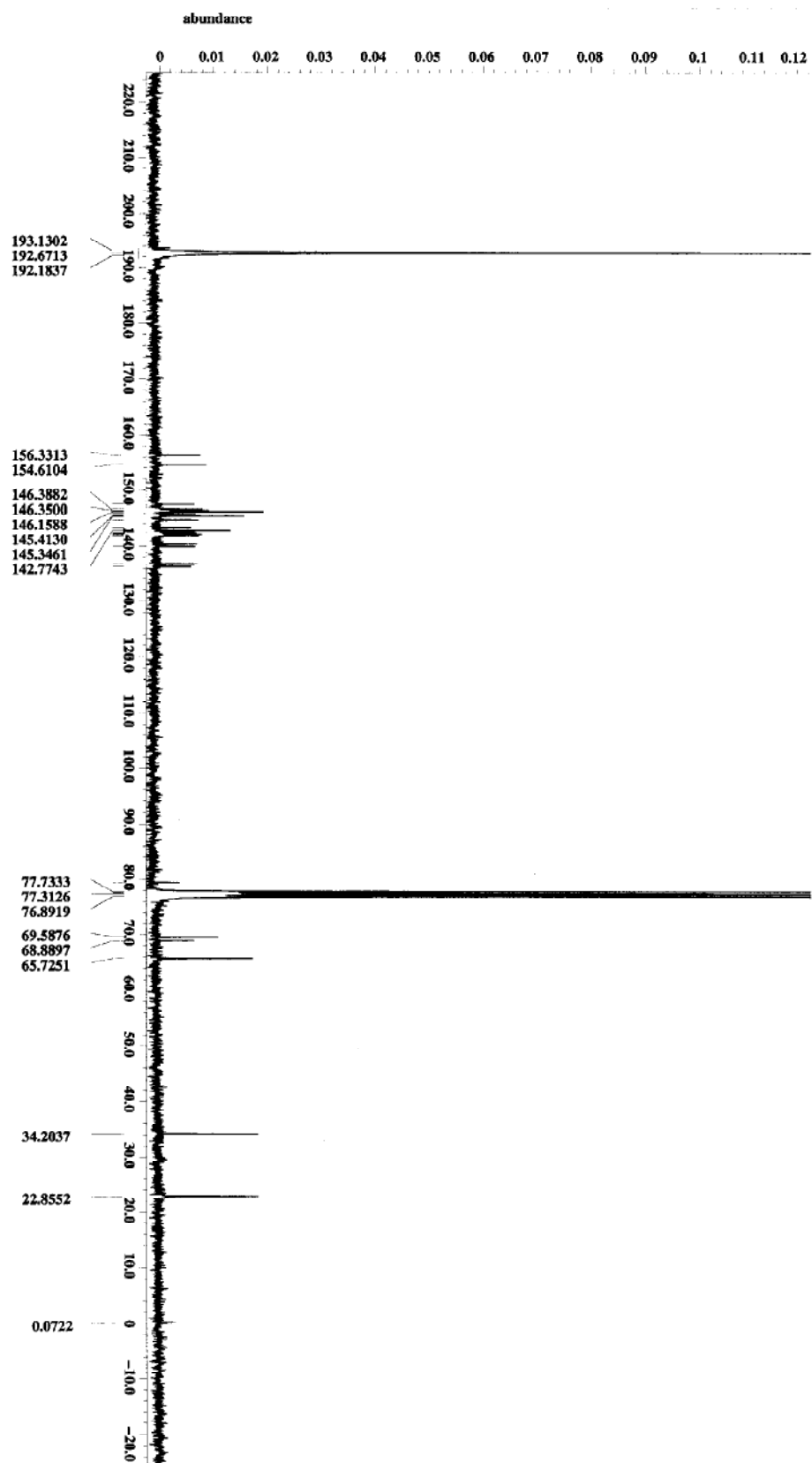**Figure A4.15** The ^{13}CNMR spectrum of **14**(75MHz, CS$_2$-CDCl$_3$)
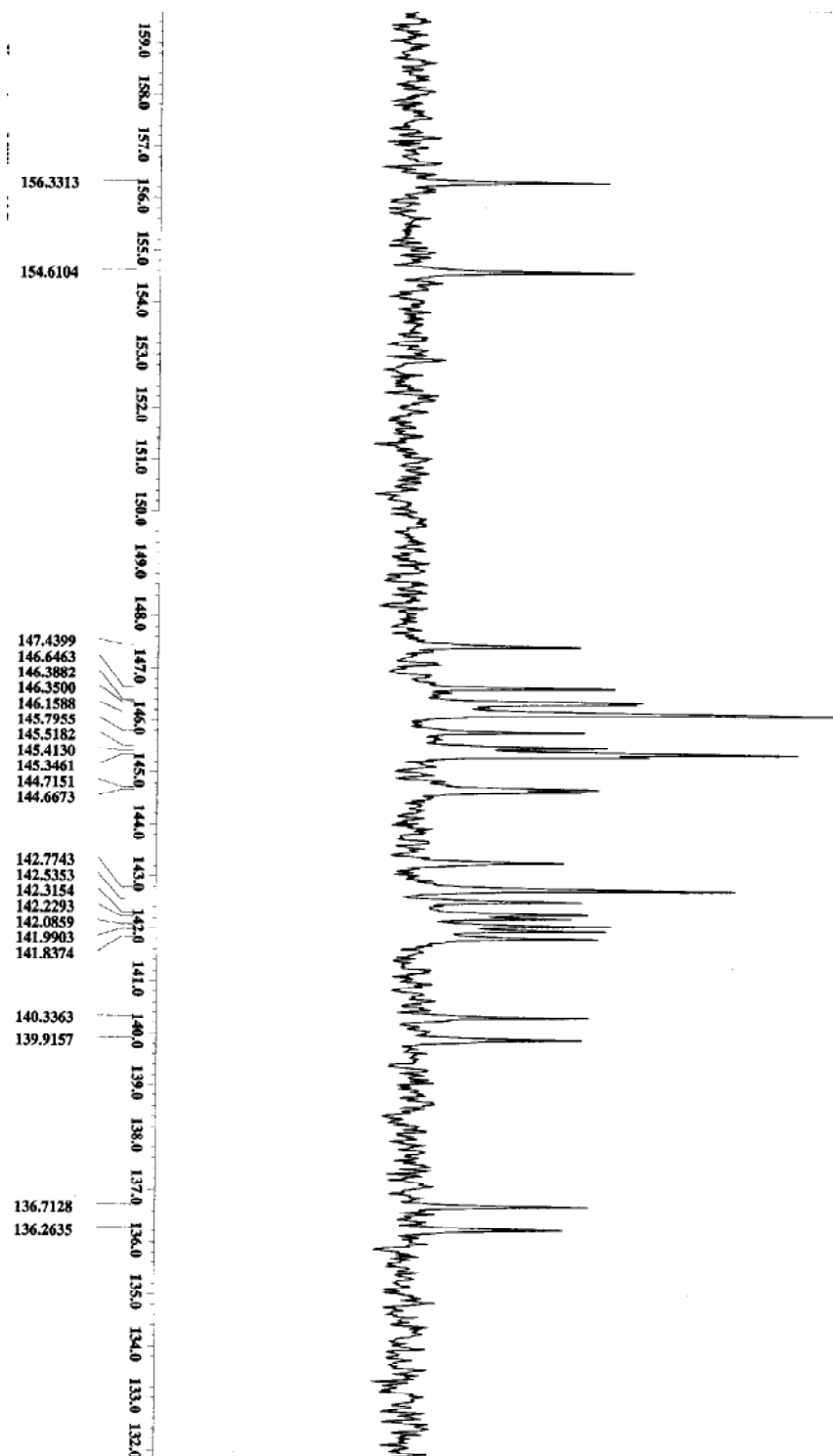
Figure A4.16 The ^{13}CNMR spectrum of **14** (75MHz, CS_2-$CDCl_3$), from 130ppm-160ppm

161

100

806.0970

%

807.1102

808.1464
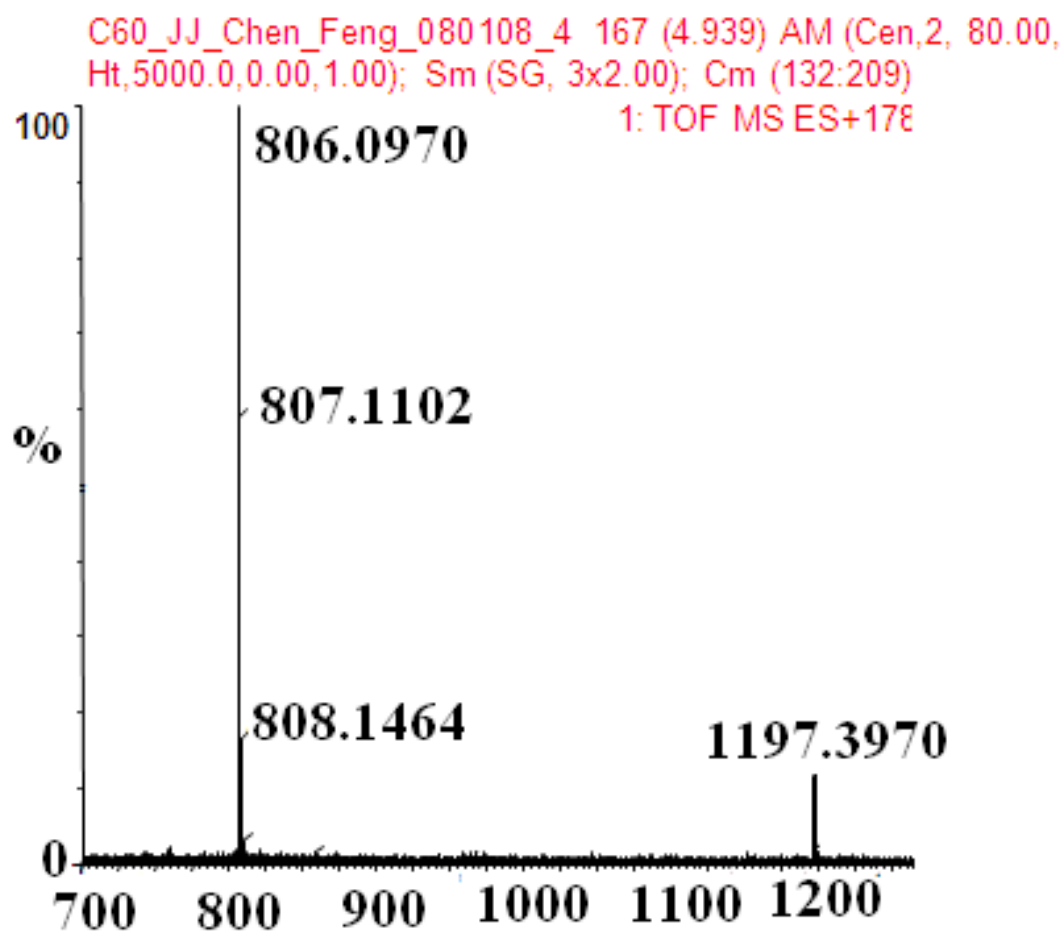
1197.3970

0

700 800 900 1000 1100 1200

Figure A4.17 The ESI-MS spectrum of **14**
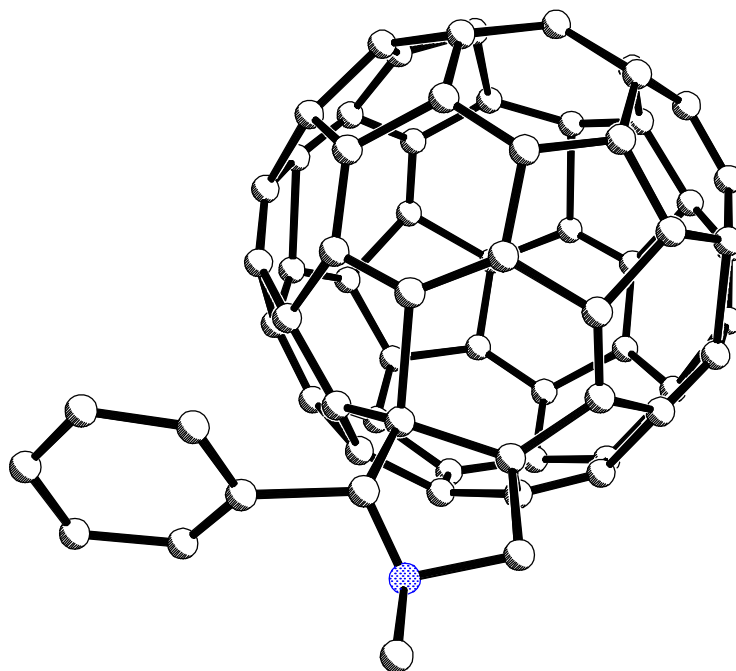
Figure A4.18 The ORTEP drawing of compound **12** with thermal ellipsoids plotted at 50% probability.

Bond precision: C-C = 0.0110 A   Wavelength=0.71073

Cell: a=10.074(2)   b=9.974(2)   c=39.648(8)

             alpha=90   beta=92.67(3)   gamma=90

Temperature: 158 K

	Calculated	Reported
Volume	3979.4(14)	3979.5(14)
Space group	P 21/c	P21/c
Hall group	-P 2ybc	?
Moiety formula	C69 H11 N, C6 H5 Cl	?
Sum formula	C75 H16 Cl N	C75 H16 Cl N
Mr	966.34	966.34
Dx,g cm-3	1.613	1.613
Z	4	4

Mu (mm-1)	0.158	0.158
F000	1960.0	1960.0
F000'	1961.35	
h,k,lmax	12,11,47	12,11,47
Nref	7060	6771
Tmin,Tmax	0.959,0.984	
Tmin'	0.942	

Correction method= Not given

Data completeness= Ratio = 0.959   Theta(max)= 25.110

R(reflections)= 0.1991(4095)   wR2(reflections)= 0.4688(6771)

S = 2.430   Npar= 694

　　*There are several methods for single crystal culture such like sublimate, co-crystallization, etc, but the most simplest and the most practical ones are slow evaporation, diffusion in liquid phase, diffusion in gas phase, we recommend the optimal amount of the sample for single crystal culture is 5-15mg, crystal nucleus could not formed in extreme diluted solution, while when the mother liquor is over concentrated, quick crystallization process results in bad crystals. In our experiment, the pretreatments of the samples include purification using preparative TLC and filtration through a cotton ball which is placed in a pipette, we found cotton balls better than a filtration paper in crystal culture. There are several solvents we use for this single crystal such as benzene, chlorobenzene, chloroform, dichloro methane or solvent mixture systems (good solvent and poor solvent in different proportion 1:2-1:4). We set five tubes for each solvent system, all the tubes were sealed with paprafilm and punched with tiny holes and were put on a stable position for a few days.

CHAPTER 5

SUMMARY

In this thesis, methylation, glycosylation and nanoconjugate reactions of the natural product-gossypol were studied. The bioactivity assays of the gossypol derivatives such as antioxidant, antidiabetic, anticancer, antitrypanosomal activities were explored. The gossypol derivatives including gossypol ethers, apogossypol, gossypolone, gossypol glycosides, unexpected N-methylfulleropyrrolidines products obtained from the gossypol based nanoconjugate reactions as well as related gossypol derivatives were synthesized and fully characterized by NMR, MS, FT-IR, UV spectrometry, HPLC and X-ray crystallography.

Firstly, hexamethyl and tetramethyl ethers of gossypol were synthesized, particularly, existence of four tautomers of gossypol tetramethyl ethers were chromatographically separated and confirmed with the assistance of NMR method. Gossypol exhibited the strongest antioxidant activity due to the high number of hydroxyl groups, while its ethers only remained partial antioxidant activity because of their conjugated naphthalene structure preserved in the derivatives. It was found that the anticancer activity of gossypol and its methylated ethers depended on the degree of methylation level of gossypol, the lower level of methylation the molecule undergoes, the higher antioxidant activity it held. Furthermore, the result of alpha-amylase inhibitory activities of gossypol and its methylated ethers showed that

the gossypol's methylated ethers were the alpha-amylase inhibitors, while gossypol was the alpha-amylase activator.

Secondly, novel glycosidic gossypol analogues were obtained by the ultrasound-assisted reaction of potassium salt of gossypol with 3, 4, 6-tetra-O-acetyl-α-D-glucopyranosyl bromide under phase transfer catalytic condition. The evaluation of anticancer, antitrypanosomal activities as well as cytotoxicity of those novel glycosidic gossypol derivatives implied that 6, 7'-gossypol diglycosidic tetraacetate (compound **8**) could be developed into a potential pharmaceutical candidate in the treatment of cancer since it exhibited powerful cancer cells inhibition with significantly low cytotoxicity. In addition, 7, 7'-gossypol diglycosidic tetraacetate (compound **7)** and 6, 7'- gossypol diglycosidic tetraacetate (compound **8)** possess strong antitrypanosomal activity with LD_{50} value low to 2.12 and 2.44 µM respectively.

Finally, gossypol reacted with fullerene [60] in the presence of sarcosine through the Prato reaction, resulting in some unexpected N-methylfulleropyrrolidines, and different products in variable yield were obtained when choosing toluene or chlorobenzene as reaction medium. During the reaction, gossypol decomposed into benzaldehyde which was successfully detected as a new intermediate through GC-MS for the first time which enriches the research of gossypol decomposition reaction. In an *in vitro* assay of NO radical induced apoptosis in 3T3L1 cells for the N-methyl-2,

2-dimethylfulleropyrrolidine (compound **14**) showed dose dependent and stronger radical scavenging activities than the parent fullerene.

The natural product-gossypol possess potential bioactivities in many aspects and certain toxicity to some extent, the chemical modification of gossypol is an efficient way to convert this two edge weapon to the more favorable direction, the prospective work about chemical reactions of gossypol can be sulfonation, halogenation, complexation etc, taking place in different reactive points of the gossypol molecule, future work will be focus on the quantitative structure-activity relationship (QSAR) of those novel gossypol derivatives and the mechanism to the molecular level of digestion, absorption, metabolism and excretion in biosystems.